Mineralization, Magmatism and Tectonics along Loei Fold Belt, Northeastern Thailand

（タイ北東部，Loei 褶曲帯における鉱化作用，
マグマ活動，およびテクトニクス）

2018

パッチャウイ ヌアルカオ
Patchawee Nualkhao
9515253

秋田大学大学院
工学資源学研究科博士後期課程
資源学専攻
2018

Abstract

Permo-Triassic granitoids from various areas along the Loei Fold Belt, northeastern Thailand, were studied. The aim of this work is to document the petrochemical characteristics of granitoids in the Loei Fold Belt. The Loei Fold Belt is an 800 km long, north-south trending fold belt that hosts several epithermal Au-Ag and skarn Au-Cu-Fe deposits. The study areas are divided into five regions *i.e.*, (1) Mung Loei, (2) Phu Thap Fah - Phu Thep, (3) Phetchabun, (4) Nakon Sawan - Lobburi and (5) Rayong - Chantaburi region. The granitoids consist of monzogranite, granodiorite, monzodiorite, tonalite, quartz-syenite and quartz-rich granitoids. These granitoids are composed of quartz, plagioclase, K-feldspar at varying proportions with mafic minerals such as hornblende and biotite. Accessory minerals, such as titanite, zircon, magnetite, ilmenite, apatite, garnet, rutile, and allanite are also present. Magnetic susceptibilities of granitoids vary from 6.5×10^{-3} to 15.2×10^{-3} in SI unit in Muang Loei, from 0.1×10^{-3} to 29.4×10^{-3} in SI unit in Phu Thap Fah – Phu Thep, from 2.7×10^{-3} to 34.6×10^{-3} in SI unit in Petchabun, from 2.4×10^{-3} to 14.1×10^{-3} in SI unit in Nakon Sawan – Lobburi and 0.03×10^{-3} to 2.8×10^{-3} in SI unit in Rayong – Chantaburi. Concentration of major elements suggests that these intermediate to felsic plutonic rocks have calc-alkaline affinities. Concentration of rare earth elements (REE) of the granitoids normalized to chondrite displays moderately elevated LREE and relatively flat HREE patterns, with distinct depletion of Eu. Rb vs. Y/Nb and Nb/Y tectonic discrimination diagrams illustrate that the granitoids from Muang Loei, Phu Thap Fah – Phu Thep, Phetchabun, Nakon Sawan – Lobburi and Rayong - Chantaburi formed in continental volcanic-arc setting. New age data from radiometric K-Ar dating on K-feldspar from granodiorite in Loei and Nakhon Sawan areas yielded 171±3 and 221±5 Ma,

respectively. K-Ar dating on hornblende separated from diorite in Lobburi yielded 219±8 Ma. These age dating data suggest magmatism of Muang Loei occurred in the Middle Jurassic, and Nakon Sawan – Lobburi occurred in Late Triassic. Both Nb vs. Y and Rb vs. (Y + Nb) discrimination diagrams and age data indicate that Nakon Sawan – Lobburi granitoids intruded in Late Triassic at Nong Bua, Nakon Sawan province and Khao Wong Phra Jun, Lobburi province in volcanic arc setting. Muang Loei granitoids at the Loei province formed later in Middle Jurassic also in volcanic arc setting. Most of $\delta^{34}S_{CDT}$ of pyrite separated from granitoids along Loei Fold Belt, range from -2.1 to +2.2‰. The negative $\delta^{34}S_{CDT}$ values of ore minerals from skarn deposit suggest that the I-type magma has been influenced by light biogenic sulfur from local country rocks. The Au-Cu-Fe-Sb deposits correlates with the magnetite-series granitoids in Phetchabun, Nakon Sawan-Lobburi and Rayong - Chantaburi areas. Metallogeny of Au and Cu-Au skarn deposits, and epithermal Au deposit are related to adakitic rocks of magnetite-series granitoids from Phetchabun and Nakon-Sawan areas. All mineralization along the Loei Fold Belt are generated in the volcanic arc related to the subduction of Paleo-Tethys. ^{T}Al content of biotite of granitoids increase in the following order: granitoids associated with Fe and Au deposit < those with Cu deposit < barren granitioids. X_{Mg} of biotite in granitoids in Muang Loei, indicate the crystallization of biotite in magnetite-series granitoids under high oxygen fugacity condition. On the other hand, low X_{Mg} (<0.4) of biotite in magnetite-series granitoids in Phu Thap Fah – Phu Thep and Rayong – Chantaburi, indicate reduced environment, low oxygen fugacity, associated with Au skarn deposit (Phu Thap Fah) and Sb-Au deposit (Bo Thong), respectively. The magnetite-series granitoids at Phu Thap Fah having low magnetic susceptibilities and low X_{Mg} of biotite, were formed by reduction of

initially oxidizing magnetite-series granitic magma by interaction with reducing sedimentary country rocks as suggested by negative $\delta^{34}S_{CDT}$ values.

Acknowledgements

Firstly, I would like to thank my supervisor Professor Akira Imai for providing me with the opportunity to entrance in this PhD research. He has given me never ending support, time and encouragement throughout the year and his patience and ideas have been instrumental. I would also like to thank my co-supervisor, Dr. Ryohei Takahashi, for his assistance in the field and laboratory work, for giving up his time for countless discussions and thesis revisions and his guidance throughout the project. His knowledge and support have been invaluable. Many thanks to Professor Punya Charusiri, my co-supervisor, for his guidance in field work, especially time spent reviewing drafts and his many thought provoking discussions.

Sincere appreciation goes to the Thung Kum Company Limited and Akara Resources Public Company Limited who made this project possible by providing access to the field area. Takamasa Sato, Ikeda Kousuke, Chaiyasit Kruasorn, Weerachon Unsen, Sasimook Chokchai are thanked for their assistance in the field. I also would like to thank to Dr. Hinako Sato for her assistance with laboratory work in sulfur isotope analysis.

Many thanks goes to Professor Ohba Tsukasa, Professor Ishiyama Daizo, Professor Shibayama Atsushi, Professor Sato Tokiyuki, Assistant Professor Kofi Adomako-Ansah, specially-appointed to the Leading Program, Dr. Ladda Tangwattanukul for suggestions and comments. My friends, Economic Geology Lab members, especially Ms. Manalo for providing me with motivation and encouragement throughout my honour year and for encouraging me and never ending support to pursue my dreams, without them I would not have these days. Lastly, I would like to thank Pikul, Peeraphol, Panuphong, and Laddawan

Nualkhao, Henrik Erkkonen and family for their love and support throughout my honours year. Without them this would not have been possible.

TABLE OF CONTENTS

LIST OF FIGURES

LIST OF TABLES

CHAPTER 1
INTRODUCTION

1.1 Introduction

The Loei Fold Belt is located at the western edge of Khorat Plateau in northeastern Thailand (Fig. 1.1). This arcuate magmatic-volcanic belt trends N-S through Thailand and Lao PDR. The district is underlain predominantly by Paleozoic rocks of the Indochina Block beneath the Khorat Group where deformed sedimentary and volcanic rocks of Silurian, Devonian, Carboniferous, and Permian ages were intruded by Triassic calc-alkaline plutons that are associated with base metal and precious metal mineralization (Crow & Zaw, 2011). The Loei Fold Belt contains a variety of mineral deposits including skarn Cu-Au deposits in the area around Loei (Jacobson *et al.,* 1969). There are many previous studies on geological, geochemistry, mineralization and tectonics but those are restricted to small study areas. Loei Fold Belt is associated with magmatism related to subduction in Late Paleozoic to Early Mesozoic (Intasopa & Dunn, 1994; Kamvong *et al.*, 2007, 2010; Boonsong *et al.,* 2011; Liu *et al.,* 2012). This magmatic event respond to subduction and formed magmatic-hydrothermal ore deposits (Richard, 2003) which were represented by the Au-Cu-Fe deposits along Loei Fold belt (Fig. 1). There are few studies that attempt to understand the magmatism and geodynamic and metallogenic evolution of the Loei Fold Belt. Kamvong (2013) investigated the hydrothermal evolution of the Puthep (PUT 1) deposit to link between tectonics, magmatism and metallogenesis in the northern part of Loei Fold Belt. Most of the studies have focused on volcanic rocks. Intasopa and Dunn (1994) studied characteristics of Sr-Nd isotope and Rb-Sr isochron age of rhyolite and basalt in the northern Loei Fold Belt. Panjasawatwong et al. (2006) studied

petrogenetic and geochemistry of basaltic rocks in Loei province. Boonsong et al. (2011) suggested that the Loei Fold belt calc-alkaline volcanic rocks formed in Permo-Triassic volcanic arc and related to crustal thickening by back-arc compression (Sone & Metcalfe, 2008; Metcalfe, 2011).

However, the relationships between deposits styles and tectonic evolution of the Loei Fold Belt still remains controversial.

1.2 Objectives

Therefore, this project presents an investigation on the geological, geochemistry characteristics of granitoids along the Loei Fold belt and has the following objectives:

- To document the geological, petrography and geochemistry of granitoids
- To determine the age of the intrusion which was related to the mineral deposits
- To develop and integrate a geotectonic and metallogenic model for the evolution and origin of the Loei Fold Belt and the overall timing and history of terrane collision in mainland SE Asia

1.3 Location and access

The Loei Fold Belt is located in the northeastern Thailand between latitude of 17˚49’36.15”N to 17˚55’15.74”N and longitude 101°51'16.05"E to 102°13'39.34"E (Fig. 1). The Loei Fold Belt covers approx. 800km in length of 10 provinces from north to south such as Loei, Phetchabun, Nakon Sawan, Lobburi, Saraburi, Chachoensao, Chonburi, Rayong, Chantaburi and Prachinburi (Fig. 1). From Bangkok, access to the study area in the northern part to Loei, Phetchabun, Nakon Sawan, Lobburi, Saraburi areas can be via

Route 201 or Saraburi-Lomsak. For the southern part to Chachoensao, Chonburi, Rayong, Chantaburi and Prachinburi areas can be via highways such as highway 304 (Bangkok-Min Buri-Chachoengsao Road) or Motorway 7 (Bangkok-Chonburi).

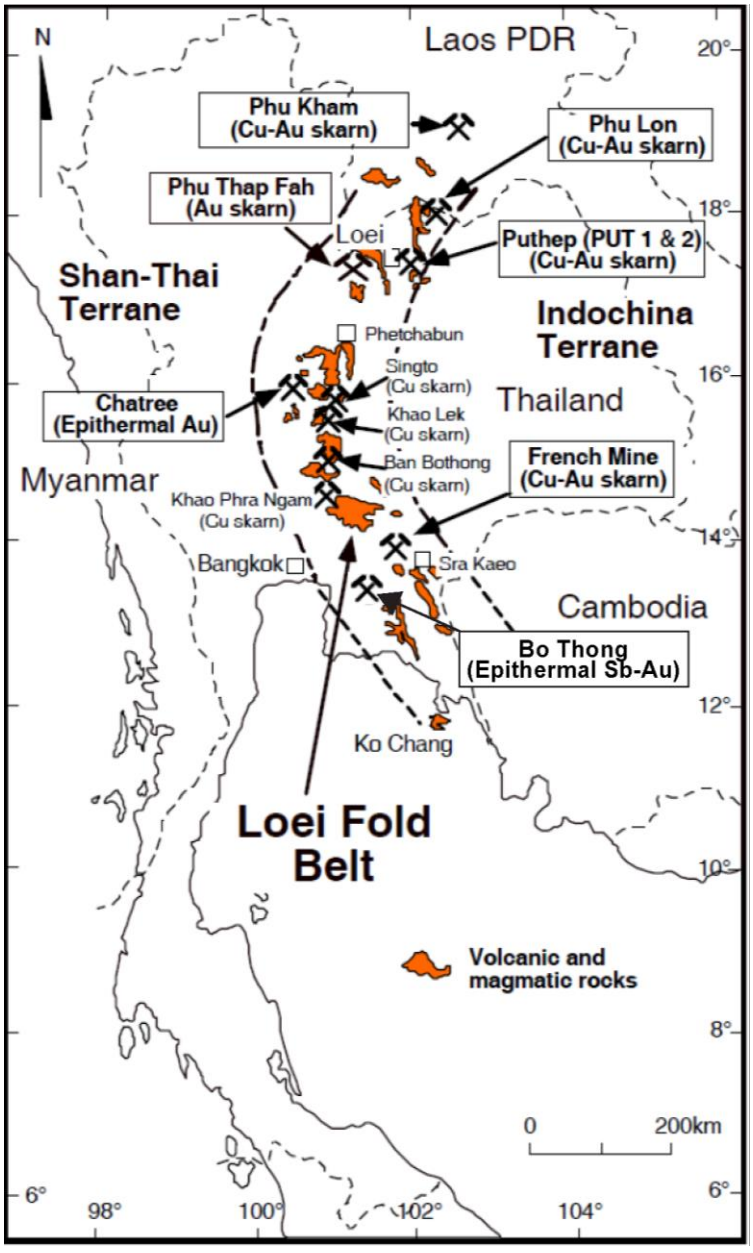

Fig. 1.1 Location of the study area in northeastern Thailand which are shown in orange colour, showing the Cu-Au skarn and epithermal Au deposits along Loei Fold Belt. (modified from Zaw *et al.*, 2009).

1.4 Land use and climate

The main land use in the study area is for agricultural in Loei, Phetchabun, Nakon Sawan, Lobburi, Saraburi, rubber plantations and crops in Rayong, Chantaburi and Prachinburi. Some areas are still covered by a deep-green forest and national park. The climate is a tropical climate dominated by annual monsoons, high both in temperature and humidity. The temperature usually averages 26 to 34 degrees Celsius, with the highest temperatures from March to May and the lowest in December and January. The study area is dominantly controlled by 2 major seasons which are the rainy season and the hot season. It rains from April to November.

1.5 Methods

Seventy-three granitoid samples were collected from the study areas along Loei Fold Belt in five regions of: (1) Mung Loei, (2) Phu Thap Fah – Phu Thep, (3) Phetchabun, (4) Nakon Sawan-Lobburi and (5) Rayong - Chantaburi (Fig. 4, Table 1).

Thin-sections were observed for petrographic analysis under a Nikon polarization optic microscope. At least 2000 points per sample were counted to identify the abundances of minerals (Table 2). Major and trace elements compositions were analyzed at ALS Minerals in Canada. Sulfur isotope of sulfide minerals were analyzed using a Thermo Scientific Inc. Flash 2000, Conflo IV and Delta V Advantage in Akita University. The sulfur isotopic ratio is presented in $\delta^{34}S$ expression relative to the $^{34}S/^{32}S$ of trotolite in Canyon Diablo iron meteorite (CDT). The analysis uncertainty is ±0.2‰.

K-Ar dating was performed on K-feldspar separated from Muang Loei Granitoids (Gr10), Nakon Sawan – Lobburi Granitoids (NDBI), and hornblende separated from Nakon Sawan – Lobburi Granitoids (WPJ-DI). The mineral separates were prepared using a magnetic separator and a heavy liquid, following Imaoka *et al.* (2011). The purity of K-feldspar and hornblende was higher than 99%, with no impurities observed under the microscope. Aliquots of the mineral separates were subsequently pulverized for K analysis. K and Ar were analyzed by isotope dilution at Actlabs, Canada, using a ^{38}Ar spike.

The magnetic susceptibility of the granitoids was measured on site using a Terraplus KT-10 magnetic susceptibility meter.

1.6 Thesis organization

This thesis is divided into seven chapters and organized as follows:

Chapter 1 provides the general background of the Loei Fold Belt. The objectives and an overview of the analytical methods are outlined and the content of each chapter is summarized.

Chapter 2 provides an overview of the tectonic setting of mainland SE Asia and the regional setting of Thailand, including the brief summaries of each terrane involved with the tectonic evolution. Moreover, the stratigraphic and tectonic framework of the Loei Fold Belt is also discussed. It is mainly based on previous studies and published literature.

Chapter 3 presents the result of the fieldwork undertaken during this study. Deposit-scale geology of mineral deposits along Loei Fold Belt is described. Petrographic and textural characteristics of intrusive rocks of each deposits have been included.

Chapter 4 focuses on the whole-rock geochemistry of intrusive rocks in each deposits and covers results of sulfur isotopes analyses of granitoids which have never been studied in Loei Fold Belt.

Chapter 5 presents the ages of those granitoids which have been determined using K-Ar dating and compares the magmatism of Loei Fold Bet to the other fold belt in SE Asia.

Chapter 6 provides details of rock-forming minerals of granitoids, particularly biotite, plagioclase, hornblende and apatite from EPMA analysis.

Chapter 7 presents discussion and conclusion of all investigation in this study, and introduces the interpretation, genesis and exploration implications of the Loei Fold Belt metallogeny. Some suggestions for future work area are stated in the last section of this thesis.

Table 1.1 Location and lithology of rock samples from Loei Fold Belt (sample location in Fig. 1.1).

Table 1 Location and lithology of rock samples from Loei Fold Belt (sample location in Fig.

Sample ID	Code	Zone	Easting	Northing	Lithology	Unit/Complex
1	Gr01	47Q	783030	1920822	granodiorite	Phu Thap Fah - Phu Thep
2	Gr02	47Q	783030	1920822	granodiorite	Phu Thap Fah - Phu Thep
3	Gr03	47Q	783030	1920822	granodiorite	Phu Thap Fah - Phu Thep
4	Gr04	47Q	782988	1920850	granodiorite	Phu Thap Fah - Phu Thep
5	Gr05	47Q	782988	1920850	granodiorite	Phu Thap Fah - Phu Thep
6	Gr07	47Q	781456	1920855	tonalite	Phu Thap Fah - Phu Thep
7	Gr08	47Q	781422	1920914	tonalite	Phu Thap Fah - Phu Thep
8	Gr09	47Q	788962	1922053	granodiorite	Phu Thap Fah - Phu Thep
9	Gr10	47Q	785286	1960980	quartz-syenit	Muang Loei
10	Gr11	47Q	785286	1960980	tonalite	Muang Loei
11	Gr12	47Q	785177	1961174	granodiorite	Muang Loei
12	Gr14	47Q	784256	1977779	granodiorite	Muang Loei
13	Gr15	47Q	784635	1978421	diorite	Muang Loei
14	Gr16	47Q	784336	1977215	granite	Muang Loei
15	Gr17	47Q	794012	1967898	tonalite	Muang Loei
16	Gr18	47Q	796117	1963434	diorite	Muang Loei
17	Gr19	47Q	796098	1963474	granodiorite	Muang Loei
18	Gr20	47Q	796817	1922781	granite	Muang Loei
19	Gr21	47Q	796788	1923496	tonalite	Phu Thap Fah - Phu Thep
20	Gr22	47Q	794832	1927353	diorite	Muang Loei
21	Gr23	47Q	795164	1925955	diorite	Muang Loei
22	Gr25	47Q	801209	1925652	granodiorite	Muang Loei
23	Gr26	47Q	686668	1789339	granite	Phetchabun
24	Gr27	47Q	686891	1789765	granodiorite	Phetchabun
25	Gr28	47Q	687431	1789993	granodiorite	Phetchabun
26	Gr29	47Q	687431	1789993	granodiorite	Phetchabun
27	Gr30	47Q	694003	1780827	granodiorite	Phetchabun
28	Gr31	47Q	696655	1774765	tonalite	Phetchabun
29	Gr32	47Q	697466	1775644	granite	Phetchabun
30	Gr33	47Q	691653	1789930	tonalite	Phetchabun
31	Gr34	47Q	699061	1793684	tonalite	Phetchabun
32	Gr35	47Q	702550	1803735	tonalite	Phetchabun
33	Gr36	47Q	701317	1807087	diorite	Phetchabun
34	Gr37	47Q	708362	1808622	diorite	Phetchabun
35	Gr38	47Q	710144	1807532	granite	Phetchabun
36	Gr39	47P	762169	1401903	granite	Rayong - Chantaburi
37	Gr40	48P	201809	1393051	granite	Rayong - Chantaburi
38	Gr41	48P	201809	1393051	granite	Rayong - Chantaburi
39	Gr42	48P	196389	1420135	granite	Rayong - Chantaburi
40	Gr43	48P	196534	1421115	granodiorite	Rayong - Chantaburi
41	Gr44	48P	196356	1422338	granite	Rayong - Chantaburi
42	Gr45	47P	801835	1431918	granite	Rayong - Chantaburi
43	Gr46	47P	801338	1432899	granodiorite	Rayong - Chantaburi
44	Gr47	47P	764975	1470643	granite	Rayong - Chantaburi
45	Gr48	47P	765071	1470672	granodiorite	Rayong - Chantaburi
46	Gr49	47P	765252	1470247	granite	Rayong - Chantaburi
47	Gr50	47P	773088	1524671	tonalite	Rayong - Chantaburi
48	Gr51	47P	773272	1524706	granodiorite	Rayong - Chantaburi
49	Gr52	47P	771607	1522038	granite	Rayong - Chantaburi
50	Gr53	47P	772914	1524766	granite	Rayong - Chantaburi
51	Gr54	47P	724697	1614473	granite	Rayong - Chantaburi
52	Gr55	47P	678794	1653835	diorite	Nakon Sawan - Lobburi
53	Di-KK	47Q	673320	1809575	diorite	Phetchabun
54	GR-LB	47Q	672115	1692684	granite	Phetchabun
55	8R5T	47Q	676945	1799311	granodiorite	Phetchabun
56	KP-DI	47Q	665924	1802933	diorite	Phetchabun
57	MKCD	47P	690042	1760386	granodiorite	Phetchabun
58	NBDI	47P	677244	1752206	granite	Nakon Sawan - Lobburi
59	NBDI1	47P	677244	1752206	granite	Nakon Sawan - Lobburi
60	NBDI1(2)	47P	677244	1752206	granite	Nakon Sawan - Lobburi
61	NBDI2	47P	677244	1752206	granitoid	Nakon Sawan - Lobburi
62	WPJ-DI	47P	681899	1655158	diorite	Nakon Sawan - Lobburi
63	WP029	47P	675213	1647563	diorite	Nakon Sawan - Lobburi
64	1R5M	47Q	676945	1799311	granodiorite	Phetchabun
65	1R1B	47Q	676945	1799311	granodiorite	Phetchabun
66	8R5T	47Q	676945	1799311	granodiorite	Phetchabun
67	4R4M	47Q	676945	1799311	granodiorite	Phetchabun
68	8R1M	47Q	676945	1799311	granodiorite	Phetchabun
69	4R5B	47Q	676945	1799311	granodiorite	Phetchabun
70	8R5B	47Q	676945	1799311	granodiorite	Phetchabun
71	4R2T	47Q	676945	1799311	granodiorite	Phetchabun
72	4R4B	47Q	676945	1799311	granodiorite	Phetchabun
73	8R3T	47Q	676945	1799311	granodiorite	Phetchabun

CHAPTER 2
GEOLOGICAL SETTING

2.1 Introduction

This chapter presents an overview of the tectonic setting and regional geology of Thailand. Many previous works have described the broader country-wide regional setting and geological events in Thailand (*e.g.*, Bunopas, 1981, 1982; Charusiri *et al.* 1997; Metcalfe *et al.* 1999; Ueno, 1999; Bunopas *et al.* 2002; Charusiri *et al.* 2002). In this chapter, recent information is summarized on the regional tectonic setting of Thailand to the district scale geology of the Loei Fold Belt, northeastern Thailand.

2.2 Regional tectonic setting of Thailand

Mainland eastern Asia (with Sundaland at its core) (Metcalfe, 2006, 2011, 2017) is composed of a complex assembly of continental blocks, arc terranes and suture zones. Thailand and its adjacent areas, comprises two major tectonic terranes: Indochina in the east and Sibumasu in the west. These two terranes are separated by Sukhothai Fold Belt (SFB) on the west side and Loei Fold Belt (LFB) on the east side (Salam *et al.* 2014). The term Sibumasu block, was proposed by Metcalfe (1984) to replace previous terms used for the Gondwana-derived block characterized by Late Palaeozoic Gondwana biotas and Late Carboniferous–Early Permian glacial-marine diamictites (Metcalfe, 2011). It is widely believed to have been rifted from the northwestern Australian part of Gondwanaland (or Gondwana in current literatures) in the early Permian (Bunopas & Vella, 1983; Gatinsky *et al.* 1984; Metcalfe, 1988; Hutchinson, 1989; Bunopas, 1991; Barber & Crow, 2002).

Indochina block is interpreted to have formed part of the India–Australian margin of Gondwana in the Early Palaeozoic and to have rifted and separated from Gondwana by the opening of the Palaeo-Tethys ocean in the Early Devonian (Metcalfe, 2011).

Loei Fold Belt lies along the western margin of the Indochina terrane (Fig. 2.1). The granitoids of Thailand are distributed in three provinces comprising a Western, Central and Eastern Province (Cobbing *et al.*, 1986; Charusiri *et al.*, 1993; Hutchison, 2007; Searle *et al.*, 2012) which are characterized by different granitoid type and ages of emplacement.

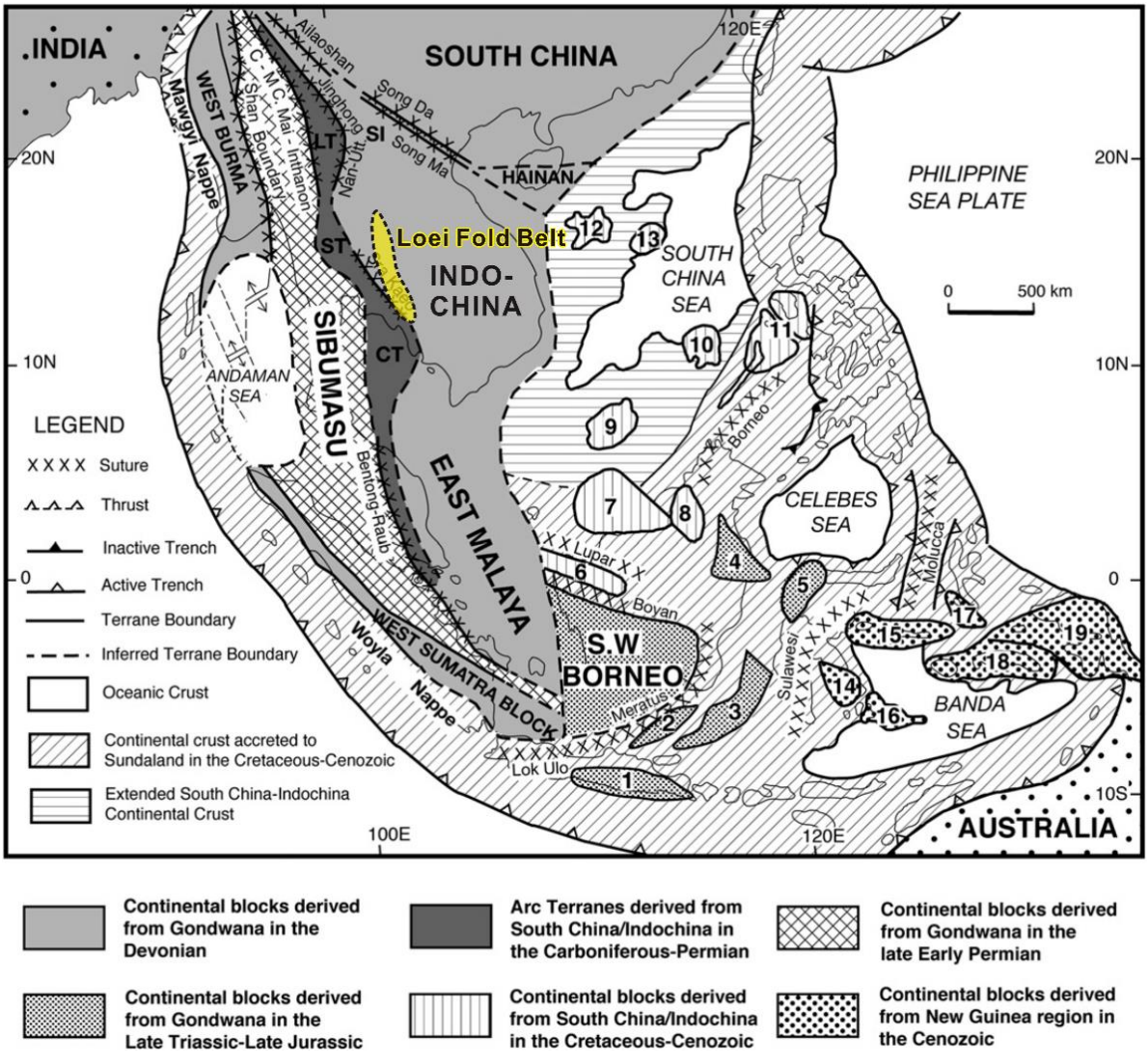

Fig. 2.1 Distribution of continental blocks, fragments and terranes, and principal sutures of Southeast Asia. Numbered micro-continental blocks, 1: East Java, 2: Bawean, 3: Paternoster, 4: Mangkalihat, 5: West Sulawesi, 6: Semitau, 7: Luconia, 8: Kelabit–Longbowan, 9: Spratly Islands–Dangerous Ground, 10: Reed Bank, 11: North Palawan, 12: Paracel Islands, 13: Macclesfield Bank, 14: East Sulawesi, 15: Bangai–Sula, 16: Buton, 17: Obi–Bacan, 18: Buru–Seram, 19: West Irian Jaya, LT: Lincang Terrane, ST: Sukhothai Terrane and CT: Chanthaburi Terrane. C–M: Changning–Menglian Suture, C.-Mai: Chiang Mai Suture, and Nan–Utt.: Nan–Uttaradit Suture, modified from Metcalfe (2011) and Simons et al. (2007). Yellow box shows location of Loei Fold belt in northeastern Thailand.

2.3 Terranes and zones

Thailand is subdivided into five major tectonic domains (Barr & Macdonald, 1987; Ueno & Hisada, 2001; Sone & Metcalfe, 2008; Sone *et al.* 2012), from east to west, the Indochina Block, Sukothai Terrane, Inthanon Terrane, Chantaburi Terrane and Shan-Thai (Sibumasu) Terrane (Fig. 2.2). The Indochina Terrane is separated from the Sukhothai Terrane to the west by Nan Suture. Sukhothai Terrane is separated from the Inthanon Terrane to the west by Chaing Mai Suture, and the Sukhothai Terrane is separated from the Shan-Thai (Sibumasu) Terrane by the Inthanon Suture Zone. Nakhon-Thai Block Terrane has been interpreted as having formed as a result of the accretion of oceanic and terrigenous materials that were mixed along the western margin of the Indochina block during Late Paleozoic to Early Mesozoic by Charusiri *et al.* (2002), Barber *et al.* (2011) and Ridd (2012).

2.3.1. Sukhothai Terrane

Sukhothai terrane or so-called Sukhothai Island Arc basin system, including the Chantaburi Terrane of Thailand, is located between the Sibumasu and Indochina terranes. It consists of Permo-Carbonifereous metamorphic rocks (Pha Som Metamorphic complex), with Permian and Triassic S-type granitoids. It was initially developed as a Permo-Triassic volcanic arc of the Indochina Block by opening of the Nan-Sa Kaeo back-arc basin. This volcanic arc system was induced by the east-dipping Paleo-Tethys subduction beneath the margin of the Indochina Block (Sone & Metcalfe, 2008). The Pha Som Metatmorphic Complex has been interpreted as an accretionary complex and occurred as a west-directed subduction zone during the Late Permian collision of the Shan-Thai and Indochina Terranes (Singharajwarapan & Berry, 2000; Sone & Metcalfe, 2008).

2.3.2. Chantaburi Terrane

The Chantaburi Terrane is the southern extension of the Sukhothai Terrane (Sone & Metcalfe, 2008). This terrane is a magmatic arc of the Indochina terrane which bounded with the Sa Kaeo Suture on the eastern side and Klaeng Fault on the western side. The formation of this terrane consists of the Permian to Triassic magmatic arc (Charisiri *et al.* 1993) which was probably emplaced during the eastward subduction of the Palaeo-Tethys Ocean beneath the Indochina Terrane.

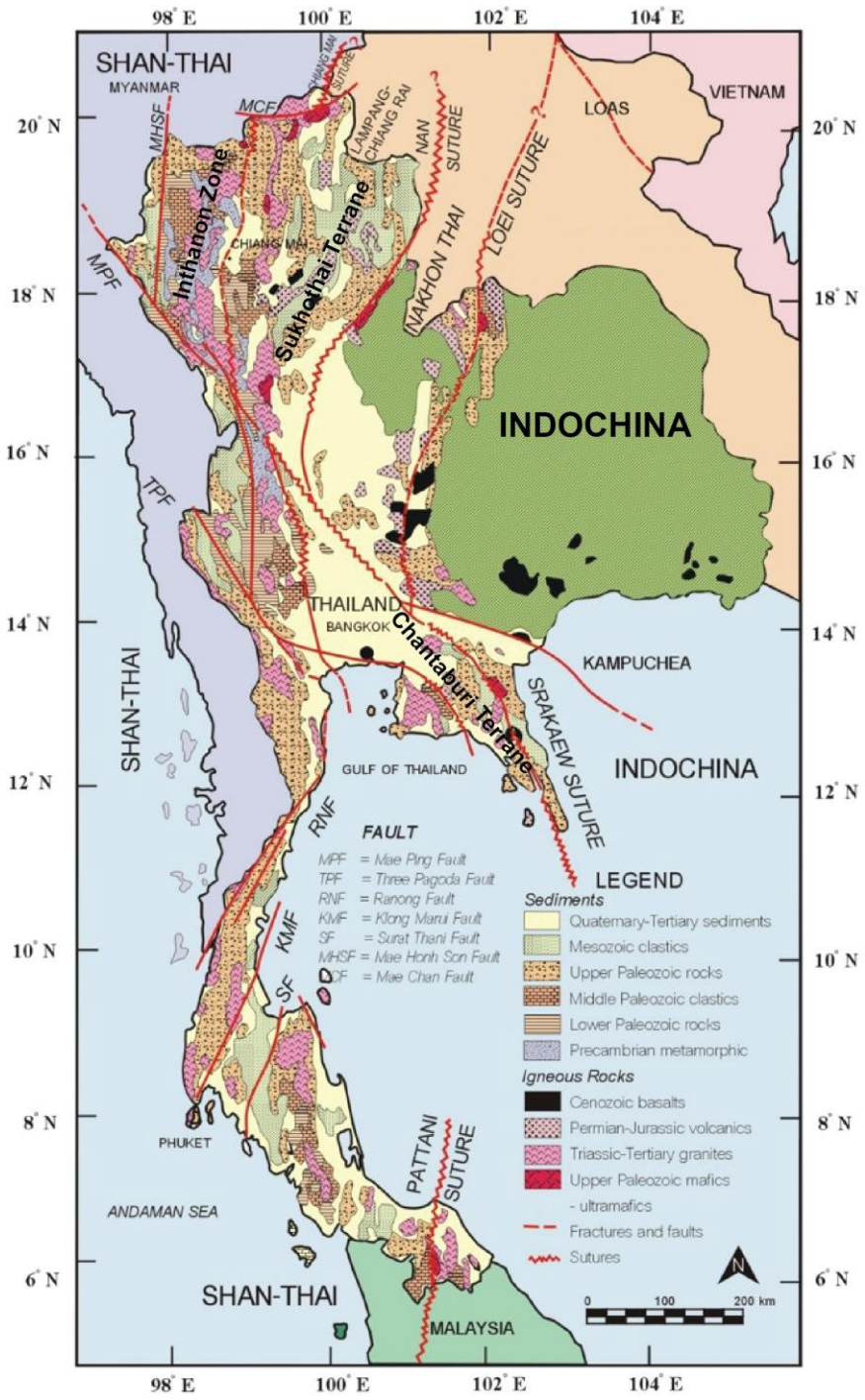

Fig. 2.2 Simplified geological map of Thailand showing the distribution of rocks of various ages, significant tectonic plates and major sutures/fault system (modified after Charusiri *et al.* 2002).

CHAPTER 3

DEPOSIT GEOLOGY

3.1 Introduction

The Loei Fold Belt occurs in Thailand between two major crustal terranes in mainland SE Asia: Shan-Thai in the west and Indochina terrane in the east. The Fold Belt hosts a diverse array of deposit styles containing significant Au and Cu. The following individual Cu-Fe-Au deposits were investigated,

1. Phu Lon skarn Cu-Au deposit, Loei
2. Phu Thep porphyry/skarn Cu deposit, Loei
3. Phu Thap Fah Cu-Au skarn deposit, Loei
4. LD epithermal Au deposit, Pichit
5. Wang Yai epithermal Au deposit, Pichit
6. Singto skarn Fe-Cu deposit, Pichit
7. Chathree epithermal Au deposit, Pichit
8. Khao Phanompha skarn Au deposit, Pichit
9. Khao Lek skarn Fe-Cu deposit, Nakhon Sawan
10. Ban Bothong skarn Cu-Au deposit, Lopburi
11. Khao Phra Ngam skarn Cu deposit, Lopburi
12. French Mine skarn Cu-Au deposit, Prachin Buri
13. Bo Thong epithermal Sb-Au deposit, Chachoensao

The location of these deposits are shown in Fig. 3.1 and their lithology of host rock/age, associated intrusions/age, ore type, alteration minerals, ore mineralogy and available tonnage/grade data are presented in Table 3.1.

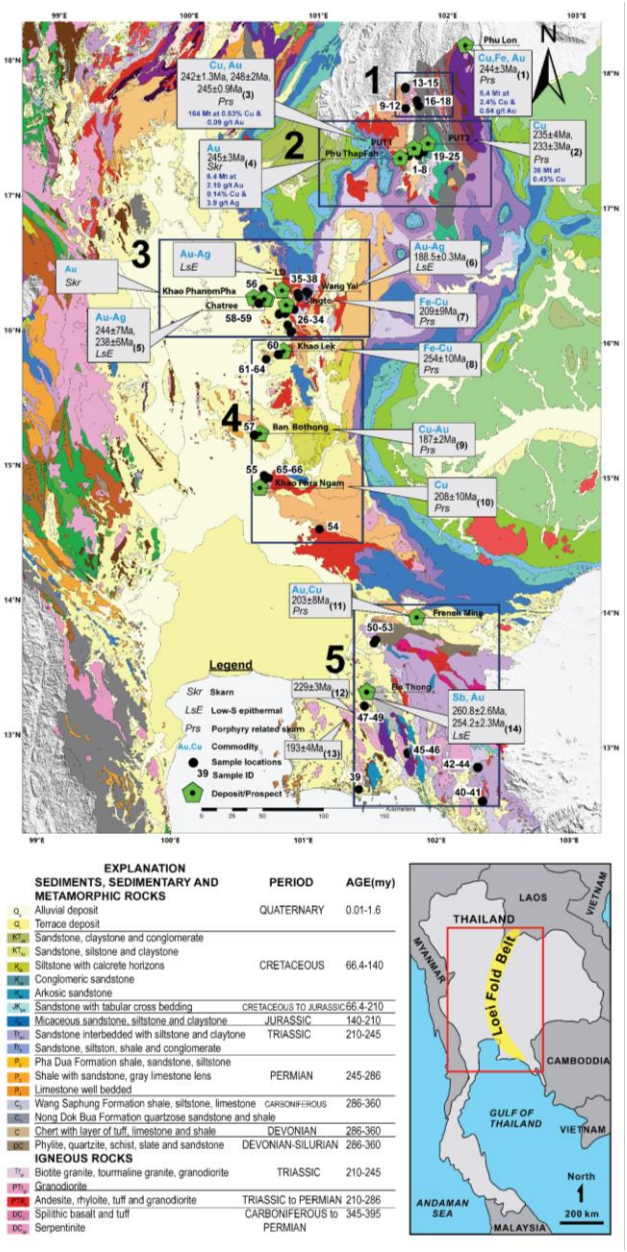

Fig. 3.1 Geologic map of the study area with locations of mines and samples. A: Muang Loei granitoids, B: Phu Tap Fah – Phu Thep granitoids, C: Phetchabun granitoids, D: Nakon Sawan – Lobburi granitoids, E: Rayong – Chantaburi Granitoids, modified from the Department of Mineral Resources (2013). Age dating data sources: (1) Kamvong (2005); (2), (3) Zaw et al. (2009); (4) Zaw et al. (2014); (5) De Little (2005); (6), (7), (8), (9) Zaw et al. (2007); (10) Muller (1999); (11), (12) Kawakami et al., (2014); (13) Paipana (2014). Section Lines of Fig. 2 are illustrated.

Table 3.1 Geological characteristics of Cu-Au deposits occurring along the Loei Fold Belt

No.	Deposit	Location	Host rock/ages	Intrusion/age	Ore type	Alteration Mineral & Type	Ore mineralogy	Tonnage	References
1	Phu Lon (Prospect)	1°47'15"N, 102°19'0.52"E	Limestone/Devonian, Volcaniclastics/U-Pb zircon 359±6 Ma (Late Devonian)	Diorite and quartz monzonite porphyry/U-Pb zircon 244±3 Ma , thermal event: Ar/Ar 187-108 Ma	Porphyry-related skarn (oxidized)	Prograde: garnet, pyroxene, wollatonite, K-feldspar Retrograde: quartz, tremolite, epidote, chlorite, calcite, sericite	Chalcopyrite, magnetite, pyrite, bornite, gold	5.4 Mt @ 2.4% Cu, 0.64 g/t Au	Kamvong (2004), Meinert et al. (2005)
2	Phu Thep								
	PUT1 (Cu-Au) (Phu Hin Lek Fai) (Prospect)	17°28'2.96"N, 101°52'1.16"E	Siliciclastics and Limestone (Wang Saphung Formation)/Carbonifereous	Diorite, monzodiorite porphyry/U-Pb zircon 248±6Ma	Porphyry-related skarn (oxidized)	Porphyry: potassic (K-feldspar, biotite, magnetite), phyllic (serecite, pyrite), propyritic (epidote, pyrite); Skarn prograde: garnet; Retrograde: chlorite, epidote, carbonate, quartz, sericite	Chalcopyrite, pyrite, magnetite	85 Mt @ 0.4% Cu (inferred)	Zaw et al. (2014)
	PUT2 (Cu-Au) (Phu Thong Dieng & Phu Tham Phra) (Prospect)	17°25'55.16"N, 101°45'35.96"E	Sandstone, siltstone, mudstone and limestone (Wang Saphung Formation)/Carboniferous	Granodiorite/U-Pb zircon 235±4 Ma(Middle Triassic) and andesitic dyke/233±3Ma(Late Triassic); whole rock K-Ar resetting age of 177, 198, 200Ma	Porphyry-related skarn (oxidized)	Porphyry; phyllic, argillic, propylitic; skarn retrograde: chlorite, epidote, carbonate, quartz, sericite, illite; supergene: kaolinite	Chalcopyrite, pyrite, magnetite, hematite	36 Mt @ 0.43% Cu (inferred)	Khositanont (2006)
3	Phu Thap Fah (Au) (Mine)	17°21'15.83"N, 101°39'10.79"E	Silisiclastic and limestone /Permian	Granodiorite/U-Pb zircon 245±3 Ma; Ar-Ar resetting age of 153-111Ma	Skarn type (reduced)	Prograde: garnet, pyroxene, quartz; retrograde: epidote, calcite, chlorite, quartz	Gold, pyrite, bismuth, pyrrhotite, magnetite, chalcopyrite	0.7 Mt @ 3.54 g/t Au (reserves) 0.7 Mt @ 7.97 g/t Au (indicated)	Rodmanee (1999); Zaw *et al.* (2006)

4	LD (Au-Ag) (Prospect)	16°17'31.2"N, 100°37'58.8"E	Plagioclase-pyroxene phyric andesite/U-Pb zircon 250±5Ma (Early Permian)	No known intrustion	Low-sulfidation epithermal	Quartz, pyrite, calcite, adularia, sericite, chlorite	Predominantly pyrite	No data	Zaw *et al.* (2007)
5	Wang Yai (Au-Ag) (Prospect)	16°21'36.79"N, 100°45'57.1"E	Volcaniclastics, rhyolite breccia Host ryolite/Ar-Ar 294±1Ma, volcanic sandstone/U-Pb zircon<247±4, Ar-Ar rehearing age at 206Ma	Post-mineral diorite intrusion/U-Pb zircon 220±5Ma, Ar/Ar age of 188.5±0.3Ma, resetting K-Ar age 124±5, 111±5Ma	Low-sulfidation epithermal	Quartz, pyrite, calcite, adularia, sericite, chlorite	Electrum, argenite, pyrite, sphalerite, galena, minor chalcopyrite	No data	De Little (2005)
6	Singto (Fe-Cu) (Prospect)	16°15'8.64"N, 100°48'3.54"E	Limestone, siliciclastics (Permian?)	Diorite/U-Pb zircon 209±9Ma, 213±10Ma(Late Triassic)	Porphyry-related skarn (oxidized)	Prograde: garnet, retrograde: quartz, epidote, chlorite, calcite	Magnetite, chalcopyrite, pyrite	No data	Müller (1999)
7	Chatree (Mine)	16°17'37.68"N, 100°38'49.20"E	Volcanoclastics, andesitic pumiceous breccia, rhyolite breccia/Permian-Early Triassic	Hornblende diorite dyke, xenocrystic granodiorite-bearing basaltic dyke, hornblende phyric dyke/U-Pb zircon 244±7Ma, 238±6Ma, 221±8Ma (Early Triassic)	Low-sulfidation epithermal	Quartz, pyrite, calcite, adularia, sericite, chlorite, illite, smectite/ Ar/Ar age of adularia (Stage 5 mineralized vein, C pit) age 280±6Ma, K-Ar 250.9±0.8Ma	Electrum, pyrite, sphalerite, galena, minor chalcopyrite	1.8 Moz Au (1.8 g/t Au, 18 g/t Ag) (reserves)	Cumming (2004), Khronkhum (2005), Salam (2006)
8	Khao Phanompha (Au) (Mine)	16°18'5.21"N, 100°33'8.96"E	Felsic andesitic volcaniclastics	No known intrustion	Mesothermal/skarn	Prograde: wollastonite, biotite; retrograde: quartz, tremolite, sericite/K-Ar age of sericite 252±5Ma (Early Permian to Late Triassic)	Pyrrhotite, pyrite, chalcopyrite, electrum	No data	Zaw *et al.* (2007)
9	Khao Lek (Fe-Cu) (Prospect)	15°53'40.17"N, 100°46'49.56"E	Limestone, siliciclastics (Permian?)	Granitoid porphyry/ U-Pb zircon 254±10 to 249±5Ma (Late Permian-Early Triassic)	Porphyry-related skarn (oxidized)	Prograde: garnet, retrograde: quartz, epidote, chlorite, calcite	Chalcopyrite, magnetite, pyrite	No data	Zaw *et al.* (2007)
10	Ban Bothong (Cu-Au) (Prospect)	15°18'17.85"N, 100°36'11.83"E		Ar-Ar amphibole age 187±2Ma	Porphyry-related skarn (oxidized)	Prograde: garnet, retrograde: quartz, epidote, chlorite, calcite	Chalcopyrite, magnetite, pyrite	No data	Zaw *et al.* (2007)

11	Khao Phra Ngam (Cu) (Prospect)	14°53'49.18"N, 100°37'40.79"E	Limestone, siliciclastics (Permian?)	Granodiorite/ U-Pb zircon 208±10Ma (Late Triassic)	Porphyry-related skarn (oxidized)	Prograde: garnet, retrograde: quartz, epidote, chlorite, calcite	Chalcopyrite, magnetite, pyrite	No data	Zaw *et al.* (2007)
12	French Mine (Prospect)	13°57'24.48"N, 101°50'1.33"E	Volcaniclastics and interbedded limestone (Lower Permian)	Granodiorite/ U-Pb zircon 203±8Ma (Late Triassic)	Porphyry-related skarn (oxidized)	Prograde: garnet, pyroxene, wollastonite, albite, biotite; retrograde: quartz, epidote, chlorite, calcite, sericite, illite	Chalcopyrite, pyrite, sphalerite, minor molybdenite	No data	Müller (1999)
13	Bo Thong (Mine)	13°22'47.90"N, 101°41'16.00"E	intermediate to felsic volcanic-sedimentary rocks	syenite, basalt porphyry dykes/260.8±2.6 Ma and 254.2±2.3 Ma (Late Permian)	Low-sulfidation epithermal	Silicic: quartz-illite-(Fe, Mg) chlorite-pyrite; phyllic: quartz-illite; propyritic: Fe chlorite-calcite-epidote; argillic: kaolinite-montmorillonite	Pyrite, arsenopyrite, galena, sphalerite and chalcopyrite	No data	Paipana (2014)

3.2 Metallogenic characteristics

The distribution of hydrothermal deposits in the belt appears to be associated with granitic intrusive rocks, which are characterized by vein type Au deposits, skarns and porphyry-type base metal deposits (Cobbing, 2011).

The Phu Lon skarn deposit had a resource of 5.4Mt at 2.4% Cu and 0.64 g/t Au which is hosted in Devonian volcano-sedimentary units and limestone (Kamvong & Zaw, 2009). The volcaniclastic units yielded Late Devonian ages 359 ± 6 Ma from U-Pb dating on zircon (Zaw *et al.*, 2009) which were intruded by plutons of oxidized, calc-alkaline quartz monzonite and diorite-monzodiorite (granodiorite porphyry) (Kamvong & Zaw, 2009). U-Pb and $^{40}Ar/^{39}Ar$ dating yielded Early Triassic ages 244 ± 4 Ma on zircon and 108-187 Ma on alkali-feldspar, respectively (Kamvong & Zaw, 2005). The presence of primary magnetite and titanite indicates that the plutons associated with mineralization are derived from oxidized magmas (Kamvong & Zaw, 2009).

Zaw *et al.* (2007a, 2009) described that the Phuthep deposits (PUT1 and PUT2) are skarn Fe-Cu (+Au) deposits which occur in fractures as veins, typically centered on at least two dioritic to granodiritic intrusions which emplaced into Carboniferous sedimentary rocks (Wang Saphung Formation) including siltstone, limestone and sandstone. The Puthep deposit (PUT1) or Phu Hin Lek Fia deposit is associated with an intrusion which yielded 242.4±1.3 Ma by U-Pb dating on zircon, and 248±2 and 247±6 Ma by $^{40}Ar/^{39}Ar$ dating on biotite (Zaw *et al.*, 2009). The Re-Os dating on molybdenite yielded 245±0.9 Ma (Kamvong *et al.*, 2014), indicating the mineralization and intrusion occurred during 248-242 Ma. The overprinted intrusions yielded younger $^{40}Ar/^{39}Ar$ ages on K-feldspar 164±0.6 Ma (Zaw *et al.,* 2014). Kamvong *et al*. (2014) reported chloritization of hornblende and sericitization of plagioclase, which may be related to skarn mineralization at PUT1 stock. Ores include both oxides (magnetite) and sulfides.

The Phu Thong Dieng deposit (PUT2) is associated with intrusions that yielded Early to Middle Triassic ages 235-233 Ma by U-Pb age on zircon (Zaw *et al.,* 2014). The Phu Thong Dieng deposit is represented by earlier phyllic alteration consisting of sericite and chlorite, replacing respectively feldspar and mafic minerals such as biotite in the host igneous rock, followed by retrograde quartz-carbonate ± epidote assemblages (Khositanont, 2008). In contrast to the Phuthep deposit, early prograde skarn minerals such as garnet and pyroxene are rarely found in the Phu Thong Dieng deposit (Crow & Zaw, 2011).

The Phu Thap Fah skarn Au deposit is hosted by a Permian sedimentary sequence consisting of shale, crystalline limestone, muddy sandstone, carbonaceous siltstone and shale, intruded by Early Triassic granodiorite (245 ± 3 Ma by U-Pb zircon age; Zaw *et al.,* 2014) and Late Triassic andesitic dyke cross-cut the mineralized skarn zone, suggesting that skarn formation and gold mineralization probably occurred during the Middle to Early Triassic (Rodmanee, 2000; Zaw *et al.,* 2007b). The deposit contains gold reserves of 0.41 Mt at 3.54 g/t Au and 0.75 Mt at 7.97 g/t Au (Zaw *et al.,* 2007b). The $^{40}Ar/^{39}Ar$ ages of biotite and amphibole in the mineralized intrusions are 111 and 153 Ma, respectively (Zaw *et al.,* 2014). The skarn mineralogy of early andraditic granet-clinopyroxene skarn was followed by retrograde alteration and mineralization (Zaw *et al.,* 2007b, 2008). The retrograde skarn assemblages consist of calcic amphibole (*e.g.*, hornblende, tremolite and actinolite), epidote, chlorite, carbonate and quartz (Zaw *et al.,* 2007b, 2008). Gold occurs as electrum, gold-bismuth and gold-bismuth-telluride associations and the greater part of the gold is confined to the massive pyrrhotite and pyrite ore with chalcopyrite in the retrograde zone (Zaw, 2007b; Rodmanee, 2000).

The Singto skarn Fe-Cu deposit is hosted by Permian limestone and siliciclastic rocks, intruded by diorite at 209 ± 9 Ma, 213± 10 Ma by U-Pb dating on zircon (Zaw *et al.*, 2014).

The Chatree epithermal deposit is located in the central portion of Loei Fold Belt which is underlain by a Paleozoic basement that is largely obscured by a wide belt of weakly deformed mostly Triassic volcanic rocks and sediments (Salam, 2008). The mineralization occured around the Permian-Triassic boundary dated as 250 Ma on the basis of U-Pb dating on zircon by Salam (2008). The Cu-Mo mineralization was discovered at the N prospect of the central part of the Chatree deposit (Tangwattananukul *et al.,* 2017). The granodiorite porphyry related to the mineralization was dated as 243 ± 5 Ma by U-Pb method on zircon (Salam *et al.,* 2013).

The Khao Lek skarn Fe-Cu deposit is located in Nong Bua district, Nakorn Sawan province. The deposit is hosted by Permian limestone and siliciclastic rocks which were intruded by granitoids dated as 254 ± 10 Ma, 249 ± 5 Ma, and 241 ± 5 Ma (Zaw *et al.,* 2014).

The Ban Bothong skarn Cu-Au deposit yielded a laser ablation $^{40}Ar/^{39}Ar$ age of Early Jurassic 187 ± 2 Ma on amphibole (Zaw *et al.,* 2007a, 2009).

The Khao Phra Ngam skarn Cu deposit is hosted by Permian limestone and siliciclastic rocks, which were intruded by a granodiorite dated as 208± 10 Ma by U-Pb method on zircon (Zaw *et al.,* 2007a).

The French Mine skarn Cu-Au deposit in the eastern part of the belt is hosted by Early Triassic vocano-sedimentary units of the Ratburi Group dated as 247 ± 6 Ma from U-Pb method on zircon, which were intruded by Late Triassic diorite at 203 ± 8 Ma from U-Pb dating on zircon (Müller, 1999). This deposit is high grade deposit with 16.8 g/t Au (Müller, 1999).

The Bo Thong deposit in Chachoensao province in the southern part of Loei Fold Belt, consists of Sb-bearing fluorite-quartz-sulfide veins hosted by intermediate to felsic volcanic-sedimentary rocks which were intruded by a syenite intrusion and basalt porphyry dykes which yielded the age 260.8±2.6 Ma and 254.2±2.3 Ma (Late Permian), respectively (Paipana, 2014).

The mineralization is characterized by fracture filling hydrothermal veins associated with breccias (Paipana, 2014). The major mineralization stages are characterized by quartz and sulfide minerals. Stages 2 and 3 consist of pyrite, arsenopyrite, galena, sphalerite and chalcopyrite. Gold, antimony, fluorite, stibnite, quartz, pyrite occurred in stage 4 that is associated with silicic alteration (Paipana, 2014).

3.3 Magmatism and metallogenic epochs

This section is the summary of the geochronological data from previous studies to constrain the magmatism in relation to metallogenic epochs along the Loei Fold Belt. A time-space evolution of the volcanic-magmatic history associated with mineralization along the Loei Fold Belt diagrammatically shows that two major mineralized epochs at Early Triassic in Figure 3.2.

The **Late Devonian** volcanism was recorded from a 359±6 Ma old volcaniclastic host rock hosting the Phu Lon Cu-Au skarn deposit, northern Loei (Zaw *et al.,* 2009). Intasopa (1993) indicated that the Devonian volcano-sedimentary sequence in the Loei district consists of sandstone, tuffaceous shale, chert, and conglomerate. The **Caboniferous** magmatism along the Loei Fold Belt was recorded from a 323 ± 5 Ma age rhyolite breccia near the Chatree epithermal Au deposit, a 321 ± 5 Ma aged rhyolite at the Wang Yai prospect, and a 327 ± 7 Ma on detrital zircon of sandstone from Wang Pong (Zaw *et al.,* 2007b). The intrusion ages were recorded from 310 ± 8 Ma and 314 ± 11 Ma granitoids at Dong Kui, near the Chatree epithermal Au deposit (Zaw *et al.,* 2007b). An **Early Permian** sandstone has detrital zircons of 331 ± 33 Ma (Zaw *et al.,* 2007b). These data suggested that oceanic to continental magmatism occured along the margin of the Loei Fold Belt in Early Carboniferous. **Late Permian** volcanism at 250 ± 6 Ma was recorded on feldspar-phyric andesite at the LD prospect and 258 ± 3 Ma old feldspar phyric flow-banded

rhyolite at Ko Chang Island where old feldspar phyric flow-banded rhyolite was recorded (Zaw *et al.,* 2007b). The intrusion ages were recorded from 261 ± 3 Ma and 254 ± 2 Ma on hornblende syenite and basalt porphyry dykes, respectively in Bo Thong (Paipana, 2014). Magmatism continued throughout the **Early Triassic** as an 233 ± 5 Ma andesite at southeast of Loei (Zaw *et al.,* 2007b). Intasopa (1999) also recorded 242 ± 3 Ma and 235 ± 4 Ma by Ar/Ar dating on hornblende, and 238 ± 1 Ma by Ar-Ar dating on K-feldspar in felsic to intermediate volcanic rocks in the Petchabun district. The felsic to intermediate magmatism was associated with mineralized events along the Loei Fold Belt in the beginning of Triassic. The mineralized event is characterized by intrusions ages, 242 ± 6 Ma to 236 ± 5 Ma at Phu Thep (PUT1) (Zaw *et al.*, 2009), 235 ± 3 Ma and 233 ± 4 Ma at Phu Thep (PUT2) (Zaw *et al.,* 2014), 244 ± 4 Ma at Phu Lon (Zaw *et al.,* 2009), 245 ± 3 Ma at Phu Thap Fah (Zaw *et al.,* 2014). These are highly mineralized Cu-Au skarn systems. The mineralization age in Phu Thep (PUT1) is 246 ± 1 Ma by Re/Os dating on molybdenite in diorite (Zaw *et al.*, 2009). This Early Triassic magmatic episode was followed by intrusions of abundant mafic to intermediated dykes, 244 ± 7 Ma, 238 ± 6 Ma, 243 ± 5 Ma, 238 ± 5 Ma (Salam, 2013) at 'N' porphyry at Chatree. The age of the 'N' porphyry intrusion was confirmed by a 244 ± 1 Ma by Re/Os dating on molybdenite (Salam, 2013). The felsic/diorite were continued to have emplaced in the Loei Fold Belt during Late Triassic to Early Jurrasic. This emplacement occurred along mineralized skarn Cu ± Au systems *e.g.,* French Mine, Singto, Khao Lek and Khao Phra Ngam.

Overall results demonstrated that the volcanic and intrusive rocks associated with most of the dozens of medium-sized ore deposits along the Loei Fold belt formed in the Late Permian-Early Triassic.

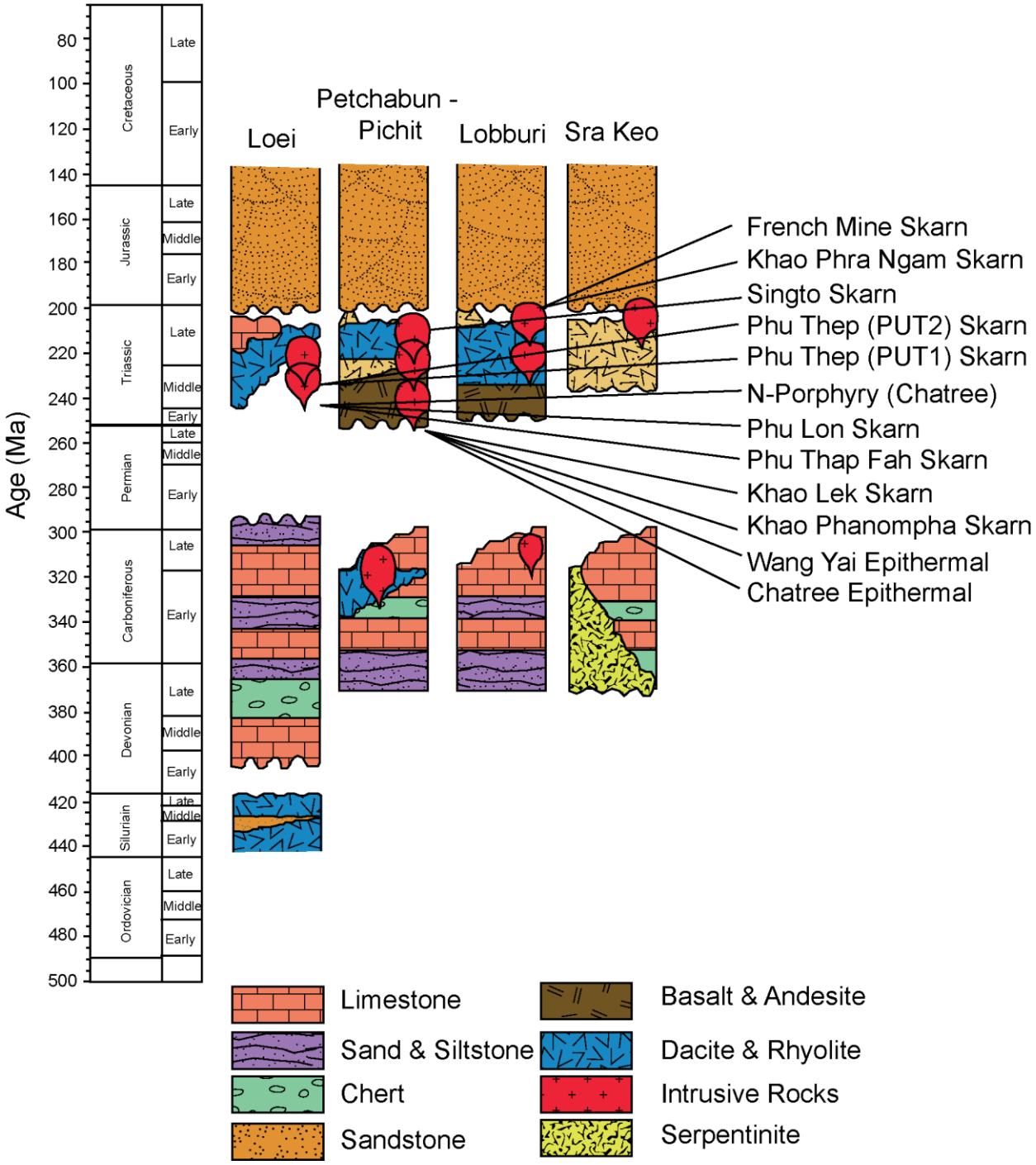

Fig. 3.2 Time-space plot showing stratigraphic columns of volcano-sedimentary sequences of Loei, Phetchabun, Lobburi and Sa Kaeo, and associated mineralized epochs. Modified from Zaw *et al.* (2009).

CHAPTER 4
MAGNETIC SUSCEPTIBILTY, PETROGRAPHY AND WHOLE-ROCK GEOCHEMISTRY

This chapter consists of three sections: (1) magnetic susceptibility (2) petrography and (3) geochemical characteristics of the granitoids from five areas along the Loei Fold Belt.

4.1. Magnetic Susceptibility

4.1.1. Introduction

The magnetic susceptibility of granitoids has been successfully used in previous studies as a crude petrographic index to distinguish between magnetite-series and ilmenite-series granitoids (Ishihaha, 1977; Takahashi *et al.,* 1980; Ishihara *et al.,* 2000). The main source of the magnetic susceptibility in magnetite-series granitoid is titanomagnetite and in ilmenite-series granitoid is ferromagnesian silicates and ilmenite, repectively. The magnitude of the magnetic susceptibility primarily reflects the abundance, nature and chemical composition of constituting minerals.

4.1.2. Analytical Method

The magnetic susceptibility of the granitoids was measured on site and inside the laboratory using Terraplus KT-10 and SM30-ZH instruments magnetic susceptibility meters (Fig. 4.1).

Fig. 4.1 Measurement of magnetic susceptibility of granitoids using SM30 magnetic susceptibility meter.

4.1.3. Result

Magnetic susceptibility of the granitoids from five areas along Loei Fold Belt (Table 4.1, Fig. 4.1) were studied to constrain their genesis. The magnetic susceptibility of the granitoids varies between 0.03 × 10^{-3} and 34.6 × 10^{-3} in SI unit. The magnetic susceptibility values of granitoids at Muang Loei range from 6.5×10^{-3} to 15.2×10^{-3} in SI unit, Phu Thap Fah - Phuthep 0.1×10^{-3} to 29.4×10^{-3} in SI unit, Petchabun from 2.7×10^{-3} to 34.6×10^{-3}in SI unit, Nakon Sawan - Lobburi from 2.4 to 14.1×10^{-3} in SI unit and Rayong – Chantaburi from 0.03×10^{-3} to 2.8×10^{-3} in SI unit.

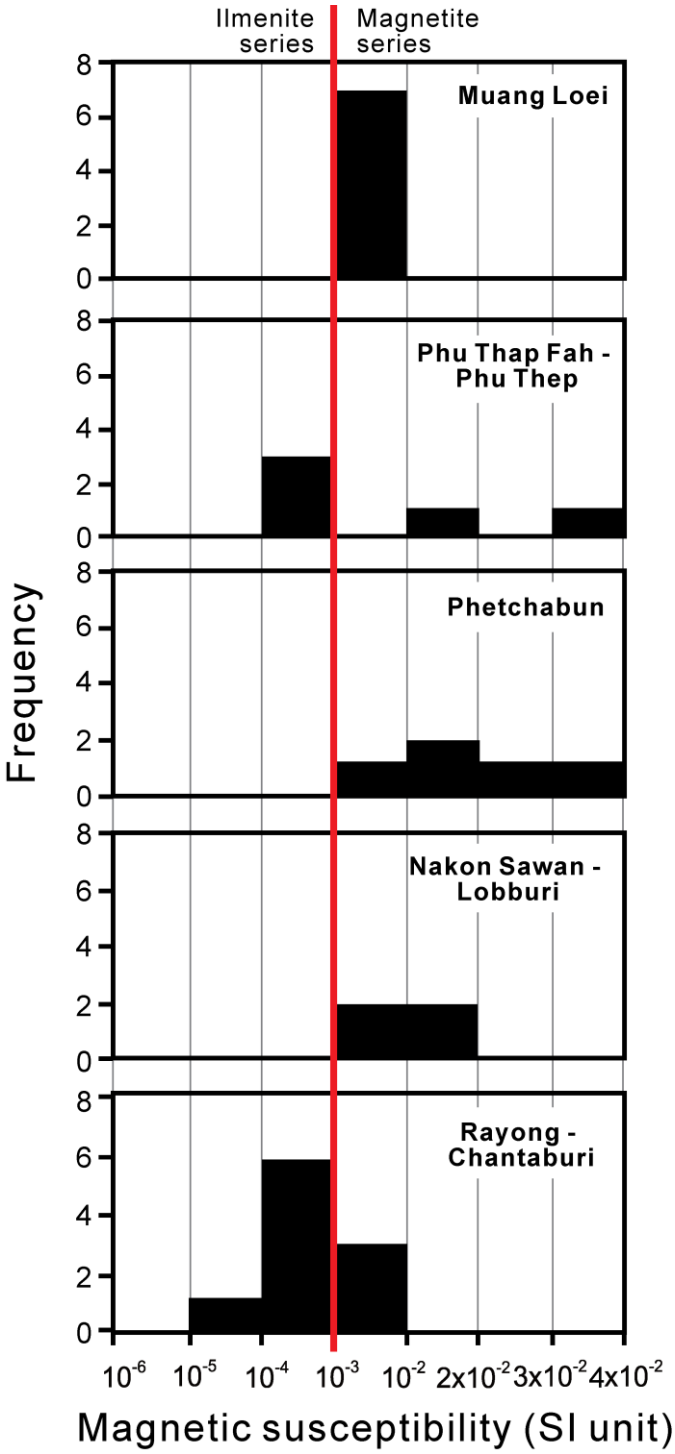

Fig. 4.2 Histogram of magnetic susceptibility of granitoids in five areas along Loei Fold Belt. A = Muang Loei granitoids, B = Phu Tap Fah – PUT granitoids, C = Phetchabun granitoids, D = Nakon Sawan – Lobburi granitoids, E = Rayong – Chantaburi Granitoids.

Table 4.1 The magnetite-series and ilmenite-granitoids of the Loei Fold Belt by number of magnetic susceptibility measurement.

Area (number of analysis)	Magnetite-series	Ilmenite-series	Mineralization	Deposit
Muang Loei				
Muang Loei (n=5)	4	0	None	
Chiang Khan (n=3)	3	0	None	
Whole area (n=7)	7 (100%)	0		
Phu Thap Fah-Phu Thep				
Wang Saphung (n=4)	2	2	Au	Phu Thap Fah
Muang Loei (n=3)	0	1	Cu	Phu Thep
Whole area (n=5)	2 (40%)	3 (60%)		
Phetchabun				
Chon Dan (n=4)	4	0	Au, Ag, Fe, Cu	Chatree, Singto
Wang Pong (n=1)	1	0	Au, Ag	Wang Yai
Whole area (n=5)	5 (100%)	0		
Nakon Sawan-Lobburi				
Nong Bua (n=2)	2	0	Fe, Cu	Khao Lek
Chon Dan (n=1)	1	0	Fe, Cu	Khao Lek
Khao Wong Phra Jun (n=1)	1	0	Cu	Khao Phra Ngam
Whole area (n=4)	4 (100%)	0		
Rayong-Chantaburi				
Makham (n=3)	0	1	None	
Phanom Sarakham(n=2)	0	2	None	
Bo Thong (n=3)	3	0	Sb, Au	Bo Thong
Khao Chamao (n=2)	0	2	None	
Muang Rayong (n=1)	0	1	None	
Si Mahosod (n=1)	0	1	None	
Whole area (n=10)	3 (30%)	7 (70%)		

4.2. Petrography

4.2.1. Introduction

Mineral content, chemical composition and texture are, together with shape and size of mineral constituents, measured by using petrographic analysis on thin-sections. The thin-sections also used for point counting for granitoids classification.

4.2.2. Analytical Method

Thin-sections and polish sections were observed for petrographic analysis under a Nikon polarization optic microscope (Fig. 4.3A). Preparation procedure of thin section and polish section are shown as follows;

Preparation procedure of thin sections

(1) Cutting hand specimen into the size of the thin section slide glass.

(2) Polishing one side of the rock chip from step (1), using the polishing powders of #120, #120, #320, #800 and #1000

(3) Drying rock chips for 1 night.

(4) Attaching the rock chips on the thin section glass using glue (E-bond) and leave it for 1 night until dry.

(5) Cutting the rock chips attached on the glass using secondary cutting machine.

(6) Making the thin sections thinner by using Preparap machine.

(7) Polishing the thin section after step (6) using polishing powder of #800.

(8) Continuing polish with the powders of #1000 until proper thickness. For example, quartz grain from yellow to grey color under crossed polars.

(9) Following polish with powders of #2000, #3000, 3µm, and 1µm.

Preparation procedure of polish sections

(1) Cutting the hand specimen part into 1cm×1cm size.

(2) Preparing molds (white/yellow) and clean them with ethanol.

(3) Mixing resin and curing agent with the ratio of 100:2

(4) Pouring the resin into the molds (10% of mold) and putting the sample inside the molds.

(5) Pouring more resin until covering the sample (90% of mold) and putting inside the vacuum machine with the 5 minutes setting.

(6) After finish from vacuuming, leaving it dry for 1 night.

(7) Removing the sample from the mold and clean them.

(8) Polishing with powder of #120, #320, #800, #1000, #2000, #3000, 3µm, and 1µm.

Performing point counting on a petrographic thin section, requires observations to be made at regular position on the sample as grid intersections. At each position, we decided to which mineral the respective grid point and its local neighborhood belong. By counting the number of points found for each mineral by using X-Y Stage Micro Topper (Fig. 4.3B), it is possible to calculate the percentage that these values represent overall the counted points. These percentages represent the relative proportions of the minerals in the sample. For quantitative examinations concerning the statically correct number of count required the image to be manipulated with the points between 1,500 and 5,000. This value is established before starting the counting procedure, based on the size (area) or each mineral phase present in the sample.

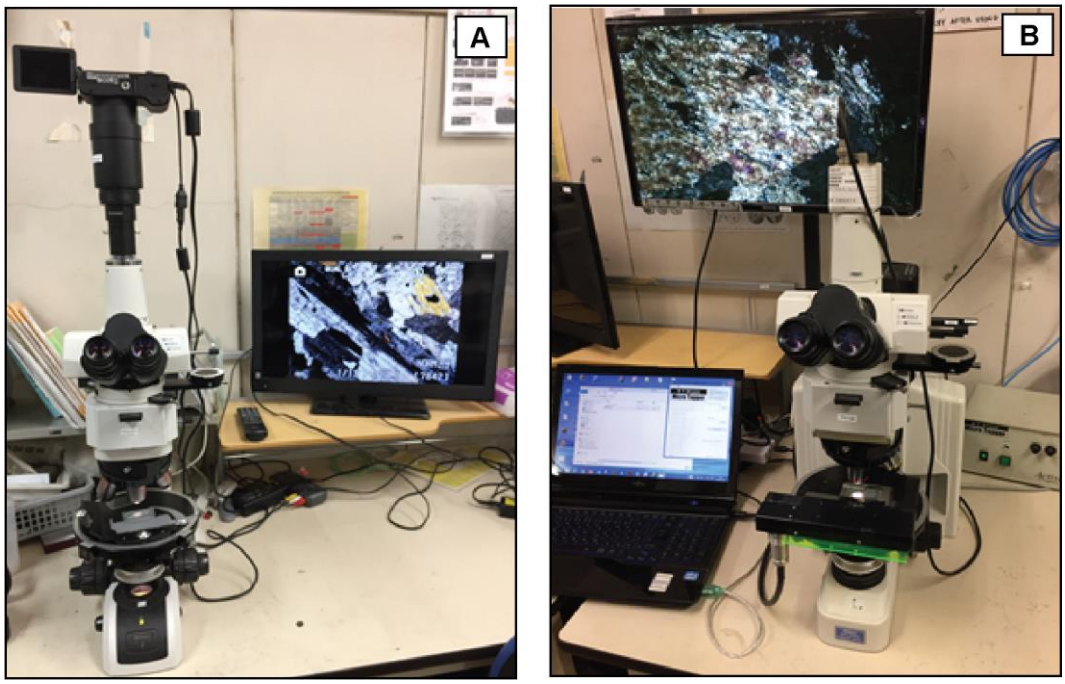

Fig. 4.3 A. a Nikon polarization optic microscope, B. X-Y Stage Micro Topper microscope.

4.2.3. Result

Modal analysis of petrographic thin section provided the relative quantity of rock forming minerals. Based on modal abundances of quartz, alkali feldspar, and plagioclase (Streckeisen, 1973; 1976), granitoids along Loei Fold Belt are classified into four main rock types i.e.,

monzogranite, granodiorite, tonalite and quartz-monzodiorite (Fig. 4.4). In addition, quartz-rich granitoid and quartz-syenite are also present (Figs. 4.4, 4.10; Table 4.2).

4.2.3.1. Granitoids at Muang Loei

Granitoids in Muang Loei complex (ca. 450 km^2, Fig. 4.5) are classified into quartz-monzodiorite, granodiorite, tonalite and quartz-syenite. Intrusive relationship between the granodiorite and the quartz-syenite has been observed based on the presence of xenolith (Fig. 4.10b). It indicates that the older granodiorite was intruded by the quartz-syenite. There is no field evidence of intrusion relationships between the quartz-monzodiorite and the tonalite. The quartz-monzodiorite is generally fine to coarse-grained, consists mainly of plagioclase, K-feldspar, quartz and hornblende with accessory biotite, magnetite, ilmenite, titanite and apatite. The abundance of hornblende and biotite of the coarse-grained quartz monzodiorite is higher than the fine-grained monzodiorite. The granodiorite is also fine to coarse-grained, composed mainly of plagioclase, K-feldspar, quartz, hornblende and biotite with accessory magnetite, ilmenite, titanite and apatite. Mafic minerals are commonly replaced by greenish fine-grained chlorite. The tonalite is fine-grained and relatively equigranular. In comparison with the other rocks in this area, color index of the tonalite is higher. It is composed of plagioclase, K-feldspar, quartz, hornblende and biotite with trace amount of clinopyroxene and accessory magnetite, ilmenite, titanite and apatite. The quartz-syenite is coarse-grained and consists of megacrystic K-feldspar, plagioclase, quartz, biotite and hornblende with accessory magnetite and ilmenite.

Granitoids from the Mung Loei are mostly tonalite, monzodiorite and granodiorite (Table 4.3, Fig. 4.4) and more dispersed within four fields of Streckeisen's diagram (Fig. 4.4). Hornblende-rich granodiorites (Gr19, Gr14) are common near the quartz-monzodiorite (Gr17, Gr15), but hornblende is rare in granodiorite (Gr12) situating further away from the quartz

monzonite (cf. Table 4.2, Fig. 4.5). Also, the granodiorites of Muang Loei include relatively much hornblende compared to other areas (Table 4.3).

Table 4.2 Modal compositions of granitoids along Loei Fold Belt.

Unit/ Complex	Locality	Sample code	Rock Name	Magnetic Susceptibility × 10^{-3} (SI)	Plg	Kfs	Qz	Cpx	Hbl	Bt	Ms	Mt	Ilm	Ttn	Apt	Zr	Gar	Rut	Aln
Muang Loei Granitoids	Muang Loei	Gr10	Biotite quartz-syenite	7.9	22.7	57.6	10.2		1.4	6.8		0.9	0.4						
	Muang Loei	Gr11	Biotite tonalite	9.0	40.8	1.6	39.3		<0.1	17.0		1.0	0.2						
	Muang Loei	Gr12	Biotite granodiorite	6.3	26.6	35.9	33.7			2.4		0.6	0.6					<0.1	
	Muang Loei	Gr14	Hornblende granodiorite	0.4*	50.9	20.8	19.2		8.3	0.1		0.1	0.1	0.6					
	Muang Loei	Gr15	Hornblende quartz-monzodiorite	11.1	52.5	19.4	14.6		11.7			1.1	0.6		0.1				
	Chiang Khan	Gr17	Biotite tonalite	15.2	55.3	3.4	24.7	<0.1	6.0	7.9		1.5	1.1		<0.1				
	Chiang Khan	Gr18	Hornblende quartz-monzodiorite	6.5	52.5	25.5	5.3		13.3	1.6		0.7	0.5	0.6					
	Chiang Khan	Gr19	Hornblende granodiorite	9.4	49.4	5.5	19.9		17.0	6.6		1.1	0.4	0.1	0.1				
Phu Tap Fah - Phu Thep Granitoids	Wang Saphung	Gr7	Hornblende tonalite	0.2	51.3	2.1	33.2		10.6	0.6		0.2	0.1		0.4		1.7		
	Wang Saphung	Gr8	Hornblende tonalite	0.1	61.6	1.8	20.7		15.4	0.2		0.1	<0.1	0.1	<0.1				
	Wang Saphung	Gr9	Biotite granodiorite	29.4	44.7	6.8	35.4		4.3	5.6		2.2	0.6		0.3	0.1			
	Wang Saphung	Gr21	Biotite tonalite	15.4	60.8	0.7	25.9		3.4	6.9		1.6	0.4		0.1				
	Muang Loei	Gr22	Hornblende quartz-monzodiorite	0.9*	57.6	14.2	16.6		10.6	0.8		0.1	0.2						
	Muang Loei	Gr23	Hornblende quartz-diorite	0.3	67.1	1.1	4.5		25.9	1.2		0.2	0.1						
	Muang Loei	Gr25	Hornblende granodiorite	0.1*	67.5	9.1	19.4		3.5	0.4		0.1	0.1	0.1					
Phetchabun Granitoids	Chon Dan	Gr26	Hornblende monzogranite	2.7	31.7	27.0	36.9		2.9	0.6		0.5	0.3		<0.1				
	Chon Dan	Gr30	Hornblende granodiorite	12.8	50.6	17.2	21.0		8.7	0.5		1.0	0.5		<0.1			0.2	
	Chon Dan	Gr35	Biotite tonalite	34.6	44.2	3.0	19.4		14.6	15.9		2.4	0.4						
	Chon Dan	Gr36	Hornblende quartz-monzodiorite	20.8	58.0	8.8	11.7		13.9	5.3		1.9	0.3		<0.1				
	Wang Pong	Gr37	Biotite quartz-monzodiorite	15.2	52.0	22.9	15.1		3.9	4.3		1.4	0.3						
Nakon Sawan - Lobburi Granitoids	Nong Bua	NDBI 2	Biotite quartz-rich granitoid	2.4	18.3	13.6	60.3		0.1	7.2		0.5	0.2						
	Nong Bua	NDBI1 (2)	Biotite monzogranite	6.8	25.2	25.8	44.4		0.3	3.3		0.6	0.2		0.1				
	Chon Dan	WP024	Biotite granodiorite	12.2	53.1	6.3	26.4		3.0	9.6		0.9	0.2	<0.1	0.2				
	Khok Samrong	Gr55	Hornblende quartz-monzodiorite	3.0*	48.6	6.3	4.3		39.7			0.1	0.1	0.3	0.7				
	Khao Wong Phra Jun	WPJ-DI	Hornblende quartz-monzodiorite	14.1	67.4	15.1	13.0		3.0	0.1		1.3			0.1				
Rayong - Chantaburi Granitoids	Makham	Gr42	Biotite monzogranite	0.0*	32.4	17.8	42.7			6.4		0.1	0.1		0.3				
	Makham	Gr43	Biotite granodiorite	0.1	44.5	5.7	21.5		6.5	21.2		0.2	0.1		0.2	0.2			
	Makham	Gr44	Biotite monzogranite	0.1*	46.1	28.1	20.4		2.4	2.5		0.1	0.1		0.2				
	Phanom Sarakam	Gr50	Biotite tonalite	0.1	49.0	5.2	24.8			20.5		0.1	<0.1	0.1	0.1				
	Phanom Sarakam	Gr53	Biotite monzogranite	0.1	23.4	35.7	32.7		0.3	7.7		0.1	0.1						
	Bo Thong	Gr47	Biotite monzogranite	1.0	21.9	25.1	43.9			8.4		0.2	0.1	0.1	0.1				
	Bo Thong	Gr48	Biotite granodiorite	2.8	43.6	15.1	30.1			9.6		0.4	0.1	1.1					
	Bo Thong	Gr49	Biotite monzogranite	1.6	33.1	24.0	39.0			3.2		0.1	0.1		<0.1	0.2		<0.1	<0.1
	Khao Chamao	Gr45	Biotite monzogranite	0.0	31.0	21.6	40.6		0.4	6.2		0.1	<0.1						
	Khao Chamao	Gr46	Biotite granodiorite	0.1	38.4	12.9	35.4			12.8		0.1	0.1	0.1		0.1			
	Muang Rayong	Gr39	Biotite monzogranite	0.2	31.2	33.0	24.4		0.8	10.2		0.1	0.1	<0.1	0.1				
	Si Mahosod	Gr51	Biotite granodiorite	0.1	48.7	20.2	24.5			4.7	1.2	0.1	0.1		0.4				
	Khlung	Gr41	Hornblende monzogranite	0.2*	27.1	19.4	28.3		14.7	9.6		0.4	0.2			0.2			

Abbreviations: Plg, plagioclase; Kfs, K-feldspar, Qz, quartz; Cpx, clinopyroxene; Hbl, hornblende; Bt, biotite; Mt, magnetite; Ilm, ilmenite; Ttn, titanite; Apt, apatite; Zr, zircon; Gar, garnet; Rut, rutile; Aln, allanite; Ms, muscovite. *, these magnetic susceptibility values were not use for granitoids series classification since the samples have been altered.

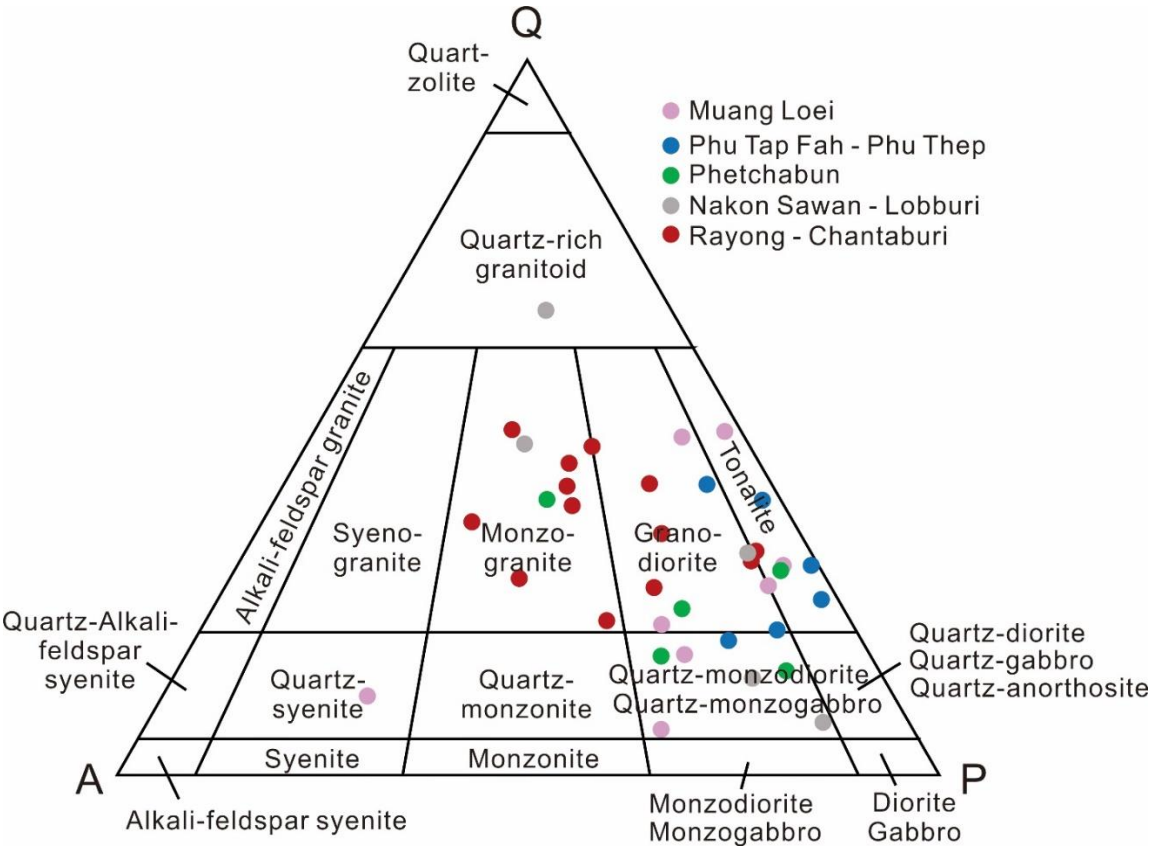

Fig. 4.4 Classification of granitoids from Muang Loei, Phu Tap Fah – Phu Thep, Phetchabun, Nakon Sawan – Lobburi, and Rayong – Chantaburi based on modal composition of quartz(Q), alkali feldspar(A) and plagioclase(P) (after Streckeisen, 1976).

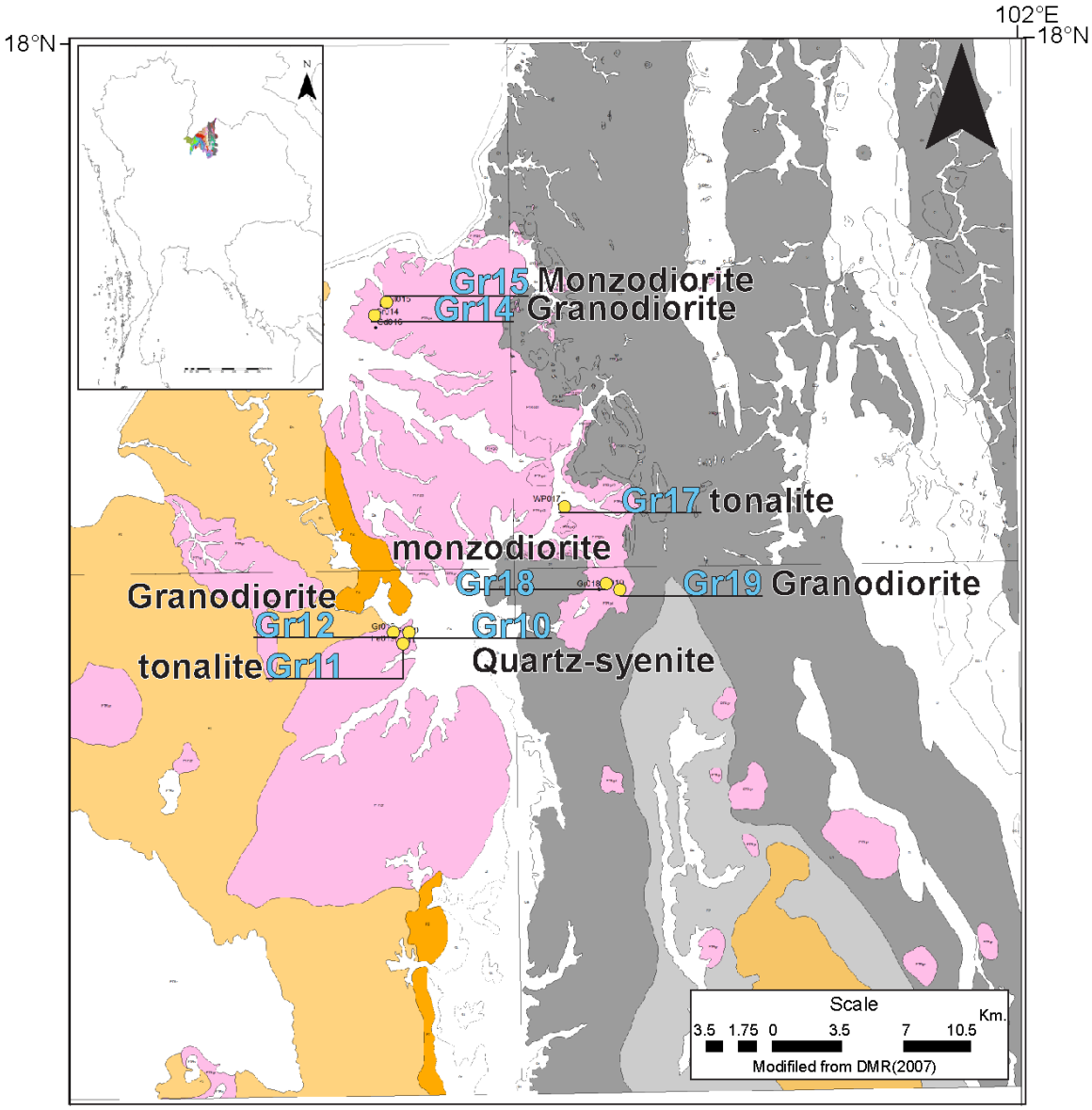

EXPLANATION

	SEDIMENTARY ROCKS	PERIOD	AGE(my)
P_3	Sandstone, siltstone and shale		
P_2	Shale, sandstone, limestone	PERMIAN	245-286
P_1	Limestone, sandstone, shale		
C_2	Shale and mudstone	CARBONIFEROUS	286-360
C_1	Conglomerate, sandstone, mudstone		
	IGNEOUS ROCKS		
PTr_{gr}	Granite, Quatz-monzonite, granodiorite	TRIASSIC	210-245

Fig. 4.5 Distribution of sedimentary rocks and granitoids in Muang Loei area.

4.2.3.2. Granitoids at Phu Thap Fah – Phu Thep (PUT)

Tonalite, granodiorite and quartz-monzodiorite are observed in Phu Tap Fah – Phu Thep granitoid complex (ca. 21 km^2, Fig. 4.6). They are generally medium to coarse-grained. Field observation indicates that the granodiorite intruded the siltstone and limestone (Fig. 4.10c). There is no observed field evidence of intrusion relationships among all granitoids in this area. The tonalite is coarse-grained and composed mainly of plagioclase, quartz, biotite and hornblende with rare K-feldspar and accessory magnetite, ilmenite, titanite and apatite. The granodiorite is composed of coarse-grained plagioclase, quartz, K-feldspar, hornblende and biotite with accessory magnetite, ilmenite, titanite, apatite, zircon and garnet (Fig. 4.11f). The fine-grained granodiorite is also observed as xenoliths within the tonalite. The quartz-monzodiorite is medium-grained, consisting of plagioclase, K-feldspar, quartz and hornblende with accessory biotite, magnetite and ilmenite.

Granitoids from the Phu Thap Fah – Phu Thep are mostly tonalite and granodiorite (Table 4.3, Fig. 4.6) and dispersed within three fields of Streckeisen's diagram (Fig. 4.4). Hornblende-rich tonalite (Gr07, Gr08) are common near the limestone unit (P3), but hornblende is rare in tonalite (Gr21) situating near the shale unit (C) (cf. Table 4.2, Fig. 4.6). Also, the quartz-diorite (Gr23) of Phu Thap Fah – Phu Thep include relatively much hornblende compared to other granitoids (Table 4.3).

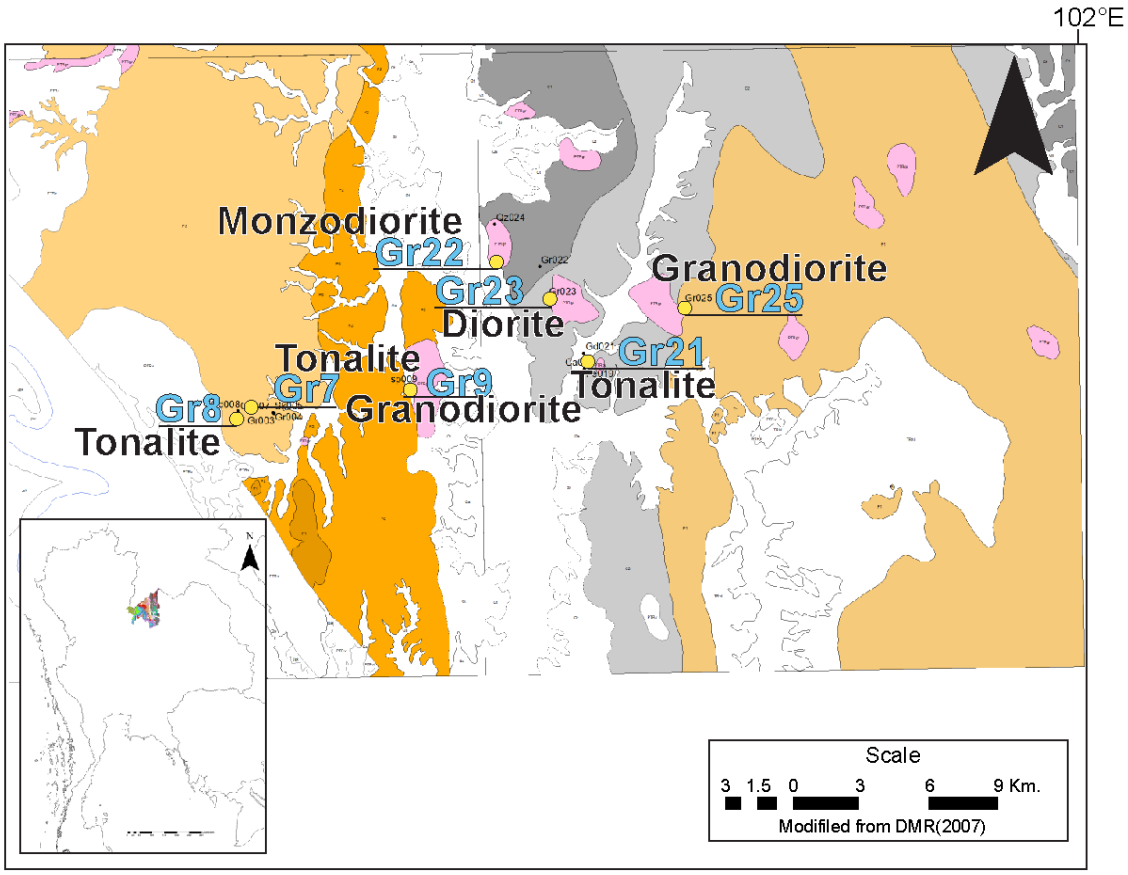

EXPLANATION

	SEDIMENTARY ROCKS	PERIOD	AGE(my)
P_3	Sandstone, siltstone and shale		
P_2	Shale, sandstone, limestone	PERMIAN	245-286
P_1	Limestone, sandstone, shale		
C_2	Shale and mudstone	CARBONIFEROUS	286-360
C_1	Conglomerate, sandstone, mudstone		
	IGNEOUS ROCKS		
PTr_{gr}	Granite, Quatz-monzonite, granodiorite	TRIASSIC	210-245

Fig. 4.6 Distribution of sedimentary rocks and granitoids in Phu Thap Fah – Phu Thep area.

4.2.3.3. Granitoids in Phetchabun

In the Phetchabun granitoid complex (ca. 100 km^2, Fig. 4.7), four rock types are present, quartz-monzodiorite, granodiorite, monzogranite and tonalite. They are generally coarse-grained. There is no observed field evidence of intrusion relationships among all granitoids in this area.

The quartz-monzodiorite is composed mainly of plagioclase, K-feldspar, quartz, hornblende and biotite with accessory magnetite, ilmenite and apatite. The granodiorite is composed mainly of plagioclase, K-feldspar, quartz, hornblende with accessory biotite, magnetite, ilmenite, apatite and rutile. The monzogranite is also composed mainly of plagioclase, K-feldspar, quartz, hornblende with accessory biotite, magnetite, ilmenite and apatite. The tonalite is also observed in this area, consisting of plagioclase, quartz, K-feldspar, hornblende and biotite with accessory magnetite and ilmenite.

Granitoids from the Phetchabun are mostly monzodiorite (Table 4.3, Fig. 4.7) and dispersed within four fields of Streckeisen's diagram (Fig. 4.4). Hornblende-rich monzodiorite (Gr36) are common near the tonalite (Gr35), but hornblende is rare in monzodiorite (Gr37) situating further away from the tonalite (cf. Table 4.2, Fig. 4.7). Also, the tonalite (Gr37) of Phetchabun include relatively much hornblende compared to other granitoids (Table 4.3).

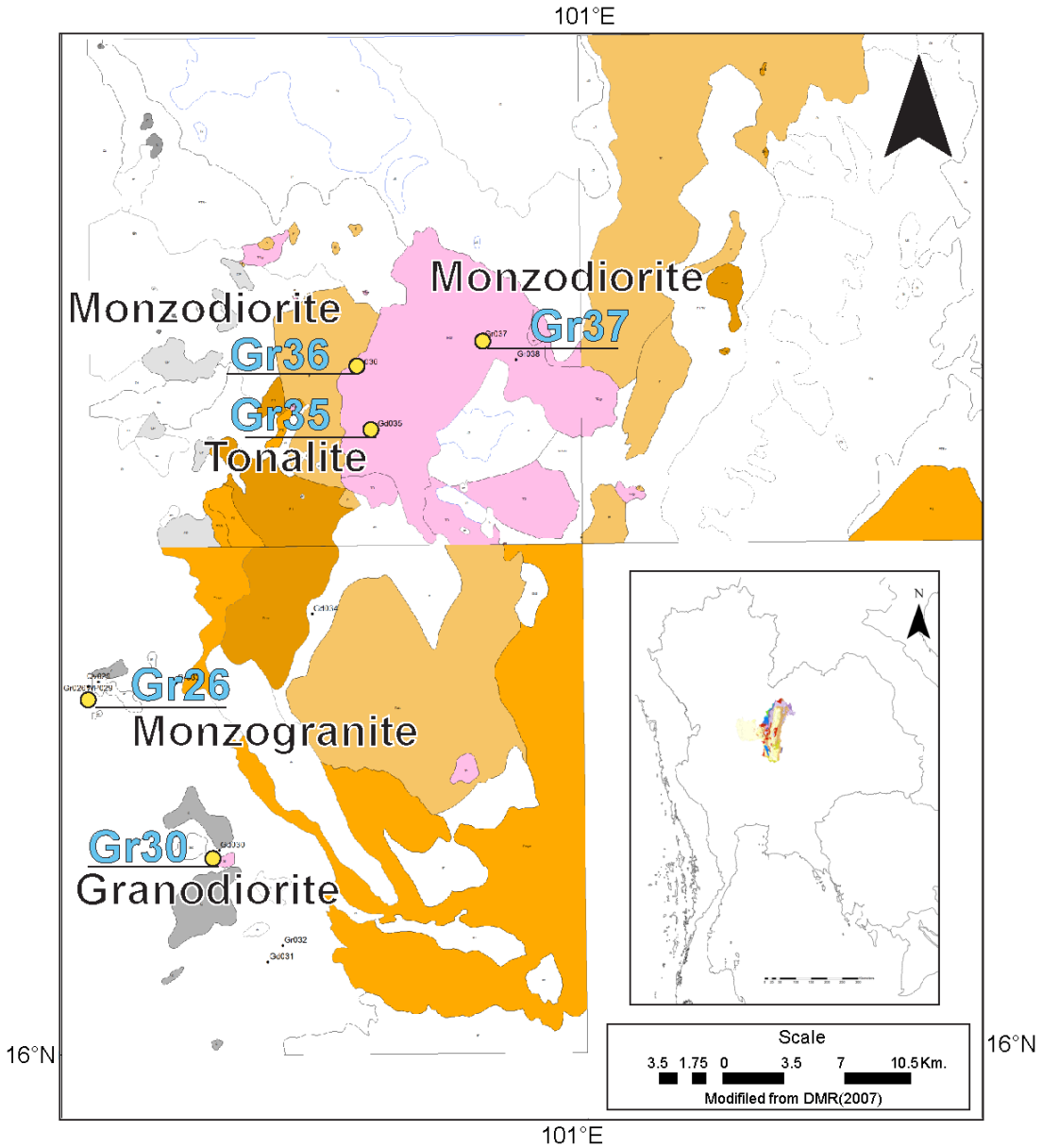

EXPLANATION

	SEDIMENTARY ROCKS	PERIOD	AGE(my)
P_3	Sandstone, siltstone and shale		
P_2	Shale, sandstone, limestone	PERMIAN	245-286
P_1	Limestone, sandstone, shale		
C_2	Shale and mudstone	CARBONIFEROUS	286-360
C_1	Conglomerate, sandstone, mudstone		
	IGNEOUS ROCKS		
PTr_{gr}	Granite, Quatz-monzonite, granodiorite	TRIASSIC	210-245

Fig. 4.7 Distribution of sedimentary rocks and granitoids in Phechabun area.

4.2.3.4.Granitoids in Nakon Sawan - Lobburi

Quartz-monzodiorite, granodiorite, monzogranite and quartz-rich granitoid are present in Nakon Sawan – Lobburi granitoid complex (ca. 87 km^2, Fig. 4.8). No field evidence of intrusion relationships is recognized among those different granitoids. They are medium to coarse-grained and some rocks such as quartz-rich granitoid and monzogranite show porphyritic texture. The coarse-grained quartz-monzodiorite is composed mainly of plagioclase, K-feldspar, quartz, and hornblende with accessory biotite, magnetite, ilmenite, titanite, and apatite. The granodiorite is also coarse-grained and composed of plagioclase, K-feldspar, quartz, hornblende and biotite with accessory magnetite, ilmenite, titanite and apatite. The porphyritic monzogranite is medium to coarse-grained, composed mainly of the phenocrysts of plagioclase, K-feldspar, quartz and biotite with accessory hornblende, magnetite, ilmenite and apatite in fine-grained groundmass mainly of plagioclase, K-feldspar and quartz. The porphyritic quartz-rich granitoid is also medium to coarse-grained and composed mainly of the phenocrysts of plagioclase, K-feldspar, quartz and biotite with less amount of hornblende, magnetite and ilmenite in fine-grained groundmass consisting mainly of plagioclase, K-feldspar, quartz and biotite.

Granitoids from the Nakon Sawan - Lobburi are mostly monzodiorite (Table 4.3, Fig. 4.8) and dispersed within three fields of Streckeisen's diagram (Fig. 4.4). Hornblende-rich monzodiorite (Gr55) are near the volcanic rock unit (PT_{rv}), but hornblende is rare in monzodiorite (WPJ-DI) situating further away the volcanic rock unit (PT_{rv}) (cf. Table 4.2, Fig. 4.8). Also, the monzodiorite (Gr55) of Nakon Sawan – Lobburi include relatively much hornblende compared to other areas (Table 4.3).

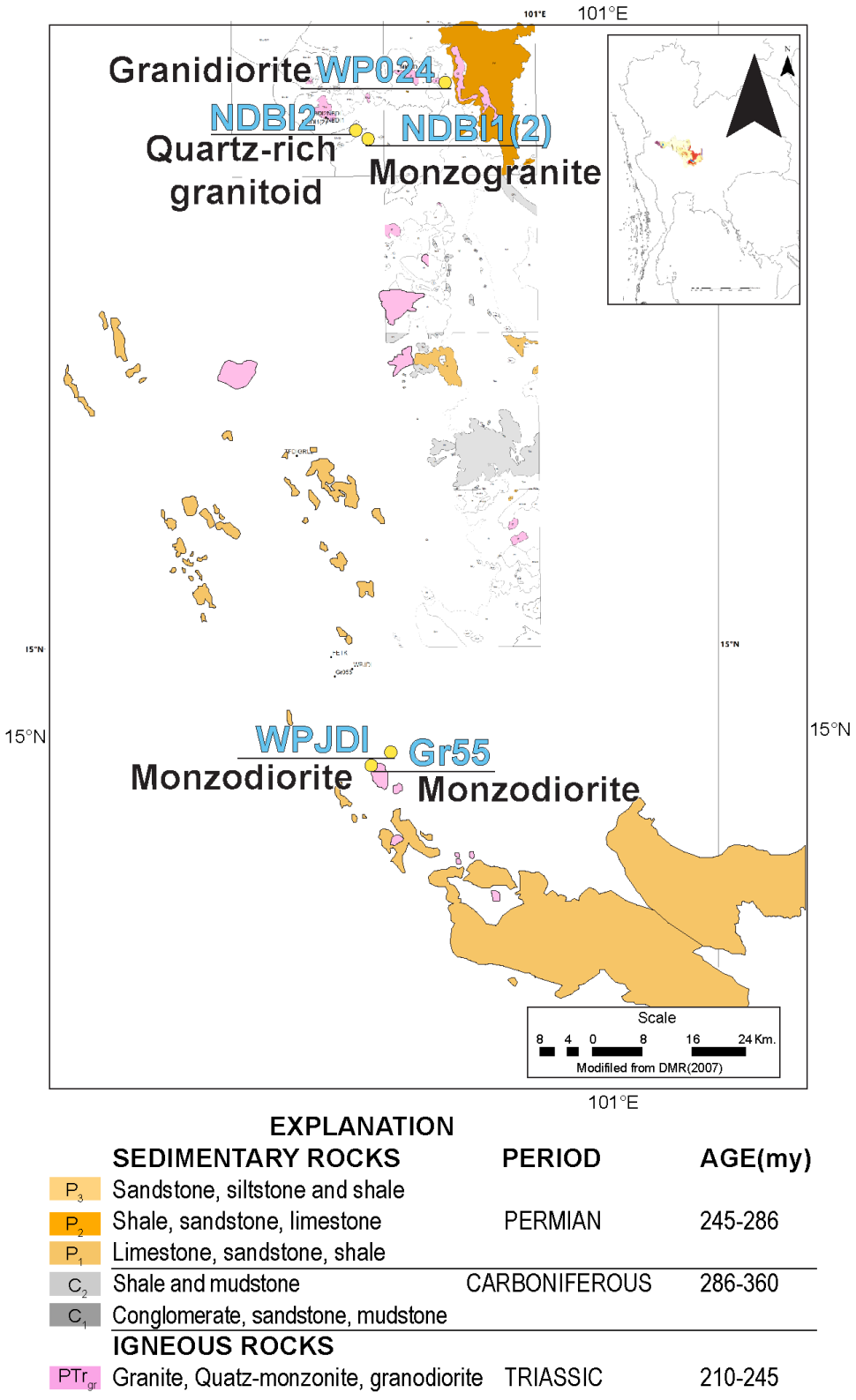

Fig. 4.8 Distribution of sedimentary rocks and granitoids in Nakon Sawan - Lobburi area.

4.2.3.5.Granitoids in Rayong - Chantaburi

Three rock types are identified in the Rayong – Chantaburi granitoid complex (ca. 1,600 km^2, Fig. 4.9) i.e., monzogranite, granodiorite and tonalite. The monzogranite is medium to coarse-grained and biotite is more abundant than hornblende. In general, it is composed mainly of plagioclase, K-feldspar, quartz, biotite and hornblende with accessory magnetite, ilmenite, titanite, apatite, zircon, rutile and allanite. A monzogranite sample shows porphyritic texture with plagioclase phenocrysts. The granodiorite is coarse-grained and composed mainly of plagioclase, quartz, K-feldspar, biotite and hornblende with accessory magnetite, ilmenite, titanite, apatite and zircon. The fine to coarse-grained tonalite is composed of plagioclase, quartz, K-feldspar and biotite with accessory titanite, apatite, magnetite and ilmenite.

Granitoids from the Rayong – Chantaburi are mostly monzogranite and granodiorite (Table 4.3, Fig. 4.9) and dispersed within two fields of Streckeisen's diagram (Fig. 4.4). Hornblende-rich monzogranite (Gr41) are situating further away from granodiorites, but hornblende is rare in monzogranite (Gr42, Gr47, 49) common near the granodiorites (cf. Table 4.2, Fig. 4.9). Also, the monzodiorite (Gr41) of Rayong – Chantaburi include relatively much hornblende compared to other areas (Table 4.3).

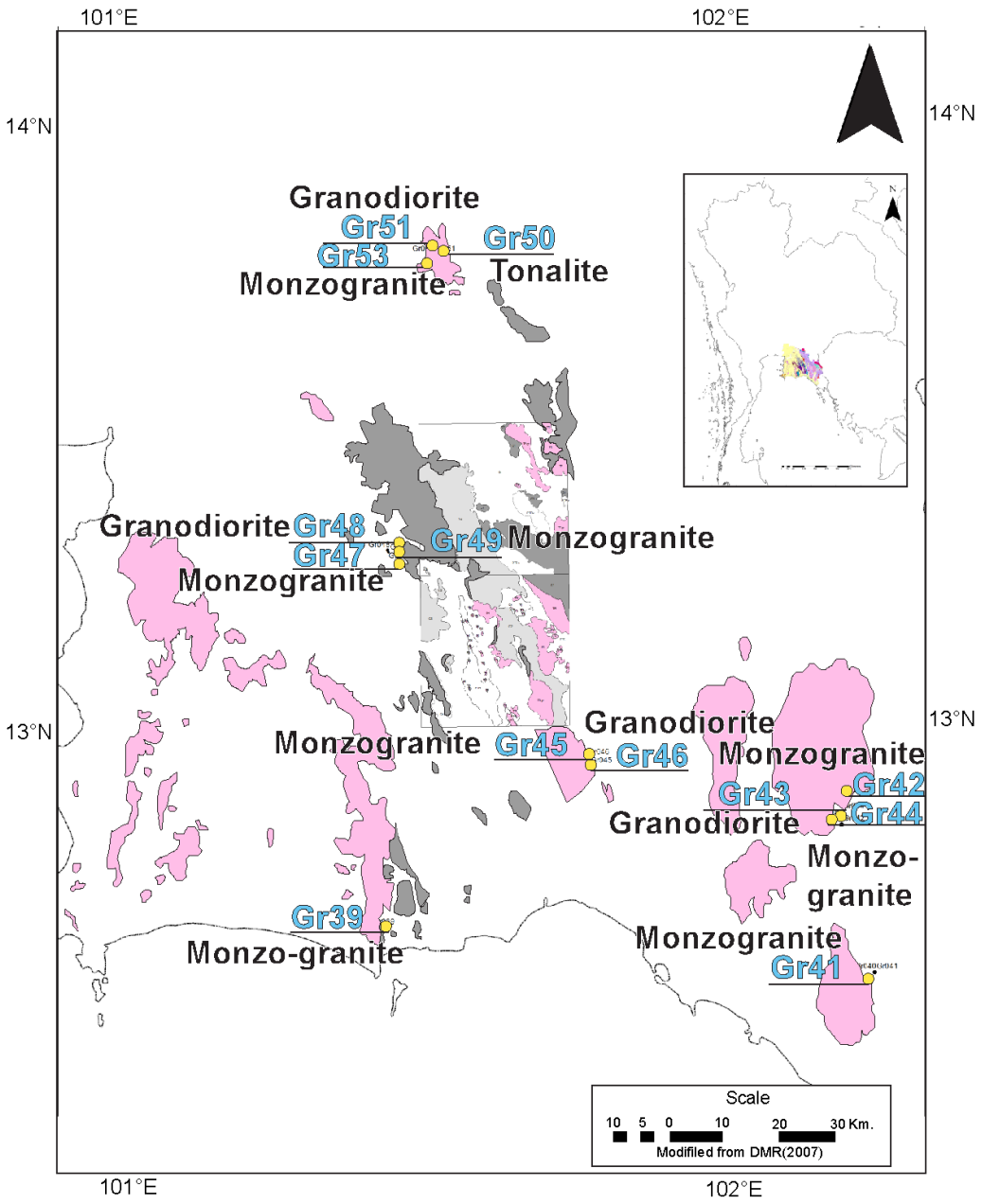

EXPLANATION

	SEDIMENTARY ROCKS	PERIOD	AGE(my)
P_3	Sandstone, siltstone and shale		
P_2	Shale, sandstone, limestone	PERMIAN	245-286
P_1	Limestone, sandstone, shale		
C_2	Shale and mudstone	CARBONIFEROUS	286-360
C_1	Conglomerate, sandstone, mudstone		
	IGNEOUS ROCKS		
PTr_{gr}	Granite, Quatz-monzonite, granodiorite	TRIASSIC	210-245

Fig. 4.9 Distribution of sedimentary rocks and granitoids in Rayong - Chantaburi area

Fig. 4.10 Outcrops and hand specimens of granitoids. A. Granodiorite outcrop in Muang Loei. B. Quartz syenite from Muang Loei with fine-grained granodiorite xenolith. C. Granodiorite sill outcrop in Phu Thap Fah – Phu Thep that intrudes Permian siliciclastic and limestone of Pha Dua Formation. D. Tonalite in Phu Thap Fah – Phu Thep, showing mafic rock inclusion. E. Granodiorite outcrop in Phetchabun. F. Weathered monzogranite from Petchabun. G. Quartz-monzodiorite outcrop in Nakon Sawan – Lobburi. H. Hand specimen of quartz-monzodiorite from Nakon Sawan – Lobburi. I. Granodiorite outcrop in Rayong – Chantaburi. J. Granodiorite in Rayong – Chantaburi, showing mafic rock inclusion.

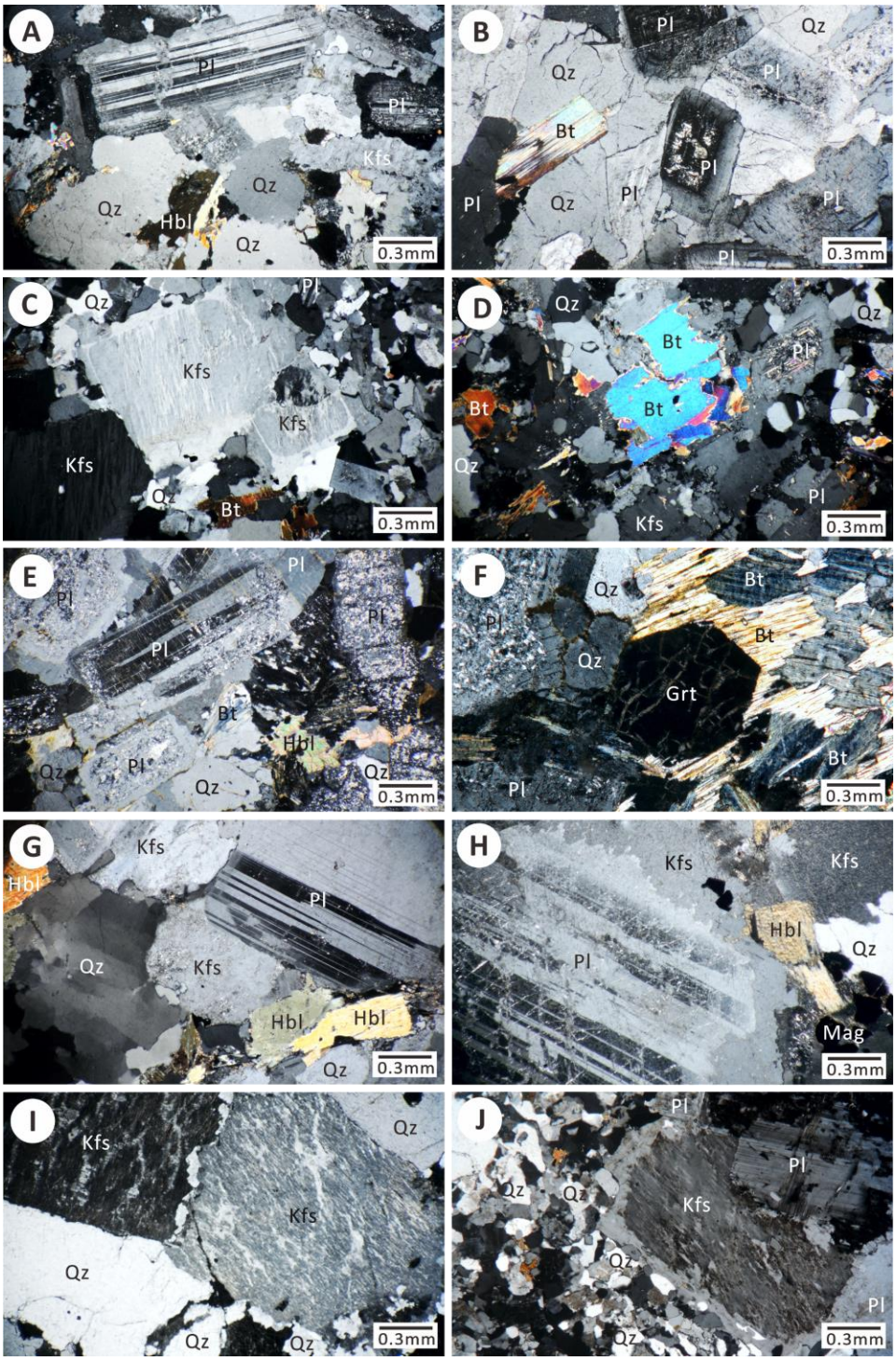

Fig. 4.11 Representative photomicrographs under cross-polarized light of the granitoids along Loei Fold Belt. A. Granodiorite from Muang Loei granitoids. B. Granodiorite from Phu Tap Fah – PUT granitoids, showing the presence of accessory magnetite. C. Monzogranite from Nakon Sawan – Lobburi granitoids. D. Monzogranite from Rayong – Chantaburi granitoids. E. Tonalite from Phu

Tap Fah – PUT granitoids. Most of the primary plagioclase is altered to sericite. F. Tonalite from Phu Tap Fah – PUT granitoids, showing the presence of accessory garnet. G. Quartz-monzodiorite from Nakon Sawan – Lobburi granitoids. H. Quartz-monzodiorite from Phetchabun granitoids. I. Quartz-syenite from Muang Loei granitoids. J. Quartz-rich granitoid from Nakon Sawan – Lobburi granitoids. Bt = biotite, Grt = garnet, Hbl = hornblende, Kfs = K-feldspar, Mag = magnetite, Pl = plagioclase, Qz = quartz.

4.3. Geochemical characteristics

4.3.1. Introduction

Determination of the major and trace element chemistry of whole rocks is the most widely used method to classify plutonic rocks, the relationship between individual intrusions and also to constrain the tectonic setting of the igneous rocks. Moreover, the chemical analysis of igneous rocks is a useful tool in distinguishing between samples of differing compositions and magmatic affinities.

4.3.2. Analytical Method

The granitoid samples collected for petrographic investigation for the deposit geology were also selected for whole-rock geochemistry analysis. Samples were first examined under the microscope and a representative sample that showed the least alteration was the chosen for analysis. All these samples were carefully screened for alteration and weathering in both hand sample and thin section examination then crushed by using a hammer before being placed into a agate motar for 5-10 minutes to obtain powdered samples with a grain size of <50 μm. Cleaning of all crushing and milling equipment was done in between samples to ensure zero contamination. Inductively Coupled Plasma Mass Spectrometry (ICP-MS) and X-ray Fluorescene Spectrometry (XRF) were used in this

study for the analysis of major and trace elements which were analyzed at ALS Minerals in Canada and at Akita University (Fig. 4.12) using Rigaku ZSX Primus II X-ray Fluorescence (XRF) spectrometer. All samples for XRF using at Akita University, were dried with drying oven and then measured the Loss on Ignition (LOI) with muffle furnace.

The formula for LOI calculation is as below;

$$LOI = \frac{weight\ of\ sample\ before\ combustion - weight\ of\ sample\ after\ combustion}{weight\ of\ sample} \times 100$$

The results obtained from XRF analysis show the concentration of major and trace elements which were plotted up on different petrologic classification schemes and tectonic discrimination diagrams using GCDKit software. Trace elements was normalized with respect to those of chondrite and primitive-mantle normalized using the value of Sun and McDonough (1989).

Fig. 4.12 Rigaku ZSX Primus II X-ray Fluorescence (XRF) spectrometer at Akita University

4.3.3. Result

4.3.3.1. Whole-rock major and trace elements geochemistry

Whole-rock compositions of 24 granitoids from different localities along Loei Fold Belt were determined (Table 4.2, 4.3). Loss on ignition (LOI) ranges from 0.18 to 1.56 wt%. The SiO_2 contents of the granitoids from Muang Loei, Phu Tap Fah – Phu Thep, Petchabun, Nakon Sawan – Lobburi and Rayong-Chantaburi vary from 60 to 76 wt%.

Binary variation diagrams of major elements oxides relative to the SiO_2 content as differentiation index indicate that as crystallization proceeds, the concentrations of TiO_2, Al_2O_3, P_2O_5, Fe_2O_3, MnO, CaO and MgO decrease (Fig. 4.13). Only the concentration of K_2O increases as SiO_2 increases.

($Na_2O + K_2O$) versus SiO_2 (wt%) diagram (Middlemost, 1994) (Fig. 4.14) indicates that granitoids in the Loei Fold Belt are classified as diorites, granodiorites and granites. The least differentiated rocks are those in Petchabun, while those in Rayong – Chantaburi are highly differentiated. K_2O versus SiO_2 (wt%) discrimination diagram (Fig. 4.15) indicates that the diorites from the Petchabun province are medium-K calc-alkaline and evolve to high-K calc-alkaline, as shown by the granitoids from Phu Tap Fah - Phu Thep and Nakon Sawan - Lobburi. The highly differentiated rocks from Muang Loei and Rayong-Chantaburi plots generally in the high-K calc-alkaline field.

Classification of rocks based on the ASI (Alumina Saturation Index = A/CNK [Al_2O_3/(CaO + Na_2O + K_2O) molar]) (Fig. 4.16A) (Maniar & Piccoli, 1989) indicates that granitoids along the Loei Fold Belt straddles between the metaluminous and peraluminous fields. Using A/CNK as an index, granitoids in this area are predominantly I-type.

Relationships between the SiO_2 content and the spatial distribution apparently indicate that the rocks are least differentiated the granitoids in Petchabun, at the central part of the Loei Fold Belt. On the other hand, SiO_2 content increases in Phu Tap Fah – Phu Thep and Nakon Sawan - Lobburi, north and south of Petchabun, respectively. SiO_2 contents of granitoids from Muang Loei and Rayong Chantaburi, at the northernmost and southernmost part of the study area, respectively, are the highest.

Nb versus Y and Rb versus (Y + Nb) tectonic discrimination diagrams indicate that the granitoids along Loei Fold Belt were generated in volcanic arcs (Fig. 4.16B, C). I further discriminated these volcanic arc granitoids to identify whether these rocks are normal volcanic arc rocks or are adakites. In the Sr/Y versus Y diagram (Defant & Drummond, 1990) (Fig. 4.17), the granitoids from Petchabun and Nakon Sawan – Lobburi dominantly plot in the adakitic field, while granitoids from Muang Loei, Phu Tap Fah and Rayong Chantaburi are considered as normal volcanic arc granites.

Rare earth element (REE) concentration patterns normalized to chondrite (Fig. 4.18) show general enrichment of light REEs (LREE) and depletion of heavy REEs (HREE). Distinct negative Eu anomaly in granitoids in Muang Loei, Nakon Sawan – Lobburi and Rayong Chantaburi indicates possible fractionation of Eu to plagioclase. Multi-element diagrams normalized to primitive mantle show distinct depletion in Nb, P and Ti (Fig. 4.18). The granitoids from Petchabun and Nakon Sawan – Lobburi which are plotted in the adakitic field (Fig. 4.17) show relatively low HREEs (Fig. 4.19).

Table 4.3 Whole-rock composition of granitoids along Loei Fold Belt.

Unit/ Complex	Locality	Sample code	Rock Name	(wt. %)											
				SiO_2	TiO_2	Al_2O_3	$Fe_2O_{3(tot)}$	MnO	MgO	CaO	Na_2O	K_2O	P_2O_5	LOI	Total
Muang Loei Granitoids	Chiang Khan	Gr18	Hornblende quartz-monzodiorite	64.68	0.84	13.49	5.90	0.09	3.21	4.71	2.68	3.36	0.20	0.69	99.85
	Chiang Khan	Gr17	Biotite tonalite	67.52	0.60	13.89	4.10	0.07	2.35	3.98	3.22	3.40	0.16	0.57	99.86
	Muang Loei	Gr10	Biotite quartz-syenite	75.25	0.17	12.72	2.27	0.06	0.40	1.19	3.78	3.61	0.05	0.14	99.79
	Muang Loei	Gr11	Biotite tonalite	70.44	0.45	14.27	3.12	0.12	1.46	2.58	5.04	1.97	0.17	0.27	99.89
	Chiang Khan	Gr19	Hornblende granodiorite	63.23	0.66	15.42	5.83	0.08	2.65	3.98	3.50	2.58	0.17	1.30	99.61
Phu Tap Fah - PUT Granitoids	Muang Loei	Gr25	Hornblende granodiorite	64.96	0.53	15.09	1.95	0.05	2.86	6.98	2.55	3.71	0.25	0.75	99.68
	Wang Saphung	Gr8	Hornblende tonalite	62.51	0.61	15.98	5.32	0.06	2.64	5.38	3.53	2.05	0.13	1.56	100.55
	Wang Saphung	Gr9	Biotite granodiorite	67.42	0.61	14.27	3.88	0.11	2.32	4.22	3.67	2.89	0.17	0.34	99.90
Phetchabun Granitoids	Chon Dan	Gr36	Hornblende quartz-monzodiorite	60.23	0.68	17.03	6.99	0.13	3.31	5.60	3.82	0.88	0.13	1.21	100.20
	Wang Pong	Gr37	Biotite quartz-monzodiorite	68.87	0.34	14.58	3.96	0.07	1.40	3.65	3.85	2.00	0.08	1.18	100.20
	Chon Dan	Gr35	Biotite tonalite	63.00	0.71	15.70	6.23	0.11	2.55	4.78	3.74	1.85	0.14	0.57	99.59
Nakon Sawan - Lobburi Granitoids	Nong Bua	NDBI 2	Biotite quartz-rich granitoid	75.24	0.17	12.88	1.54	0.04	0.21	0.87	4.14	4.11	0.02	0.25	99.64
	Nong Bua	NDBI1(2)	Biotite monzogranite	76.20	0.13	11.95	1.15	0.03	0.65	0.80	4.24	3.94	0.01	0.18	99.26
	Chon Dan	WP024	Biotite granodiorite	65.43	0.67	14.79	4.41	0.06	2.93	4.66	3.89	2.14	0.15	0.71	99.84
	Khao Wong Phra Jun	WPJ-DI	Hornblende quartz-monzodiorite	62.13	0.48	18.40	3.77	0.05	2.01	5.99	4.94	0.65	0.16	0.50	99.25
Rayong - Chantaburi Granitoids	Makham	Gr44	Biotite monzogranite	74.49	0.18	12.24	1.96	0.03	0.67	1.23	3.89	4.97	0.03	0.20	99.89
	Phanom Sarakam	Gr53	Biotite monzogranite	74.81	0.23	11.89	2.29	0.04	0.97	1.53	2.86	4.93	0.04	0.28	99.87
	Phanom Sarakam	Gr50	Biotite tonalite	74.38	0.20	12.04	2.28	0.07	0.98	1.61	2.85	5.09	0.05	0.31	99.86
	Makham	Gr43	Biotite granodiorite	71.72	0.22	14.88	1.94	0.04	0.61	2.16	3.67	4.12	0.08	0.26	99.85
	Bo Thong	Gr47	Biotite monzogranite	70.82	0.34	13.86	2.17	0.05	1.22	2.42	3.15	5.43	0.12	0.25	99.83
	Bo Thong	Gr49	Biotite monzogranite	71.08	0.39	13.47	2.60	0.06	1.43	2.51	3.10	4.77	0.14	0.27	99.82
	Khao Chamao	Gr46	Biotite granodiorite	71.59	0.41	12.90	2.80	0.05	0.93	1.73	2.64	6.50	0.08	0.18	99.81
	Muang Rayong	Gr39	Biotite monzogranite	73.75	0.25	14.23	1.96	0.04	0.53	2.01	3.58	3.16	0.14	0.46	100.25
	Khlung	Gr41	Hornblende monzogranite	70.51	0.50	12.35	4.81	0.07	1.00	2.18	3.12	4.67	0.11	0.51	99.83

Table 4.4 Trace elements and REE contents of granitoids along Loei Fold Belt.

Sample	Gr07	Gr08	Gr09	Gr10	Gr11	Gr12	Gr17	Gr18	Gr19	Gr25	Gr33	Gr35	Gr36	Gr37	Gr38	Gr39	Gr41
Rock type	tonalite	tonalite	granodiorite	quartz-syenite	tonalite	granodiorite	Biotite tonalite	monzodiorite	granodiorite	granodiorite	tonalite	tonalite	monzodiorite	monzodiorite	granite	monzogranite	monzogranite
Locality	Wang Saphung	Wang Saphung	Wang Saphung	Muang Loei	Muang Loei	Muang Loei	Chiang Khan	Chiang Khan	Chiang Khan	Muang Loei	Chon Dan	Chon Dan	Chon Dan	Wang Pong	Wang Pong	Muang Rayong	Khlung
La (ppm)	16.8	15.4	19.4	43.8	30.6	56.6	15.0	30.5	1.1	29.2	7.3	21.6	12.8	8.7	8.0	12.2	23.5
Ce	33.8	30.1	35.3	89.9	60.3	107.5	31.8	54.9	2.0	50.2	19.6	46.6	28.1	21.4	17.6	28.5	44.1
Pr	4.1	3.6	4.2	10.3	7.0	11.5	4.1	5.9	0.2	5.3	2.9	5.6	3.8	3.0	2.1	3.7	4.7
Nd	16.5	15.0	15.5	37.1	25.5	39.5	16.7	22.1	1.0	19.6	14.8	22.2	16.1	13.8	8.4	16.6	17.3
Sm	4.0	3.7	3.0	7.7	5.1	6.2	3.4	4.3	0.2	3.5	4.2	4.8	3.7	3.7	1.9	4.1	3.4
Eu	0.9	1.0	0.9	0.4	0.6	0.5	0.9	0.9	<0.03	0.9	1.5	1.3	1.0	1.0	0.6	0.9	0.6
Gd	3.7	3.5	2.6	5.8	4.6	4.5	3.1	3.7	0.2	3.1	5.1	4.1	4.0	3.8	1.8	3.9	2.8
Tb	0.6	0.6	0.4	1.0	0.7	0.7	0.5	0.6	0.0	0.5	0.9	0.6	0.7	0.6	0.3	0.6	0.5
Dy	3.7	3.7	2.8	5.1	4.1	3.9	3.0	3.6	0.3	2.6	5.5	3.5	4.2	4.0	1.6	4.1	2.6
Ho	0.8	0.8	0.6	1.1	0.8	0.7	0.6	0.8	0.1	0.6	1.1	0.7	0.9	0.8	0.4	0.8	0.5
Er	2.5	2.4	1.6	3.1	2.4	1.9	2.0	2.3	0.2	1.5	3.3	2.0	2.6	2.5	1.1	2.6	1.4
Tm	0.4	0.4	0.3	0.5	0.3	0.3	0.3	0.3	0.0	0.2	0.5	0.3	0.4	0.4	0.2	0.4	0.2
Yb	2.6	2.5	1.9	2.9	2.2	1.8	1.9	2.0	0.2	1.4	3.0	1.9	2.6	2.4	1.2	2.4	1.4
Lu	0.4	0.4	0.3	0.4	0.4	0.3	0.3	0.4	0.0	0.2	0.5	0.3	0.4	0.4	0.2	0.4	0.2
Rb	80.1	79.0	56.4	98.3	110.5	129.5	99.2	94.1	2.1	60.6	3.1	14.4	42.8	14.6	39.9	36.3	240.0
Ba	413.0	402.0	528.0	409.0	328.0	733.0	430.0	544.0	13.0	621.0	52.1	201.0	292.0	178.0	351.0	302.0	397.0
Th	5.6	5.5	6.7	15.4	8.2	13.4	12.7	14.1	0.3	9.1	0.9	3.9	3.8	1.3	5.1	2.7	16.4
U	2.1	2.2	2.4	3.0	2.4	1.9	2.4	2.1	0.6	2.7	0.3	1.0	0.9	0.6	1.3	0.9	6.1
Nb	5.4	5.8	4.6	12.8	12.8	9.4	6.5	6.6	0.4	7.6	5.2	7.9	4.4	3.4	3.0	3.7	15.5
Ta	0.4	0.4	0.3	1.1	0.8	0.6	0.6	0.5	<0.1	0.7	0.3	0.5	0.3	0.2	0.3	0.3	2.9
Sr	346.0	356.0	432.0	143.0	240.0	162.0	341.0	351.0	60.2	743.0	905.0	589.0	368.0	404.0	337.0	443.0	101.0
P	611.0	567.3	654.6	349.1	698.2	218.2	654.6	829.2	916.4	1047.4	1265.6	611.0	654.6	349.1	741.9	654.6	436.4
Zr	146	144	147	104	168	80	139	160	4	127	140	180	167	113	122	189	111
Hf	4.0	4.3	4.3	4.1	4.8	2.8	4.5	4.8	0.2	3.7	3.7	4.6	5.3	3.6	3.8	5.5	3.4
Ti	2998	3657	2758	1019	2698	779	3597	5036	3957	3177	9532	4256	4077	2038	4496	1499	2998
Y	22.1	21.0	16.0	30.9	22.9	19.2	17.5	20.7	1.8	14.5	29.3	18.6	23.8	22.5	10.2	23.3	14.8

Table 4.4 Trace elements and REE contents of granitoids along Loei Fold Belt. (continue)

Sample	Gr42	Gr43	Gr44	Gr46	Gr47	Gr49	Gr50	Gr51	Gr52	1R5M	0R3T	MKCD	NDBI1	NDBI2	TFDI	WPJDI	WP029
Rock type	monzogranite	granodiorite	monzogranite	granodiorite	monzogranite	monzogranite	tonalite	granodiorite	granite	granodiorite	granodiorite	granodiorite	monzogranite	monzogranite	tonalite	monzodiorite	diorite
Locality	Makham	Makham	Makham	Khao Chamao	Bo Thong	Bo Thong	Phanom Sarakam	Si Mahosod	Phanom Sarakham	Chatree	Chatree	Chon Dan	Nong Bua	Nong Bua	Lam Phayon	Khao Wong Phra Jun	Khao Phra Ngam
La (ppm)	30.1	13.2	28.5	37.0	41.4	18.4	35.3	22.2	17.4	10.3	10.3	15.8	41.6	9.4	6.4	8.2	6
Ce	60.3	28.0	52.9	76.7	74.5	37.5	70.9	45.2	35.6	20.9	21.1	33.1	82.6	19.7	14.8	17.6	14.0
Pr	7.0	3.4	5.8	9.1	8.3	4.3	8.1	5.4	4.1	2.6	2.6	4.2	10.1	2.4	1.8	2.3	1.85
Nd	27.2	13.7	20.4	35.5	28.6	16.1	30.0	21.5	15.2	11.4	12.1	17.1	39.3	10.6	8.4	10.2	8.4
Sm	6.8	3.2	3.7	8.0	4.6	3.3	5.0	4.8	3.3	2.2	2.4	3.9	9.1	2.1	1.6	2.2	1.97
Eu	1.1	0.4	0.6	0.4	0.7	0.5	0.8	0.6	0.5	0.8	0.8	0.9	0.7	0.8	0.6	0.8	0.6
Gd	6.6	3.2	2.6	7.6	3.1	2.9	3.2	4.4	3.0	2.0	1.9	3.1	8.8	1.6	1.8	2.3	1.97
Tb	1.1	0.6	0.4	1.2	0.5	0.4	0.4	0.8	0.6	0.2	0.3	0.6	1.4	0.3	0.3	0.4	0.3
Dy	7.4	3.7	2.3	7.6	2.7	2.7	2.4	4.7	3.6	1.3	1.5	2.7	9.5	1.5	1.5	2.0	1.93
Ho	1.6	0.8	0.5	1.7	0.6	0.6	0.5	1.0	0.7	0.2	0.3	0.6	2.2	0.2	0.3	0.4	0.35
Er	4.8	2.3	1.4	4.6	1.7	1.7	1.3	3.0	2.1	0.7	0.8	1.6	6.6	0.7	0.8	1.2	1.1
Tm	0.7	0.3	0.2	0.7	0.3	0.3	0.2	0.5	0.4	0.1	0.1	0.2	0.9	0.1	0.1	0.2	0.15
Yb	5.1	2.2	1.5	4.6	1.5	1.7	1.5	3.3	2.3	0.7	0.8	1.7	5.6	0.7	0.9	1.1	1.12
Lu	0.8	0.3	0.3	0.7	0.3	0.3	0.2	0.5	0.4	0.1	0.1	0.2	0.9	0.1	0.1	0.2	0.19
Rb	183.0	196.5	290.0	170.5	297.0	129.5	261.0	226.0	141.5	5.7	9.8	53.3	110.0	6.4	9.7	9.7	3.2
Ba	233.0	372.0	427.0	283.0	475.0	626.0	408.0	224.0	450.0	165.5	175.0	359.0	651.0	194.5	190.0	252.0	71.5
Th	24.5	13.3	25.6	20.1	35.6	13.5	17.4	18.9	12.8	0.6	0.6	4.2	9.3	0.6	1.4	0.6	1.95
U	6.8	3.1	9.3	4.5	27.6	4.0	2.3	6.3	4.9	0.3	0.3	1.6	3.3	0.3	0.5	0.3	0.55
Nb	7.4	4.4	15.7	8.1	16.8	4.2	6.6	8.7	5.4	3.2	3.1	4.5	14.1	3.1	1.7	3.3	3.6
Ta	0.8	0.4	1.9	0.7	2.3	0.5	0.3	0.8	0.6	0.2	0.2	0.4	0.8	0.2	0.2	0.2	0.4
Sr	139.0	43.5	180.0	46.6	195.5	152.0	133.0	85.2	174.5	694.0	761.0	432.0	42.1	706.0	977.0	839.0	744
P	131	349	131	349	524	611	218	393	262	709.0	927	655	44	87	655	698	546
Zr	217	86	136	190	150	64	216	176	84	82	116	199	184	76	89	134	85
Hf	6.6	3.2	5.2	7.0	5.3	2.4	6.3	6.2	3.2	2.3	2.9	5.5	6.1	2.0	2.5	3.3	2.5
Ti	839	1319	1079	2458	2038	2338	1199	2158	1319	2098	2548	4017	779	1019	1724	2878	2848
Y	47.3	20.6	15.4	42.8	20.9	17.2	13.4	32.5	21.1	6.5	6.9	14.8	57.7	6.1	7.7	10.3	10.1

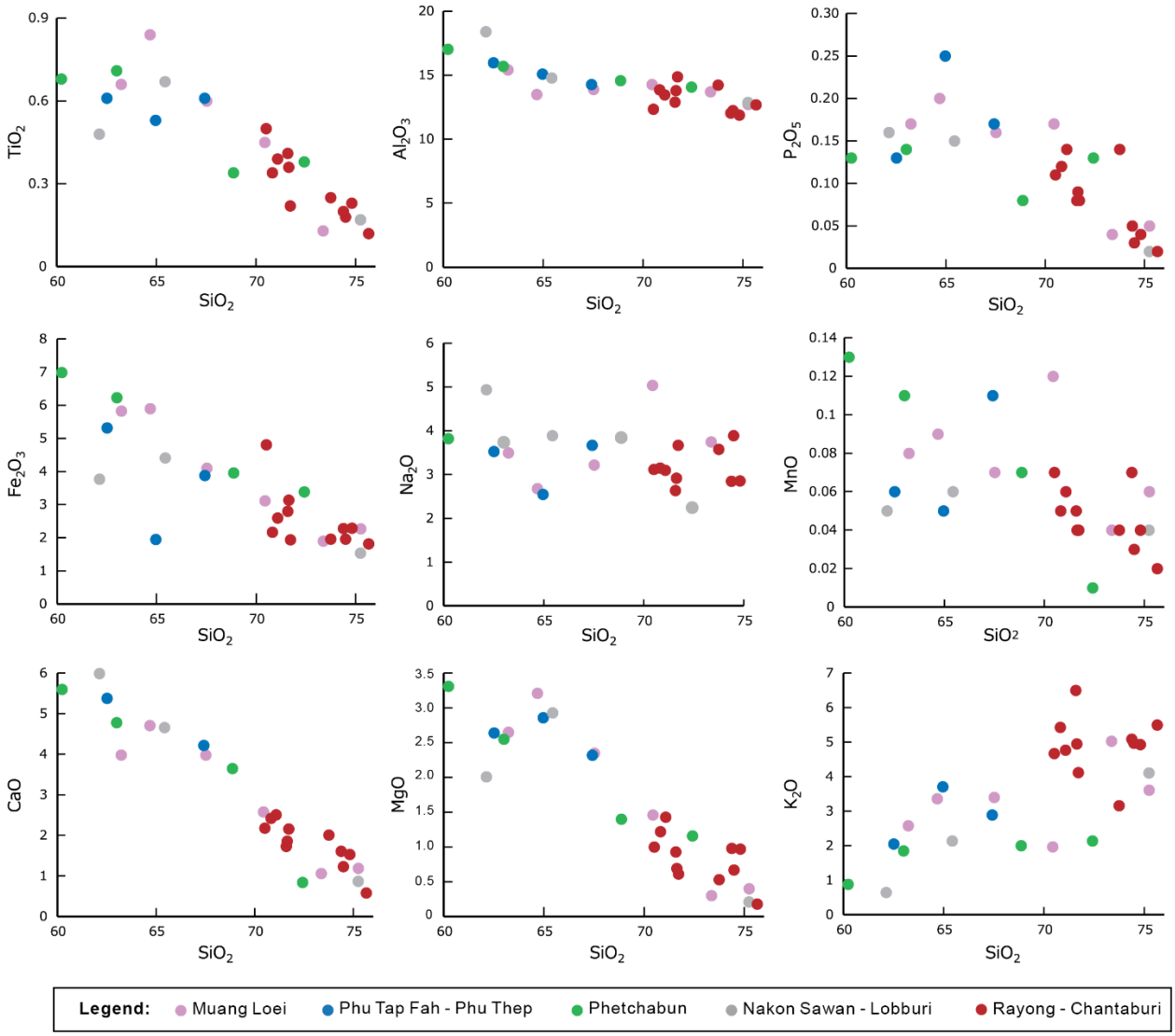

Fig. 4.13 Binary variation diagrams of whole-rock major elements with respect to SiO_2 (wt%) oxides of granitoids from Loei Fold Belt.

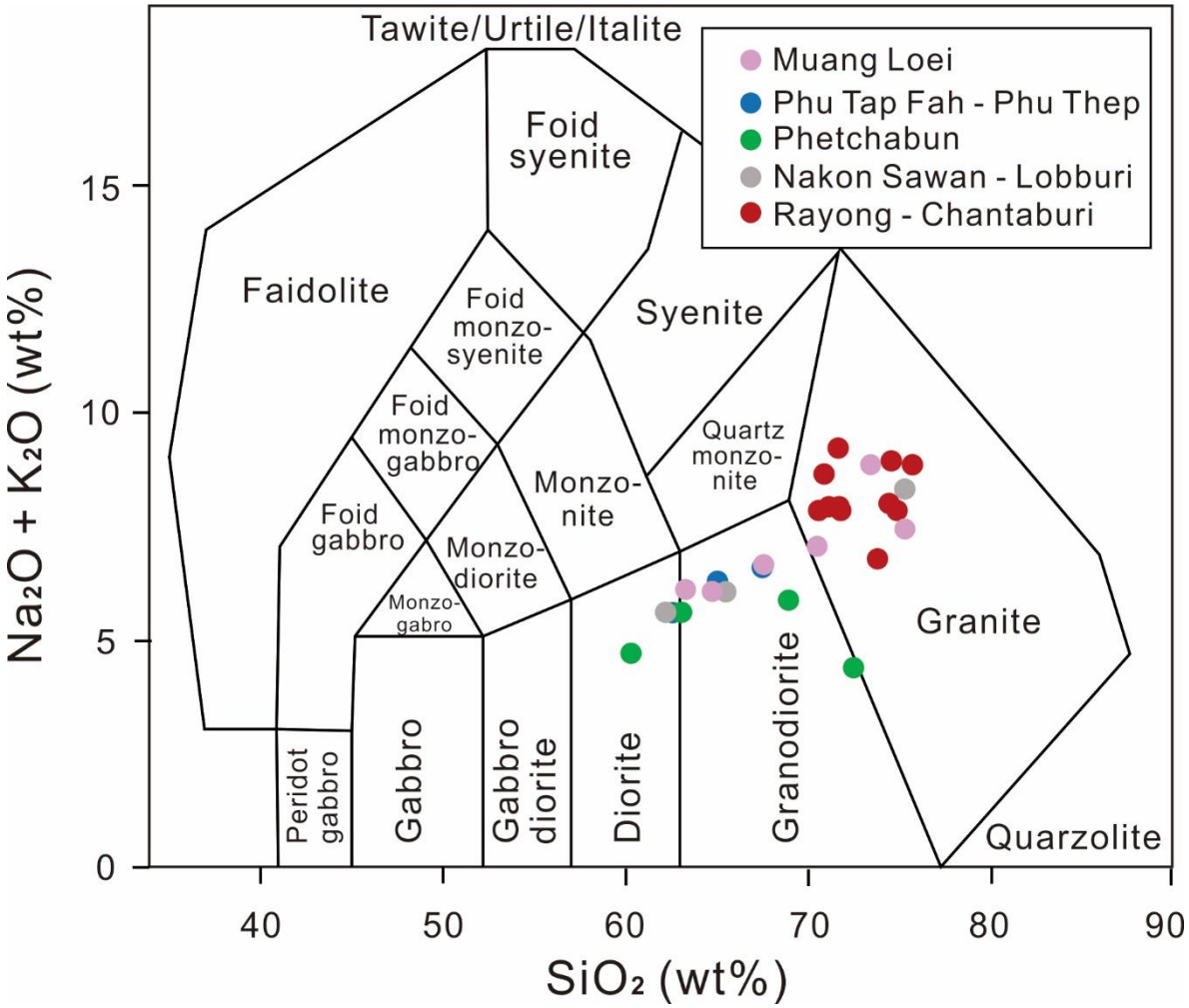

Fig. 4.14 Classification of granitoids from Muang Loei, Phu Tap Fah – Phu Thep, Phetchabun, Nakon Sawan – Lobburi, and Rayong – Chantaburi based on whole-rock SiO_2 and ($Na_2O + K_2O$) contents (Middlemost et al., 1994).

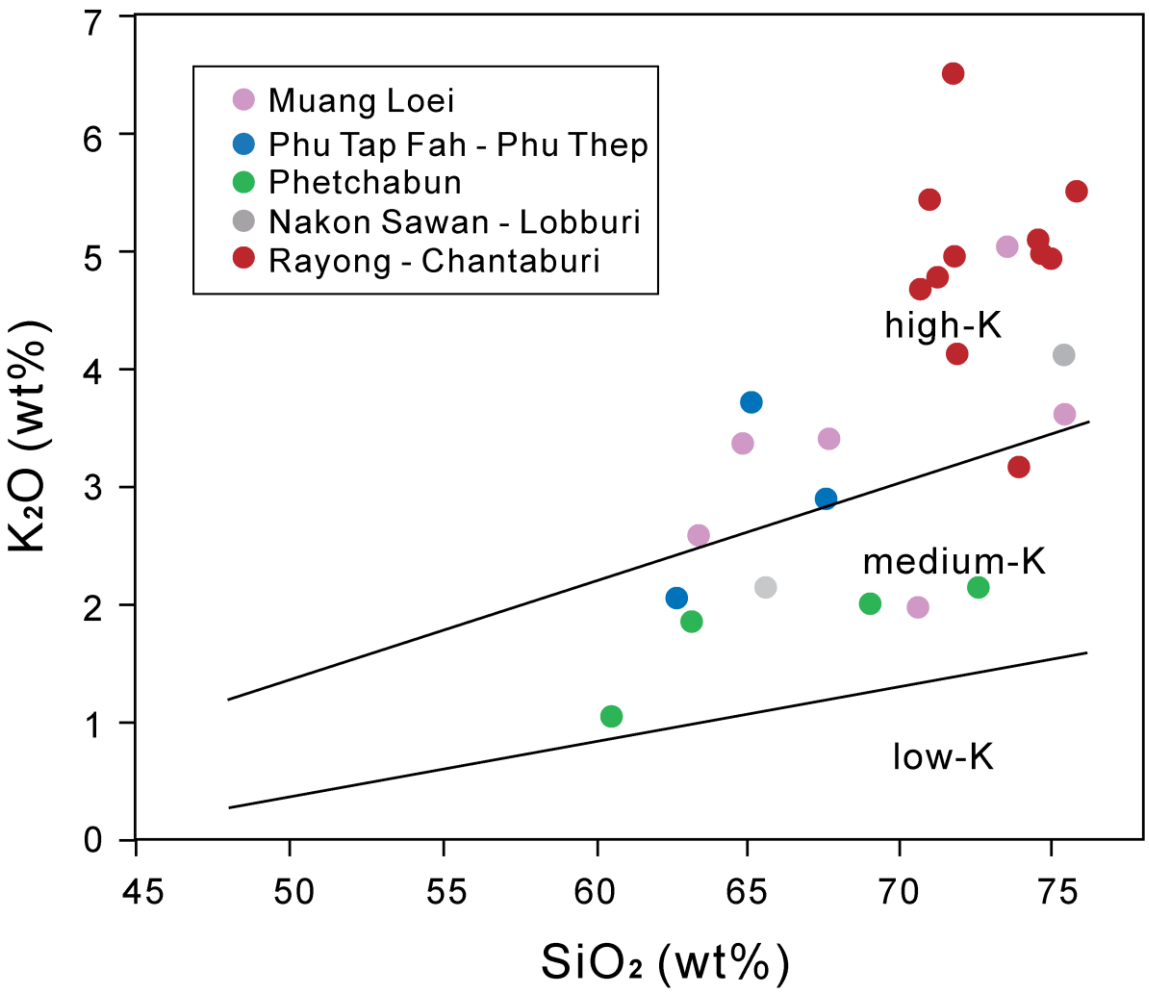

Fig. 4.15 SiO_2 vs. K_2O (wt%) diagram of Peccerillo et al. (1976) dividing the granitoids from Muang Loei, Phu Tap Fah – Phu Thep, Phetchabun, Nakon Sawan – Lobburi, and Rayong – Chantaburi into two groups; high-K calc-alkaline and medium-K calc-alkaline groups. Some plutons consist of combination of more than one series.

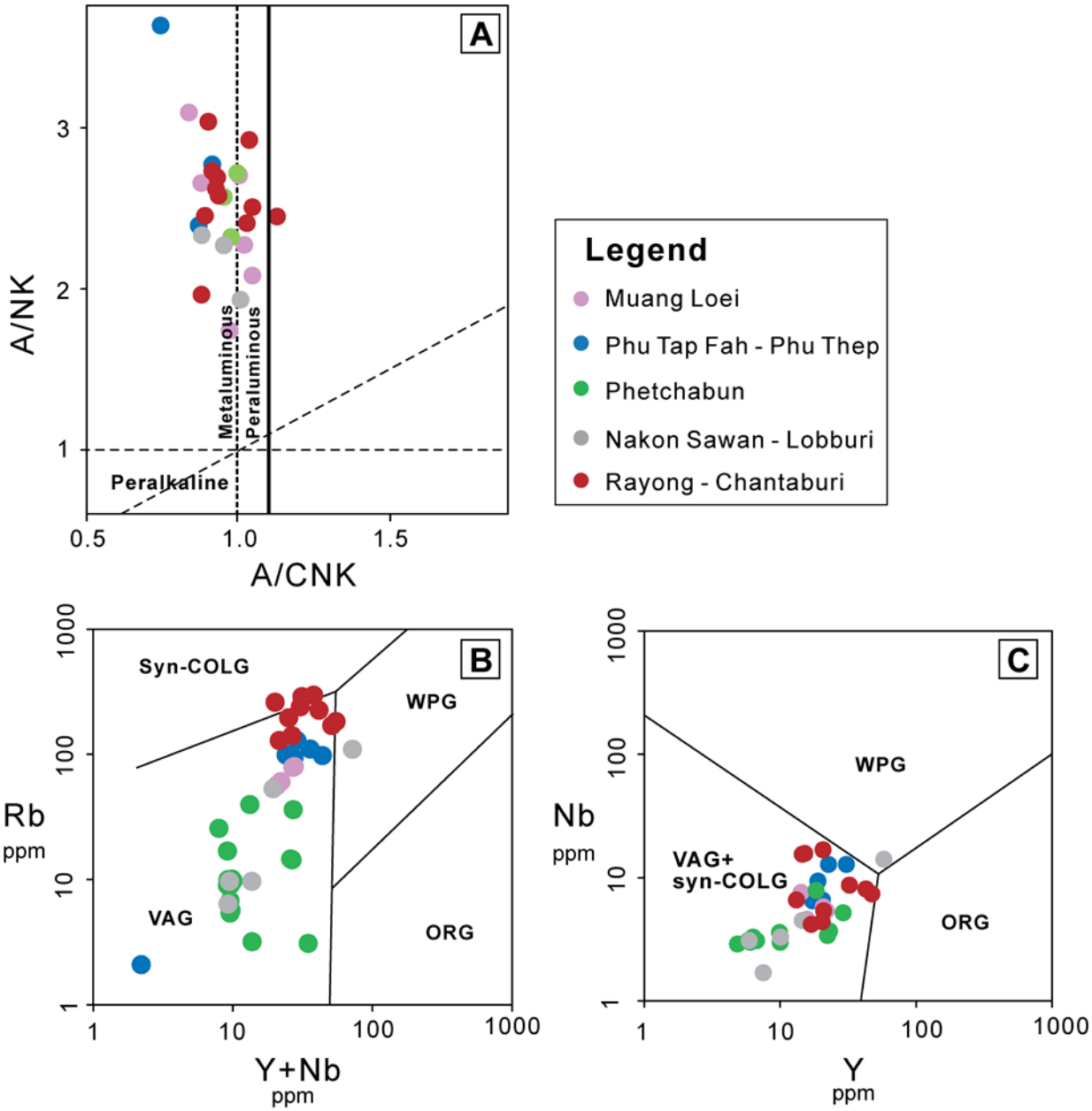

Fig. 4.16 (a) A/CNK [Al_2O_3/(CaO + Na_2O + K_2O) molar] vs A/NK[(Al_2O_3/Na_2O + K_2O) molar] diagram (Maniar & Piccoli, 1989), (b), (c) discrimination diagram of tectonic environment (Pearce et al., 1984) of granitoids along Loei Fold Belt. Abbreviation: VAG = volcanic-arc granite; syn-COLG = syn-collision granite; WPG = within plate granite; ORG = oceanic ridge granite.

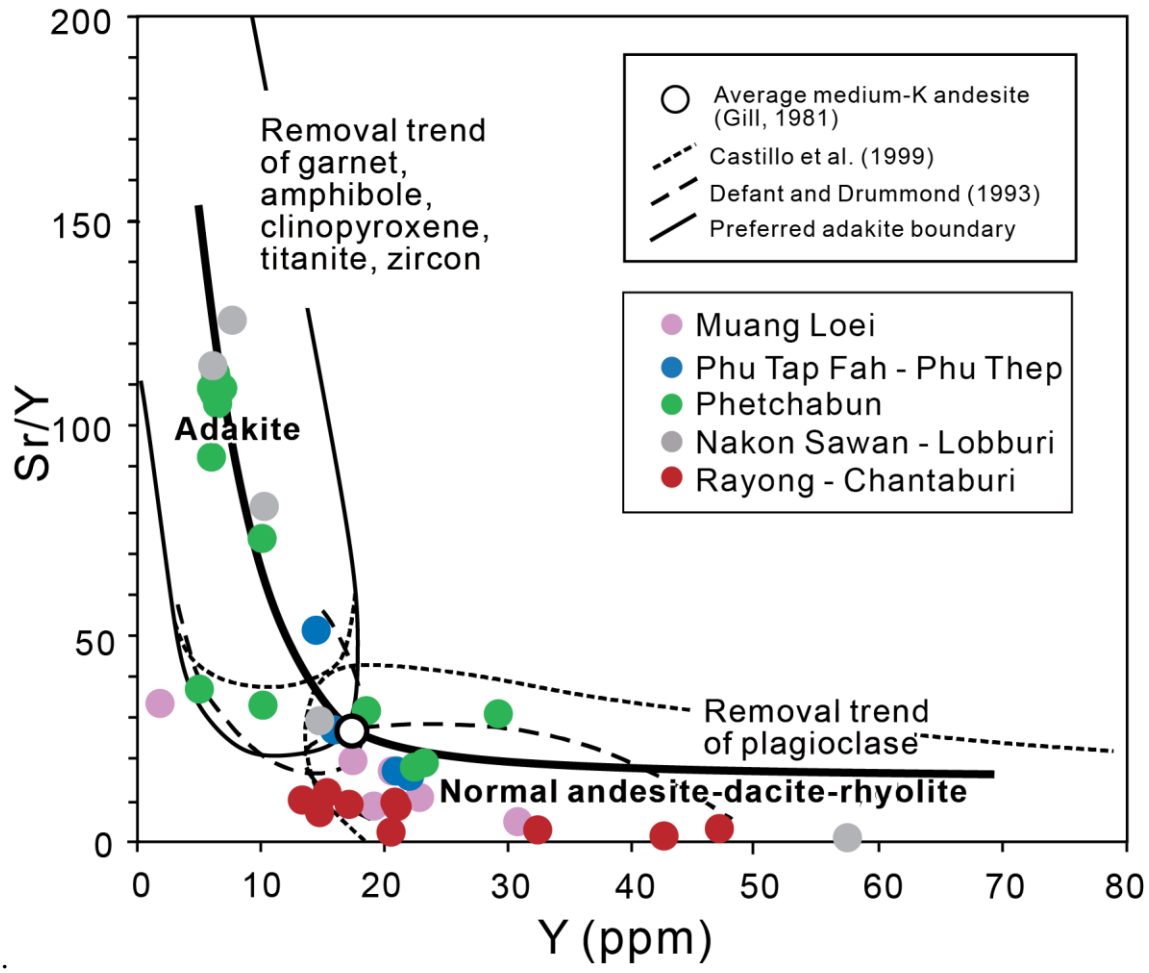

Fig. 4.17 Sr/Y vs. Y (a; Drummond & Defant, 1990) and La/Yb vs. Yb (b; Matin, 1986) diagrams discriminating between adakitic and arc calc-alkaline compositions. Arrows show fractionation trends.

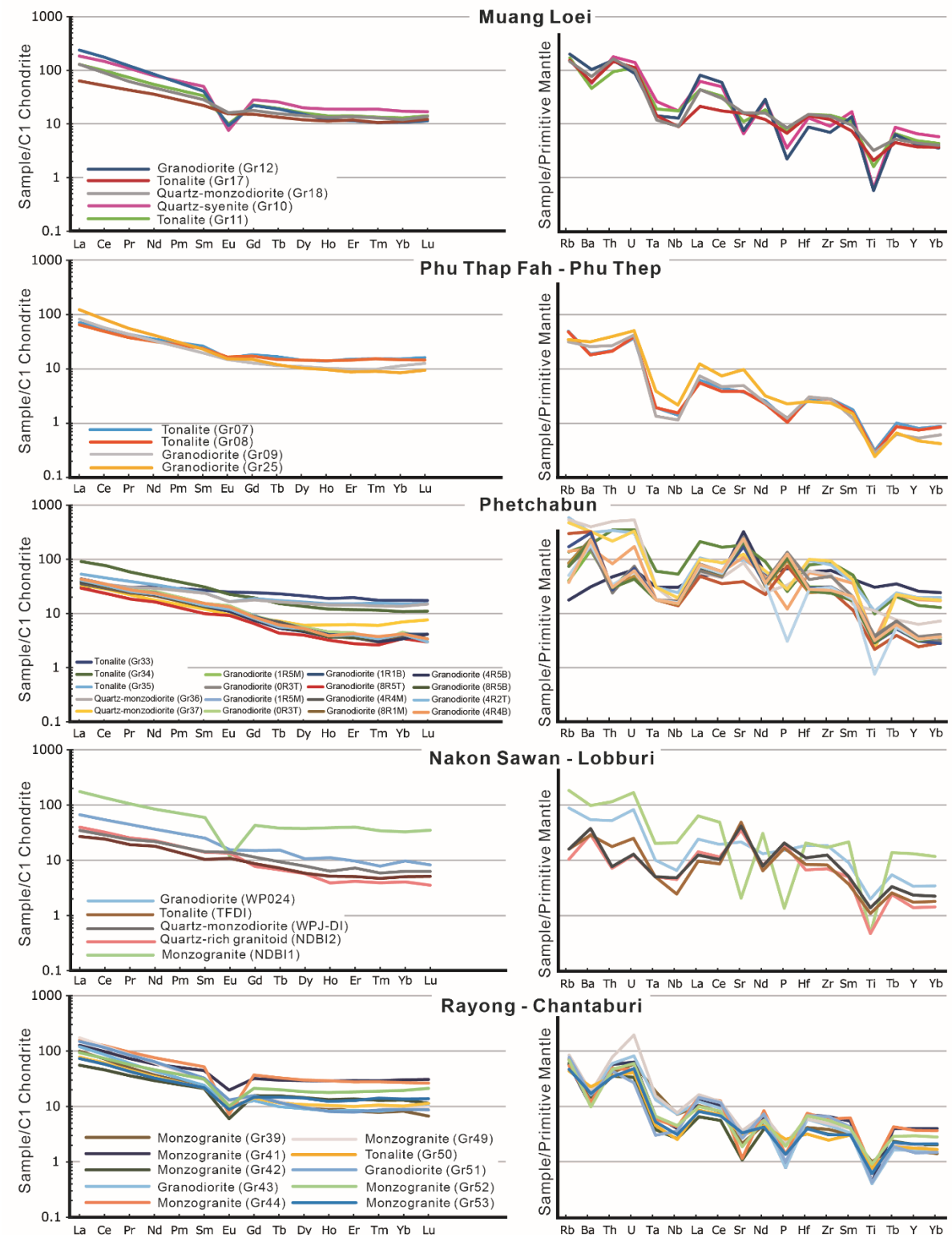

Fig. 4.18 Chondrite normalized rare earth elements and primitive-mantle normalized trace elements patterns of granitoids along Loei Fold Belt (Chondrite are values from Sun & McDonough).

4.3.3.2. Granitoids from Muang Loei

Granitoids from the Muang Loei plot as high-K calc-alkaline (CAK) series (K_2O= 2.58-5.0 wt%) and mid-K calc-alkaline series (K_2O=1.97 wt%) (Fig. 4.15). The SiO_2 content ranges from 63.2 to 75.2 wt%. Five granitoids from Muang Loei, tonalite (Gr17), quartz-monzodiorite (Gr18), granodiorite (Gr19, Gr12) and quartz-syenite (Gr10) are high-K calc-alkaline with K_2O ranging from 2.6 to 5.1 wt% and SiO_2 ranging from 63.2 to 75.3 wt%. The SiO_2 and K_2O content of tonalite (Gr11) at Muang Loei is 70.4 wt% and 2.0 wt%, respectively, which plot in the mid-K calc-alkaline field.

The ASI of the granitoids from Muang Loei ranges from 0.8 to 1.0. In the A/NK[Al_2O_3/(Na_2O + K_2O) molar] vs. A/CNK diagram (Fig. 4.16A), tonalite (Gr17, Gr11) and monzodiorite (Gr18) from Muang Loei are metaluminous (A/CNK < 1.0). The granodiorite (Gr12) and quartz-syenite (Gr10) are peraluminous (A/CNK > 1.0). The granodiorite (Gr19) straddles along the metaluminous and peraluminous field boundary.

In tectonic environment discrimination diagram (Pearce *et al.*, 1984) (Fig. 4.16A), tonalite (Gr17, Gr11), monzodiorite (Gr18), granodiorite (Gr19, Gr12) and quartz-syenite (Gr10) plotted in the I-type field (A/CNK < 1.1). According to the diagrams of trace elements (Y, Nb, Rb) (Fig. 4.16B, C) (Pearce *et al.*, 1984), all granitoids in Muang Loei are in the range of volcanic-arc granite (VAG).

Sr/Y vs. Y (Fig. 4.17) of tonalite (Gr17, Gr11), monzodiorite (Gr18), granodiorite (Gr12) and quartz-syenite (Gr10) are plotted in normal andesite-dacite-rhyolite field whereas granodiorite (Gr19) from Muang Loei are plotted close to adakite field (Defant & Drummond, 1990).

In the binary diagrams (Fig. 4.13), the TiO_2, Al_2O_3, P_2O_5, Fe_2O_3, CaO and MgO contents of tonalite (Gr17, Gr11), monzodiorite (Gr18), granodiorite (Gr19, Gr12) and quartz-syenite (Gr10) are negatively correlated with the SiO_2 content whereas the Na_2O and K_2O contents are positively correlated with the SiO_2 content.

Rare earth and trace elements of tonalite (Gr17, Gr11), monzodiorite (Gr18), granodiorite (Gr19, Gr12) and quartz-syenite (Gr10) were normalized to chondrite and primitive mantle values (Sun & McDonough, 1989; Fig. 4.18). LREE of granodiorite (Gr12), tonalite (Gr17, Gr11), monzodiorite (Gr18), quartz-syenite (Gr10) are slightly enriched with negative Eu anomaly and relatively flat HREE patterns (Fig. 4.18). The level of negative Eu decrease from quartz-syenite (Gr10), through granodiorite (Gr12), tonalite (Gr17), monzodiorite (Gr18) to tonalite (Gr17). LREE are highly enriched with flat HREE pattern with strongly negative Eu anomaly in quartz-syenite (Gr10) and granodiorite (Gr12), but slightly negative Eu anomaly in a quartz-monzodiorite (Gr18). Large ion lithophile elements (LILE: Ba) are enriched while high field strength elements (HFSE: P and Ti) are depleted in most of the granitoids from Muang Loei (Fig. 4.18).

4.3.3.3. Granitoids from Phu Tap Fah – Phu Thep

Granodiorites (Gr09, Gr25) from the Phu Thap Fah – Phu Thep plot in the field of CAK series (K_2O 2.9-3.1 wt%) and a tonalite (Gr08) plots in the field of mid-K calc-alkaline series (K_2O 2.1 wt%) (Fig. 4.15). The SiO_2 content narrowly ranges from 62.5 to 67.4 wt%. Two granodiorites from Muang Loei (Gr25) and Wang Saphung (Gr09) belong to high-K calc-alkaline series with K_2O ranging from 2.9 to 3.7 wt% and SiO_2 ranging from 65.0 to 67.4 wt%. The SiO_2 and K_2O

content of tonalite (Gr08) from Wang Saphung is 62.5 wt% and 2.1 wt%, respectively, which plot in the mid-K calc-alkaline field.

The ASI of the granitoids from Phu Thap Fah – Phu Thep ranges from 0.7 to 0.9. The granodiorite (Gr09, Gr25) and tonalite (Gr08) are metaluminous (A/CNK < 1.0) (Fig.4.16A). In this diagram, granodiorite (Gr09, Gr25) and tonalite (Gr08) are plotted in the I-type field (A/CNK < 1.1). According to the diagrams of trace elements (Y, Nb, Rb) (Fig. 4.16B, C) (Pearce *et al.*, 1984), all granitoids in Phu Thap Fah – Phu Thep are in the range of VAG granites.

Sr/Y vs. Y (Fig. 4.17) of granodiorite (Gr25) is plotted in adakite field, whereas granodiorite (Gr09) and tonalite (Gr07, Gr08) are plotted in normal andesite-dacite-rhyolite field (Defant & Drummond, 1990).

LREE are highly enriched with flat HREE pattern of granodiorite (Gr09, Gr25) and tonalite (Gr07, Gr08) in Phu Thap Fah – Phu Thep, in chondrite-normalized REE patterns but higher enrichment of LREE in granodiorite (Gr25) than tonalite (Gr07, Gr08) and granodiorite (Gr09). In primitive-mantle normalized trace element diagram show that the LILE (Ba) are enriched while HFSE (P and Ti) are depleted in granodiorite (Gr25, Gr09) and tonalite (Gr07, Gr08) (Fig. 4.18).

4.3.3.4. Granitoids from Phetchabun

The TiO_2, Al_2O_3, Fe_2O_3, Na_2O, MnO, CaO and MgO contents of monzodiorite (Gr36, Gr37), tonalite (Gr35) and granodiorite (8R5T) are negatively correlated with SiO_2 content whereas the K_2O content is positively correlated with the SiO_2 content (Fig. 4.13).

Tonalite (Gr35), monzodiorite (Gr36, Gr37), and granodiorite (8R5T) from the Phetchabun plot as mid-K calc-alkaline series (K_2O=0.9-2.0 wt%) (Fig. 4.15). Two granitoids from Chon Dan, tonalite (Gr35), monzodiorite (Gr36, Gr37) from Wang Pong belong to mid-K calc-alkaline series with K_2O ranging from 0.8 to 2.0 wt% and SiO_2 ranging from 60.2 to 68.9 wt%.

The ASI of the granitoids from Phetchabun ranges from 0.9 to 1.0. In the A/NK vs. A/CNK diagram (Fig. 4.16A), monzodiorite (Gr37) and tonalite (Gr35) are metaluminous (A/CNK < 1.0) and monzodiorite (Gr36) is between metaluminous and peraluminous. In this diagram, monzodiorite (Gr37, Gr36) and tonalite (Gr35) are plotted in the I-type field (A/CNK < 1.1). According to the diagrams of trace elements (Y, Nb, Rb) (Fig. 4.16B, C) (Pearce *et al.,* 1984), all granitoids in Phetchabun are in the range of VAG with syncollisional granites (syn-COLG).

Sr/Y vs. Y (Fig. 4.17) of granodiorite (8R5T, 8R5B, 4R4M, 0R3T, 4R4B, 4R5B, 8R1M, 4R2T, 1R1B, 1R5M), diorite (WP029) and monzodiorite (Gr37) are plotted in adakite field, whereas tonalite (Gr33, Gr34, Gr35) from Chon Dan, monzodiorite (Gr36) and granodiorite (Gr38) from Wang Pong are plotted in normal andesite-dacite-rhyolite field (Defant & Drummond, 1990).

LREE of the granitoids from Phetchabun are enriched with relatively flat HREE patterns (Fig. 4.18). LREE contents of all tonalite are higher than that of quartz-monzodiorite and granodiorite. LILE (Ba, Sr) are enriched and HFSE (P and Ti) are depleted in the granitoids from Phetchabun (Fig. 4.18).

4.3.3.5. Granitoids from Nakon Sawan - Lobburi

The Al_2O_3, P_2O_5, Na_2O and CaO contents of granodiorite (MKCD), monzogranite (NDBI1) and monzodiorite (WPJ-DI) are negatively correlated with the SiO_2 content whereas the K_2O content is positively correlated with the SiO_2 content (Fig. 4.13).

Monzogranite (NDBI1) from Nakon Sawan - Lobburi plots as CAK series (K_2O 4.1 wt%), and granodiorite (MKCD) plots as mid-K calc-alkaline series (K_2O 2.1 wt%) (Fig. 4.15). SiO_2 and K_2O contents of monzogranite (NDBI1) from Nongbua is 75.2 wt% and 4.1 wt% respectively, which plots in CAK field. SiO_2 and K_2O contents of granodiorite (MKCD) is 65.4 wt% and 2.1 wt%, respectively which plots in CK series.

The ASI of the granitoids from Nakon Sawan - Lobburi ranges from 0.9 to 1.0. In the A/NK vs. A/CNK diagram (Fig. 4.16A), granodiorite (MKCD) and monzodiorite (WPJ-DI) are metaluminous (A/CNK < 1.0) except monzogranite (NDBI1) from Nong Bua which is peraluminous (A/CNK > 1.0). In this diagram, granodiorite (MKCD) and monzodiorite (WPJ-DI) and monzogranite (NDBI1) are plotted in the I-type field (A/CNK < 1.1). According to the diagrams of trace elements (Y, Nb, Rb) (Fig. 4.16B, C) (Pearce *et al.*, 1984), all granitoids in Nakon Sawan - Lobburi are in the range of VAG with syn-COLG granites.

Sr/Y vs. Y (Fig. 4.17) of monzodiorite (WPJ-DI) are plotted in adakite field, whereas monzogranite (NDBI1) from Nongbua and granodiorite (MKCD) from Chon Dan are plotted in normal andesite-dacite-rhyolite field (Defant & Drummond, 1990).

LREE of the granitoids from Nakon Sawan - Lobburi are slightly enriched with relatively flat HREE patterns (Fig. 4.18). Monzogranite sample (NDBI1) from Nong Bua shows negative Eu anomaly. LILE (Ba, Sr) and HFSE (P and Ti) are depleted in the granitoids from Nakon Sawan - Lobburi (Fig. 4.18).

4.3.3.6. Granitoids from Rayong - Chantaburi

The Al_2O_3, P_2O_5, Fe_2O_3, MnO, CaO and MgO contents of granodiorite (Gr51, Gr46, Gr43), monzogranite (Gr53, Gr47, Gr49, Gr44, Gr42, Gr41, Gr39) and tonalite (Gr50) are negatively correlated with the SiO_2 content (Fig. 4.13).

Monzogranite (Gr47, Gr42) and granodiorite (Gr46) from the Rayong - Chantaburi plot as shoshonitic (HK) series (K_2O 5.1-6.5 wt%), tonalite (Gr50), granodiorite (Gr51, Gr46, Gr43) and monzogranite (Gr53, Gr49, Gr44, Gr41) plot as CAK series (K_2O 4.1-5.5 wt%) and monzogranite (Gr39) plots as mid-K calc-alkaline series (K_2O 3.2 wt%) (Fig. 4.13). Most of the granitoids including monzogranite (Gr41) from Klung, granodiorite (Gr42) and monzogranite (Gr44) from Makham, monzogranite (Gr49) from Bo Thong, granodiorite (Gr51) from Si Mahosod and monzogranite (Gr53) from Phanom Sarakam belong to CAK with K_2O ranging from 4.1 to 5.5 wt% and SiO_2 ranging from 71.7 to 75.7 wt%. SiO_2 and K_2O contents of tonalite (Gr50) from Panom Sarakam, monzogranite (Gr47) from Bo Thong, and granodiorite (Gr46) from Khao Chamao show HK character with SiO_2 and K_2O ranging from 70.8 to 74.4 wt% and from 5.1 to 6.5 wt% respectively. The SiO_2 and K_2O content of monzogranite (Gr39) from Muang Rayong is 73.8 wt% and 3.2 wt%, respectively which plots in CK series.

The ASI of the granitoids from Rayong - Chantaburi ranges from 0.9 to 1.1. Tonalite (Gr50), monzogranite (Gr53, Gr47, Gr49, Gr44, Gr41) and granodiorite (Gr46) are metaluminous (A/CNK < 1.0) except granodiorite (Gr51) from Phanom Sarakham, granodiorite (Gr39) from Wat Khao Banchob (Gr43) and monzogranite (Gr42) from Chaman which are peraluminous in the A/NK vs. A/CNK diagram (Fig. 4.16A). In this diagram, tonalite (Gr50), monzogranite (Gr53, Gr47, Gr49, Gr44, Gr42, Gr41) and granodiorite (Gr51, Gr46, Gr43) are plotted in the I-type field

(A/CNK < 1.1), except a monzogranite (Gr39) from Muang Rayong which is S-type. According to the diagrams of trace elements (Y, Nb, Rb) (Fig. 4.16B, C) (Pearce *et al.*, 1984), all granitoids in Rayong - Chantaburi are in the range of VAG with syn-COLG granites.

Sr/Y vs. Y (Fig. 4.17) of identity are plotted in normal andesite-dacite-rhyolite field (Defant & Drummond, 1990).

LREE of granodiorite (Gr51, Gr46, Gr43), monzogranite (Gr53, Gr47, Gr49, Gr44, Gr42, Gr41, Gr39) and tonalite (Gr50) from Rayong - Chantaburi are slightly enriched with negative Eu anomaly and relatively flat HREE. LILE (Ba, Sr) of the granitoids from Rayong – Chantaburi are enriched and HFSE (P and Ti) are depleted in primitive-mantle normalized trace element diagram (Fig. 4.18).

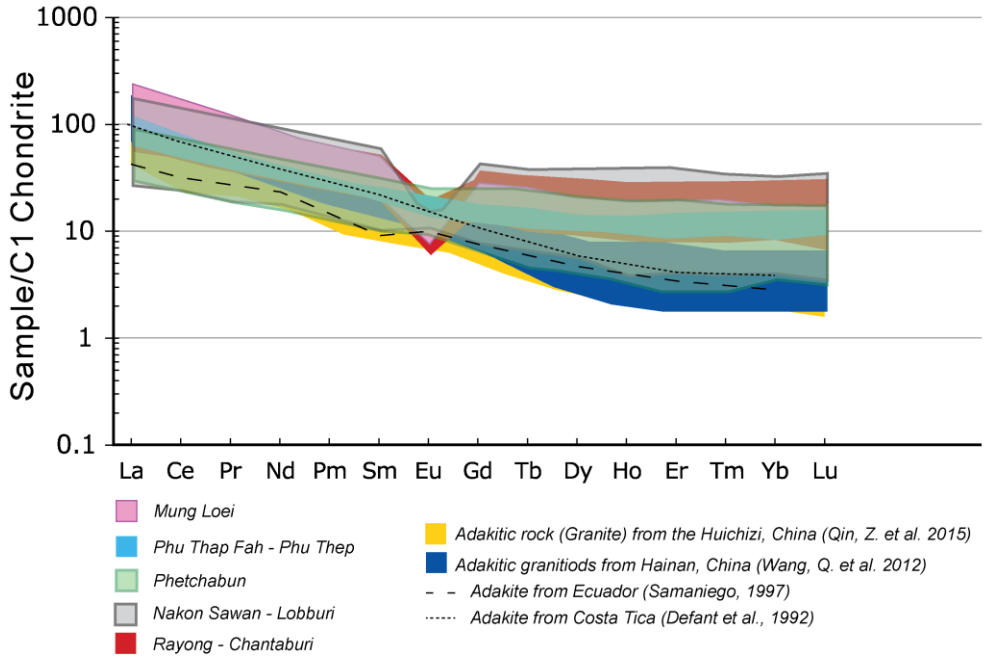

Fig. 4.19 Chondrite normalized rare earth elements patterns of granitoids along Loei Fold Belt (Chondrite are values from Sun & McDonough). Typical adakites are from Huichizi, China (Qin et al., 2015), Hainan, China (Wang et al., 2012), Costa Rica (Defant et al., 1992) and Ecuador (Samaniego, 1997).

CHAPTER 5
MINERAL CHEMISTRY AND SULFUR ISOTOPES

5.1. Composition of biotite

5.1.1. Introduction

Mineral composition of minerals provides a means of evaluating P-T condition and the nature of the magma during the emplacement of granitoids. Biotite is a significant ferromagnesian mineral in most intermediate and felsic igneous rocks. Biotite compositions depend largely upon the nature of magma from which they have crystallized (Abdel-Rahman, 1994; Moazamy, 2006; Shabbani & Lalonde, 2003). The composition of the biotite reflects the nature and the physicochemical conditions of magma from which it formed. Also, they can be used to provide valuable petrogenetic information.

5.1.2. Analytical Method

In this study, we present electron microprobe data to examine the possible link existing between the chemistry of biotite and the original magma and estimate the pressure and temperature at which plutons is emplaced. Before the EMPA, we need to prepare thin section samples as the procedure below;

(1) Marking observation points on the thin section using carbon pen.

(2) Carbon coating for the analyzing sample.

(3) Putting the sample on the sample holder of EPMA.

(4) Fixing the samples using carbon tape and for electric conductivity, and taking photo.

The samples selected for present study were derived from quartz-syenite, tonalite, granodiorite, monzodiorite, quartz-rich granitoid and monzogranite. Mineralogy of studied samples is summarized in Table 4.2. Mineral compositions were determined using an electron probe microanlyzer JXA-8800R (JEOL Ltd.) at Akita University. The quantitative analyses of selected minerals were performed with a 15keV accelerating voltage, a 10nA beam current and a 5 μm beam size. Biotite was analyzed with a probe diameter of 5 μm at an accelerating voltage 15 kV and a probe current of 12nA, and hornblende was analyzed with a probe a diameter of 15 μm at an accelerating voltage of 15kV and a probe current of 12nA. The analytical conditions are shown in Table 5.1 (biotite and hornblende).

Biotite is rather homogeneous and their compositions are uniform throughout individual samples. Most analyses represent averages of three or more individual several spot analyses from different biotites. The color of the biotite in magnetite-series biotite granodiorite at Wang Saphung in Phu Thap Fah - Phu Thep area (Fig. 5.1A) is greenish brown, because the mineral is rich in Mg due to iron consumed to form an earlier crystallized magnetite as Fe^{3+} (black cubes) (Ishihara, 1998). Biotite in ilmenite-series tonalite at Phanom Sarakam in Rayong -Chantaburi area is reddish brown, because its Fe^{2+}-rich (Ishihara, 1998) (Fig. 5.1B).

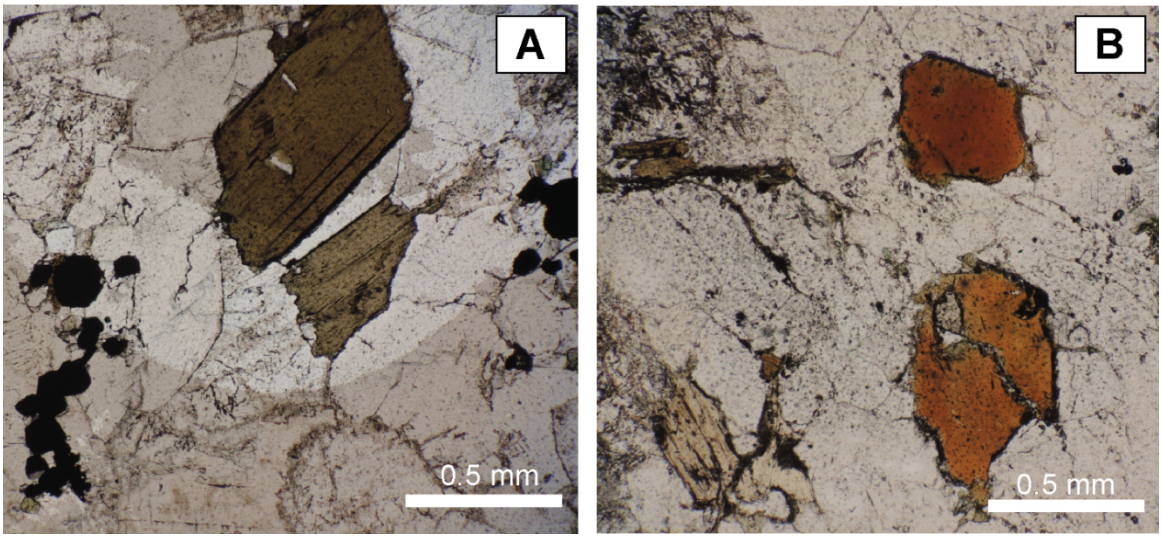

Fig. 5.1 A. Magnetite-series biotite granodiorite at Wang Saphung in Phu Thap Fah - Phu Thep area, B. Ilmenite-series biotite tonalite at Phanom Sarakam in Rayong-Chantaburi area.

Table 5.1 Analytical condition for biotite and hornblende.

Element	*Crystal*	*Fluorescence line analyzed*	*Standard*	*Counting time (s) (peak/background)*	*Detection limit (ppm)*
F	TAP	Kα	Fluorapatite	30/16	2200
Fe	LIF	Kα	Hematite	20/10	270
Cl	PETJ	Kα	Sodalite	60/30	60
Na	TAP	Kα	Albite	20/10	100
Mn	LIF	Kα	Manganosite	30/15	200
Ca	PETJ	Kα	Wolasstonite	20/10	130
Al	TAP	Kα	Corundum	20/10	580
K	PETJ	Kα	KTiOPO4	30/15	70
Mg	TAP	Kα	Periclase	20/10	90
Ti	PETJ	Kα	Rutile	20/10	200
Si	TAP	Kα	Albite	20/10	130

5.1.3. Result

5.1.3.1. Biotite composition

The chemical compositions of some analyzed biotites in granitoids along Loei Fold Belt are given in Table 5.2 The number of ions on the basis of 22 oxygen was calculated from the oxide values (Table 5.2). Ternary MgO-FeO_{tot}-Al_2O_3 tectono-magmatic discrimination diagram (Abdel-Rahman, 1994) suggests that biotite compositions from the Loei Fold Belt granitoids fall within calc-alkaline field (Fig. 5.2), except for quartz-rich granitoid (NDBI2, NDBI2(1)) and

granite (Gr45) plotted in alkaline field. The biotite composition of monzogranite (Gr39, Gr47, Gr53), granite (Gr49) and tonalite (Gr50) from Rayong – Chantaburi plotted in peraluminous field.

In Muang Loei granitoids, total Al content (^{T}Al) of biotite in fine to coarse-grained granodiorite is higher than that of fine-grained and relatively equigranular tonalite, fine to coarse-grained granodiorite and coarse-grained quartz-syenite, respectively. The ^{T}Al content of biotite of medium to coarse-grained granodiorite in Phu Thap Fah-Phu Thep is high. The ^{T}Al content of biotite of medium to coarse-grained with porphyritic texture quartz-rich granitoid in Nakon Sawan-Lobburi is lowest among the granitoids in all area. In Rayon-Chantaburi granitoids, the ^{T}Al content of biotite of coarse-grained granite is higher than that of medium to coarse-grained with porphyritic texture monzogranite, coarse-grained granodiorite and fine to coarse-grained tonalite.

Atomic Mg/(Mg+Fe) or X_{Mg} of biotite in tonalites (Gr11, Gr17) in Muang Loei range from 0.47 to 0.56, granodiorites (Gr12, Gr19) range from 0.51 to 0.52, quartz-syenite (Gr10) is 0.46. and monzodiorite (Gr18) is 0.55. X_{Mg} of biotite in granodiorite (Gr09) from Phu Thap Fah – Phu Thep is highest 0.60, while X_{Mg} of biotite in quartz-rich granitoid (NDBI2) from Nakon Sawan – Lobburi is lowest 0.26. The X_{Mg} of biotite in granitoids in Rayong – Chantaburi widely range from 0.22 to 0.48.

Fluorine concentrations of biotite in granitoids in Muang Loei range from 0.07 to 0.51 atoms per formula unit (apfu). F concentrations of biotite from tonalite (Gr11) and granodiorite (Gr12) are highest, 0.44 apfu and 0.51 apfu, respectively. F concentration of biotite in monzodiorite (Gr18) is 0.07 apfu. Cl concentrations of biotite in granitoids taken from the west of Muang Loei, quartz-syenite (Gr10), tonalite (Gr11) and granodiorite (Gr12), are 0.03, 0.05 and 0.07 apfu., respectively. Cl content of biotite in granitoids taken from the east of Muang Loei, tonalite (Gr17), monzodiorite (Gr18) and granodiorite (Gr19) are 0.08, 0.11 and 0.06 apfu., respectively.

Fluorine and chlorine contents of granodiorite (Gr09) in Phu Thap Fah are relatively low at 0.12 and 0.03 apfu., respectively. F and Cl contents of biotite of quartz-rich granitoid (NDBI2) in Nakon Sawan – Lobburi are 0.48 and 0.12 apfu., respectively.

Chlorine contents of biotite from granitoids in Rayong - Chantaburi are not significant, except monzogranite (Gr42) and granodiorite (Gr46) with concentrations of 0.10 and 0.02 apfu., respectively. Fluorine concentrations of biotite, on the other hand, widely vary from 0.02 to 0.41 apfu. F concentration of biotite in monzogranites range from 0.02 to 0.31 apfu. F concentrations of biotite in granodiorites range from 0.23 to 0.36 apfu. F concentrations of biotite in granites range from 0.21 to 0.41 apfu, while that in the tonalite is 0.17 apfu.

F concentrations versus X_{Mg} of the biotite from granitoids in Rayong - Chantaburi (Fig. 5.3B) are positively correlated. F contents and X_{Mg} of biotite in the western granitoids in Muang Loei are positively correlated along with the slope of the biotite in granitoids from Rayong - Chantaburi.

Chlorine concentrations and X_{Mg} of biotite in granitoids from Rayong - Chantaburi and Muang Loei are distinct. Chlorine content and X_{Mg} of biotite in granitoids from Rayong - Chantaburi are negatively correlated (Fig. 5.3C).

5.1.3.2. Hornblende composition

The total Al content of hornblende in granodiorite (Gr19) and quartz-monzodiorite (Gr18) from Muang Loei, granodiorite (Gr09) from Phu Thap Fah – Phu Thep and granodiorite (Gr30) from Phetchabun were analyzed (Table 5.3). The oxygen fugacity relative to nickel-nickel oxide (ΔNNO) was calculated based on 23 oxygen on the basis of Ridolfi *et al.* (2009). The log fO_2 of hornblende of granitoids from Muang Loei, Phu Thap Fah – Phu Thep, and Phetchabun ranging from NNO+0.7 to NNO+1.7 which indicates a high oxidized state of magma.

CHAPTER 6
GEOCHRONOLOGY

6.1. Geochronology

6.1.1. Introduction

K-Ar dating technique is based upon the decay of a naturally occurring isotope of potassium, ^{40}K to an isotope of argon, ^{40}Ar. The decay of ^{40}K is by a branching process; 10.48% of ^{40}K decays to ^{40}Ar by β^+ decay (Beckinsale & Gale 1969), followed by γ decay to the ground state, and by electron capture direct to the ground state, and 89.52% decays to ^{40}Ca by β^- to the ground state. Argon is a rare trace element and radiogenically produced ^{40}Ar generally exceeds the levels of trapped ^{40}Ar. The naturally occurring isotopes of argon are measured by mass spectrometry for K-Ar dating (^{36}Ar, ^{38}Ar and ^{40}Ar). The $^{36}Ar/^{38}Ar$ ratio is almost constant, although cosmogenic ^{38}Ar can be detected in some Ca-rich samples (Renne *et al.* 2001). Absolute argon concentrations, required for the K-Ar technique, are measured as a ratio with respect to a known amount of ^{38}Ar tracer gas. In K-Ar dating, potassium is measured generally using flame photometry, and atomic absorption spectroscopy.

The date measured by K-Ar techniques reflects the time since radiogenic argon produced by decay of ^{40}K, become trapped in the mineral or rock. This maybe be the age of the rock of the most recent cooling event and in some samples may even reflect an integrated cooling age for a range of sub-grains.

In this study, I report new results of K-feldspar and hornblende K-Ar dating for 3 samples representing the quartz-syenite from Muang Loei, monzogranite and monzodiorite from Nakon Sawan – Lobburi (Table 6.1).

6.1.2. Analytical Method

The rock samples were crushed using a stainless steel mortar and sieved into 0.25-0.35 and 0.35-0.5 mm size-fractions. The material was then washed in water and dried in an oven temperature at about 50°C. Heavy liquid, magnetic separation and handpicking under a binocular microscope produced about 0.5 g of K-feldspar and 0.7 g of hornblende separates which were subsequently cleaned in distilled water. The two samples of K-feldspar (NDBI, GR10), and one sample of hornblende (WPJ-DI) have been concentrated at Akita University and submitted for Geochronology test by K-Ar method to Actlabs, Canada.

Aliquots of the samples were weighted into Al container, loaded into sample system of extraction unit, degassed at ~100°C during 2 days to remove the surface gases. Argon was extracted from the sample in double vacuum furnace at 1,700°C. The determination of radiogenic argon content was carried out twice on MI-1201 IG mass-spectrometer by isotope dilution method with ^{38}Ar as spike, which was introduced to the sample system prior to each extraction. The extracted gases were cleaned up in two step purification system. Then pure Ar was introduced in to custom built magnetic sector mass spectrometer (Reinolds type). The test was done twice to ensure the consistency of the result. Two globally accepted standards (P 207 Muscovite and 1/65 “Asia” rhyolite matrix) were measure for ^{38}Ar spike calibration.

For age calculations the international values of constants were used as follow:

$$\lambda_K = 0.581 \times 10^{-10} y^{-1},\ \lambda_\beta = 4.962 \times 10^{-10} y^{-1},\ {}^{40}K = 0.01167\ (at.\%)$$

6.1.3. Result

Pure K-feldspar concentrates were extracted from fresh quartz-syenite (Gr10) in Muang Loei and monzogranite (NDBI) in Nakon Sawan – Lobburi as well as hornblende from quartz-monzodiorite (WPJ-DI) in Nakon Sawan – Lobburi. K-Ar age dating yielded the age 171±3, 221±5, and 219±8 Ma, respectively (Table 6.1). The certainty of the ages calculated fall within 2σ error.

Table 6.1 Summary of age dating of granitoids.

Sample no.	Location	Rock Type	Method	Dated mineral	K, % ± σ	^{40}Ar rad, (ng/g)	Age (Ma)
Gr10	Muang Loei	quartz-syenite	K-Ar	K-feldspar	9.76±0.10	121.4±0.4	171±3
NDBI	Nakon Sawan	monzogranite	K-Ar	K-feldspar	6.07±0.07	99.0±0.3	221±5
WPJDI	Lobburi	quartz-monzodiorite	K-Ar	Hornblende	0.650±0.015	10.49±0.04	219±8

CHAPTER 7
DISCUSSION AND CONCLUSIONS

7.1. Discussion

7.1.1. Geodynamic implications

Various geodynamic models have been proposed to explain the genesis of the Permian to Early Triassic magmatism along the Loei Fold Belt (e.g. Kamvong *et al.*, 2014, Charusiri, 1989; Charusiri *et al.,* 1993; Intasopa, 1993; Charusiri *et al.*, 2007; Barr and Charusiri, 2011; Boonsoong *et al.,* 2011; Zaw *et al.*, 2014; Salam *et al.*, 2014). These magmatism produced high-K calc-alkaline (high-K) and calc-alkaline (medium-K) plutonic rocks and have contributed to the magmatic-hydrothermal fluids that gave rise to a variety of ore deposit types along the Loei Fold belt (e.g. Charusiri *et al.*,1993; Charusiri *et al.*, 2007; Kamvong & Zaw, 2009; Zaw *et al.*, 2009; Crow & Zaw, 2011; Salam *et al.*, 2013). Previous classification of the granitoids along the Loei Fold Belt suggested features of both "I" type granites (Cobbing *et al.,* 1986; Charusiri et al., 1993, Barr & Mcdonald, 1991) and "S" type granites (Metcalfe, 2011; Sone & Metcalfe, 2008). However, geochemical and petrographic data of samples I collected across the length of Loei Fold Belt, suggest the predominance of I-type granitoids throughout the belt. Notable features of these granitoids are:

(a) mafic minerals are invariably hornblende and biotite;

(b) muscovite, garnet and cordierite are absent;

(c) accessory minerals present include titanite, apatite, zircon; monazite is not present;

(d) in terms of A/CNK, A/CNK of most of the collected granitoids are < 1.1;

(e) there are Au and Cu mineralization but no Sn or W mineralization;

All these features are consistent with “I” type granite.

Different tectonic discrimination diagrams show consistently that the granitoids from Petchabun, Phu Tap Fah and Nakon Sawan-Lobburi were generated in a volcanic arc setting, while granitoids of Muang Loei and Rayong – Chantaburi are plotted in both volcanic arc and collisional zone fields. This transition from volcanic arc to collisional setting reflects the initiation of continental collision (Fig. 7.1). Geochemistry and the age of Muang Loei suggest that the Paleo-tethys ocean must have been closed by the late Middle Jurassic.

Moreover, the new geochronological data from this study suggest that magmatism along Loei Fold Belt continued further to late Middle Jurassic instead of ceasing at late Early Jurassic, as suggested by previously reported ages (Zaw *et al.*, 2009; Kawakami, 2014). This new finding has further implications for tectonic reconstructions being carried out in Asia and surrounding regions.

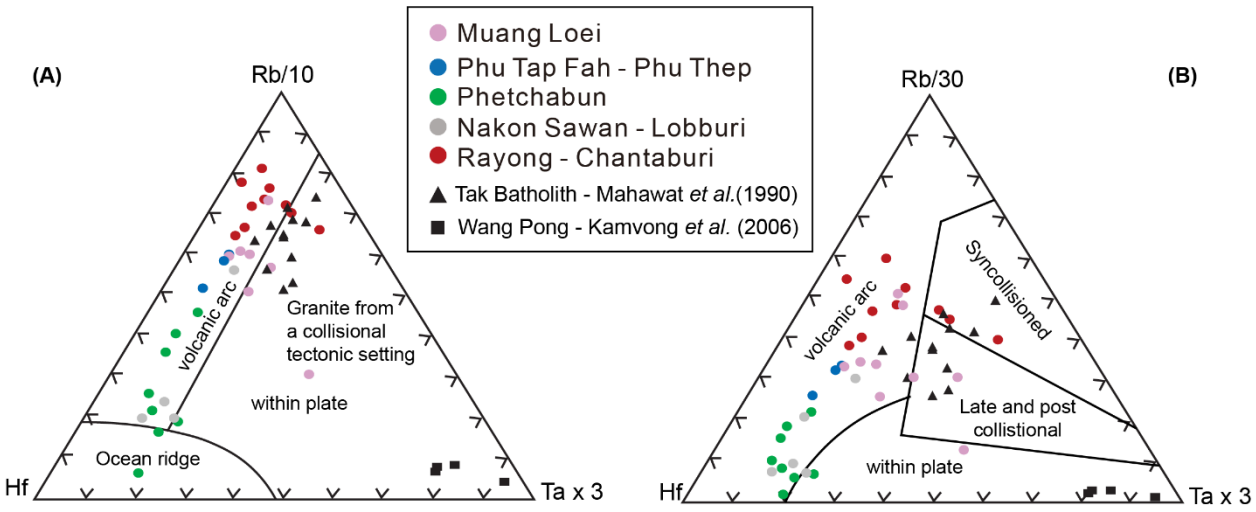

Fig. 7.1 Trace-element tectonic discrimination diagrams. (A) Hf-Rb/10-Ta×3 and (B) Hf-Rb/30-Ta×3 discrimination diagrams for plate granites after Harris et al. (1986).

7.1.2. Metallogenic implications

The magnetic susceptibility of the granitoids show wide range variation between 0.03 × 10^{-3} and 34.6 × 10^{-3} in SI unit, corresponding respectively to ilmenite-series (<1 × 10^{-3} in SI unit) and magnetite-series (>1 × 10^{-3} in SI unit). Low magnetic susceptibility value is due to hydrothermal alteration. Magma derived from partial melting of subducted slab materials in a volcanic arc setting would have assimilated sedimentary materials not only in deep levels but also at the site of intrusion to have formed the relatively reduced I-type granitoids with low magnetic susceptibility. The local reduction of granodiorite magma by sedimentary rocks of the Phu Thap Fah Au skarn deposit suggested that the contrasting lithology of the crust formed by the collision controlled oxygen fugacities and chemical trends of granitoids through magma-wall-rock interactions (Sato, 1991). Magnetite-series granitoids are in Muang Loei, Phu Thap Fah – Phu Thep, Phetchabun, Nakon Sawan – Lobburi and Rayong - Chantaburi. The abundance of magnetite, as observed under the microscope, suggests that the granitoids along Loei Fold Belt belong to magnetite-series.

X_{Mg} of biotite and the assemblage of high X_{mg} hornblende-magnetite-titanite-quartz in granitoids in Muang Loei, indicating oxidized environment, high oxygen fugacity, which corresponds with the occurrence of magnetite-series granitoids. Hornblende oxybarometry indicates a high oxidized state of magma (log fO_2 ranging from NNO+0.7 to NNO+1.7) (Table 5.5). X_{Mg} of biotite in Phu Thap Fah – Phu Thep and Rayong – Chantaburi is low (<0.6), indicating reduced environment, low oxygen fugacity which also corresponds with the occurrence of magnetite-series granitoids associated with and Sb-Au deposit (Bo

Thong) in Rayong – Chantaburi. Low magnetic susceptibility values for the magnetite-series granitoids may probably suggest that granitic magmas in Phu Thap Fah – Phu Thep and Rayong – Chantaburi areas were contaminated by C-bearing sedimentary host rocks.

Regionally, granitoids along the Loei Fold Belt are magnetite-series based on the classification of granitoid series by Ishihara (1977). The magnetite-series granitoids predominate in the Muang Loei area, Phetchabun area related to the Au-Ag (Chatree, Wang Yai) and Fe-Cu (Singto) deposits and Nakon Sawan - Lobburi area related to the Fe-Cu (Khao Lek) and Cu (Khao Phra Ngam) deposits while the magnetite-series granitoids were reduced in the Phu Thap Fah - Phu Thep area which related to Au (Phu Thap Fah) and Cu (Phu Thep) deposits and Rayong - Chantaburi area related to the Sb-Au (Bo Thong) deposit. A few residual iron deposits (e.g. Khao Lek deposit) were mined in magnetite-rich magnetite-series plutons (Nakon Sawan - Loburi area).

The granitoids along the Loei Fold Belt related to skarn mineralization are adakitic (e.g. Salam, 2013; Kamvong et al., 2014; Paipana, 2014). The granodiorite in Phu Thap Fah - Phu Thep area, granodiorite, diorite and monzodiorite in the Petchabun area and monzogranite, monzodiorite and granodiorite in Nakon Sawan - Lobburi area associated with skarn Cu-Au deposit are adakitic (Fig. 4.12). Skarn deposits are absent in the Muang Loei area and Rayong -Chantaburi area. Geochemistry of tonalite, granodiorite and quartz-syenite in the Muang Loei area, granodiorite and tonalite in the Phu Thap Fah - Phu Thep area, and monzogranite, granodiorite and tonalite from Rayong – Chantaburi area indicates that these are normal typical volcanic arc rocks.

Most of the mineralization are related to granodiorite, monzodiorite and tonalite from Muang Loei, Phu Thap Fah - Phu Thep, Phetchabun, Nakon Sawan - Lobburi and

Rayong -Chantaburi that show volcanic arc signatures. Quartz syenite and tonalite from the Muang Loei and monzogranite from Rayong - Chantaburi areas which indicate formation in a collisional setting are not associated with significant mineralization. Metallogeny of Cu-Au skarn deposits, Au skarn deposit, epithermal Au deposit and epithermal Sb-Au deposit along the Loei Fold Belt must have been related to the subduction of the Paleo-Tethys, and ceased upon initiation of continental collision (Fig. 7.2).

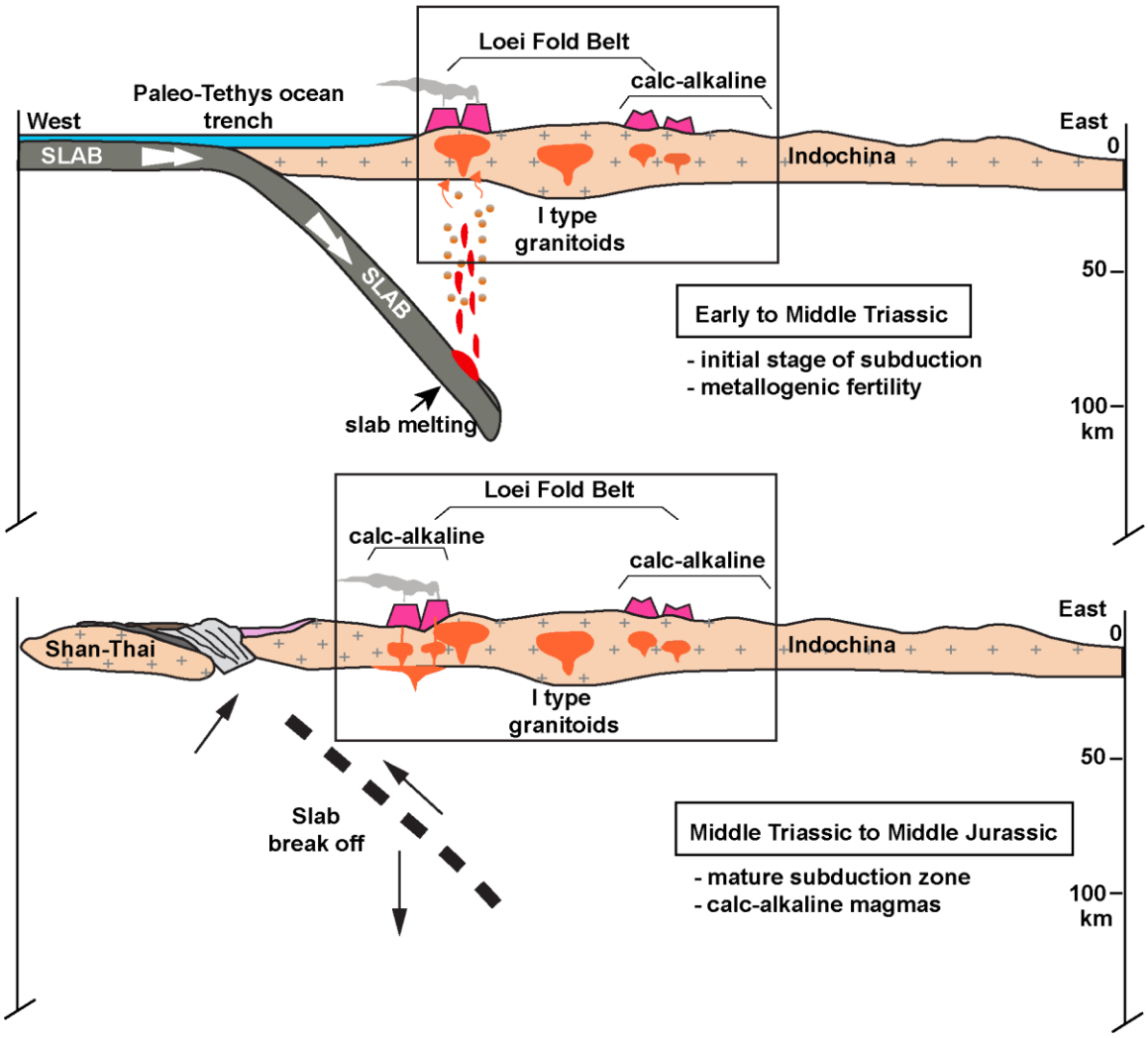

Fig. 7.2 Schematic model for the arc magma genesis, tectonic and metallogenic evolution of the Loei Fold Belt during Early Triassic to Middle Jurassic. Enclosed within the box is the cross-section of Loei Fold Belt, as interpreted in this study. Modified from Kamvong et al. (2014).

7.1.3. Relationship between solidification depth of granitoids and formation of hydrothermal ore deposits

Chemical compositions of biotite from granitoids in the Loei Fold Belt are presented in Table 5. Ternary MgO-FeO_{tot}-Al_2O_3 tectono-magmatic discrimination diagram (Abdel-Rahman, 1994) suggests that biotite compositions from the Loei Fold Belt granitoids fall within calc-alkaline field (Fig. 7.3), except for granodiorite (Gr30) from Petchabun plotted in alkaline field and granodiorite (Gr46, Gr43), monzogranite (Gr44, Gr39, Gr42, Gr45, Gr53) and tonalite (Gr50) from Rayong – Chantaburi plotted in peraluminous field.

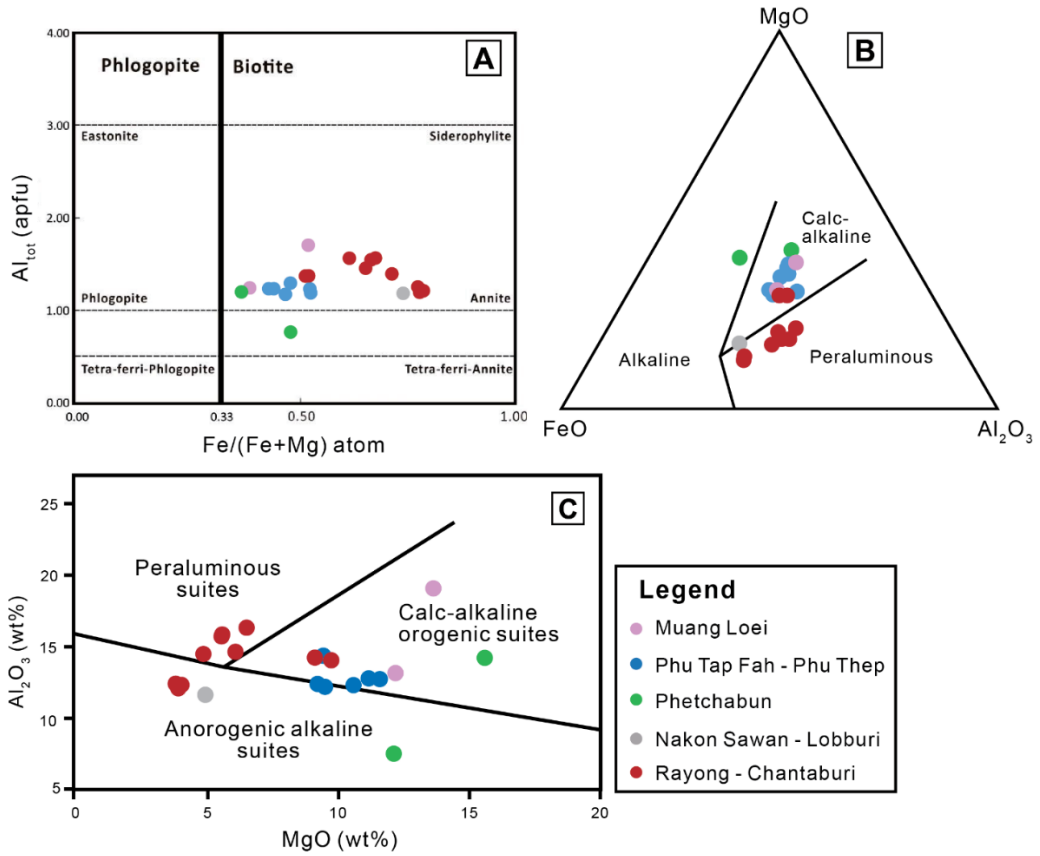

Fig. 7.3 (a) A/CNK [Al_2O_3/(CaO + Na_2O + K_2O) molar] vs A/NK[(Al_2O_3/Na_2O + K_2O) molar] diagram (Maniar & Piccoli, 1989), (b), (c) discrimination diagram of tectonic environment (Pearce et al., 1984) of granitoids along Loei Fold Belt. Abbreviation: VAG = volcanic-arc granite; syn-COLG = syn-collision granite; WPG = within plate granite; ORG = oceanic ridge granite.

The relationship between the estimated solidification pressure of granitic magma and Al_{total} content of biotite proposed by Uchida *et al*. (2007) is applied to estimate the solidification pressure of granitoids along the Loei Fold Belt. The estimation of solidification pressures of granitoids are 0.5 to 1.9 kb in Muang Loei, 1.1 kb in Phu Tap Fah – Phu Thep, 0.6 kb in Nakon Sawan – Lobburi, and 1.0 to 3.1 kb in Rayong – Chantaburi (Table 5).

The total Al content changes with the metal type of the accompanying hydrothermal ore deposits and increases in the following order: Fe-Cu deposit (Khao Lek) and Au deposit (Phu Thap Fah) < Cu deposit (Phu Thong Dieng or PUT2) < barren granitic rocks (Fig. 7.4).

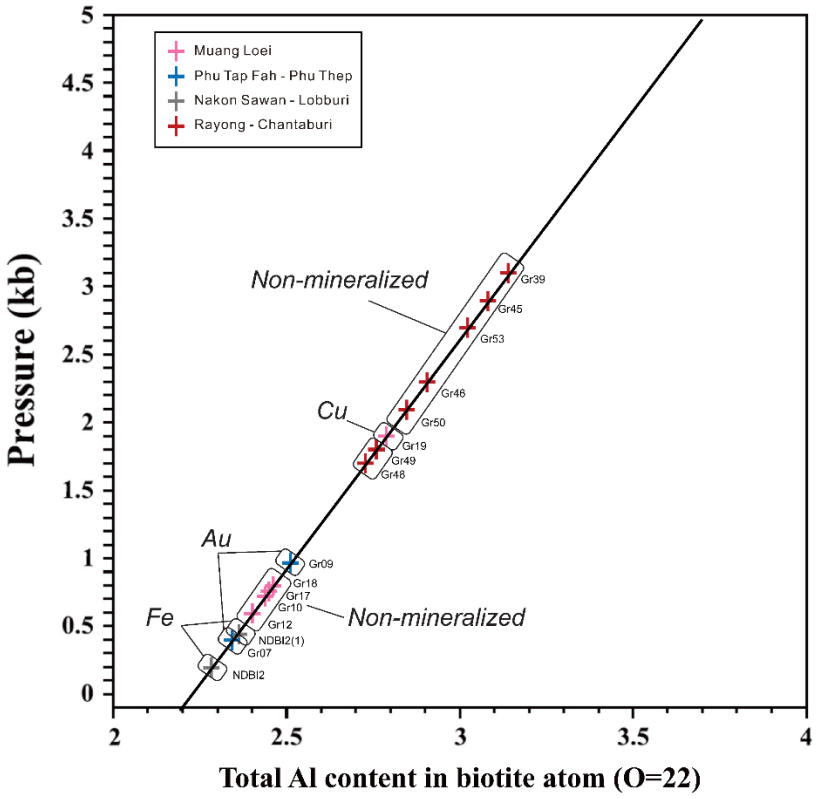

Fig. 7.4 The relationship between the estimated solidification pressure of granitoids along Loei Fold Belt and the TAl content of biotite. Modified from Uchida et al. (2006).

7.2. Summary and Conclusions

Integration of existing data with new geochemistry, petrography, magnetic susceptibility, mineral chemistry and field data leads to the following conclusions.

(1) Granitoids along Loei Fold Belt are petrographically classified into four main rock types i.e., monzogranite, granodiorite, tonalite and quartz-monzodiorite. In addition, quartz-rich granitoid and quartz-syenite are also present locally. Whole-rock SiO_2 vs. ($Na_2O + K_2O$) plot also indicates that those granitoids are classified into granite, granodiorite and diorite.

(2) According to the whole-rock SiO_2 vs. K_2O plot, granitoids along Loei Fold Belt are medium-K calc-alkaline and high-K calc-alkaline series, while monzogranite and granodiorite from Rayong Chantaburi are shoshonite series.

(3) Biotite ternary MgO-FeO_{tot}-Al_2O_3 tectono-magmatic discrimination diagram suggests that biotite compositions from the Loei Fold Belt granitoids fall within calc-alkaline magmas field, except for granodiorite from Petchabun and granodiorite, monzogranite and tonalite from Rayong – Chantaburi which fall within peraluminous.

(4) All granitoids are I-type, except a monzogranite from Rayong - Chantaburi. Tonalite and monzodiorite from Muang Loei are metaluminous, whereas granodiorite and quartz-syenite are peraluminous. All granodiorites and tonalites from Phu Tap Fah – Phu Thep are metaluminous. Monzodiorite and tonalite from Phetchabun, granodiorite, monzogranite and monzodiorite from Nakon Sawan – Lobburi are metaluminous. Tonalie, monzogranites, and granodiorites from Rayong – Chantaburi are metaluminous, whereas some of monzogranites and granodiorites are peraluminous.

(5) In the whole-rock Sr/Y ratio vs. Y concentration diagram, granodiorite, diorite and monzodiorite from Petchabun, granodiorite from Phu Thap Fah – Phu Thep and

monzodiorite from Nakon Sawan – Lobburi are plotted in adakite field, whereas tonalite, granodiorite and quartz-syenite from Muang Loei, granodiorite and tonalite from Phu Thap Fah – Phu Thep and monzogranite, granodiorite and tonalite from Rayong Chantaburi are plotted in the normal volcanic arc andesite-dacite-rhyolite field.

(6) The K-Ar age on K-feldspar of quartz-syenite from Muang Loei is 171±3 Ma, K-Ar age on K-feldspar of monzogranite from Nakon Sawan is 221±5 Ma, and K-Ar age of hornblende of quartz-monzodiorite from Loburi is 229±8 Ma. These age data suggest magmatism of Muang Loei occurred in the Middle Jurassic, and Nakon Sawan – Lobburi occurred in Late Triassic. Both Nb vs. Y and Rb vs. (Y + Nb) discriminations and age data indicate that the Paleo-Tethys subducted under the Indochina plate in Nakon Sawan – Lobburi area during Late Triassic, while volcanic arc in Muang Loei formed later in Middle Jurassic.

(7) $\delta^{34}S_{CDT}$ value of pyrite ranging from -1.3 to +2.2‰ indicates that sulfur in that hydrothermal fluid was derived from magmatic materials. Likewise, low magnetic susceptibility values of granodiorite at Phu Thap Fah Au deposit in Phu Thap Fah – Phu Thep area ($<1\times10^{-3}$ in SI unit) suggest that the rocks are hydrothermally altered. Especially magnetite-series the Au-Cu-Fe deposits along Loei Fold Belt is related to adakitic rocks of magnetite-series granitoids from Phetchabun and Nakon-Sawan areas that were generated in the volcanic arc related to the subduction of Paleo-tethys.

(8) Chemical analysis of biotite in granitoids indicates that the ^{T}Al content of biotite differs with metal type, that is, ^{T}Al content increases in the following order: Fe-Cu-

Au deposit < Cu deposit < barren granitioids, reflecting that the ^{T}Al content of biotite of granitoids depends on the crystallization pressure.

References

Abdel-Rahman, A.M. (1994) Nature of biotites from alkaline, calc-alkaline, and peraluminous magmas. J. Petrol, 35, 525-541.

Barber, A.J. and Crow, M.J. (2002) An evaluation of plate tectonic models for the development of Sumatra. Gondwana Research, 6, 1-28.

Barber, A.J., Ridd, M.F. and Crow, M.J. (2011) The origin, movement and assembly of the pre-Tertiary tectonic units of Thailand. In: Ridd, M.F., Barber, A.J. and Crow, M.J. (eds.), The Geology of Thailand. Geological Society, London, 507-538.

Barr, S.M. and Charusiri, P. (2011) Volcanic rocks. In: Ridd, M.F., Barber, A.J. and Crow, M.J. (eds.), The Geology of Thailand. Geological Society, London, 415-439.

Barr, S.M. and Macdonald, A.S. (1991) Toward a late Palaeozoic-early Mesozoic tectonic model for Thailand. J. Thai Geosci., 1, 11-22.

Beckinsale, R.D. and Gale, N.H. (1969) A reappreaisal of decay constants and branching ratio of 40K. Earth Planet. Sci. Lett, 6, 289-294.

Blevin, P.L. and Chappell, B. W. (1995) Chemistry, origin and evolution of mineralised granites in the Lachlan Fold Belt, Australia; The metallogeny of I- and S-type granites. Econ. Geol., 90, 1604-1619.

Boonsoong, A., Panjasawatwong, Y. and Metparsopsan, K. (2011) Petrochemistry and tectonic setting of mafic volcanic rocks in the Chon Daen-Wang Pong area, Phetchabun, Thailand. Island Arc, 20, 107-124.

Bunopas, S. (1991) The Pre-late Triassic collision and stratigraphic belts of Shan-Thai and Indochina microcontinents in Thailand. In Proceedings of Papers Presented at

the 1st International Symposium of the IGCP Project 321, Gondwana Dispersal and Accretion of Asia, Kunming, China, 25-30 November 1991, 25-30.

Bunopas, S. and Vella, P. (1983) Opening of the Gulf of Thailand – Rifting of Contiental Southeast Asia and Late Cenozoic Tectonics. J. Geol. Soc. Thailand, 6, 1-12.

Castillo, P.R., Janney, P.E. and Solidum, R.U. (1999) Petrology and geochemistry of Camiguin Island, southern Philippines: Insights to the source of adakites and other lavas in a complex arc setting. Contrib. Mineral. Petrol., 134, 33-51.

Chappell, B.W. and White, A.J.R. (2001) Two contrasting granite types: 25 years later. Australian J. Earth Sci., 48, 489-499.

Charusiri, P. (1989) Lithophile Metallogenic Epochs of Thailand: A Geological and Geochronological Investigation. (Unpublished PhD Thesis) Queen's University, Ontario, 819p.

Charusiri, P., Clark, A.H., Farrar, E., Archibald, D. and Charusiri, B. (1993) Granite belts in Thailand: evidence from the $^{40}Ar/^{39}Ar$ geochronological and geological syntheses. J. Earth Sci., 8, 127-136.

Charusiri, P., Khamphavong, K., Sutthirat, C., Lunwongsa, W. and Inthasopa, S. (2007) Multiple tectono-magmatic and metallogenic episodes of Eastern Thailand and Central Lao PDR. European Geosciences Union, 9, 580.

Charusiri, P., Daorerk, V., Archibald, D., Hisada, K. and Ampaiwan, T. (2002) Geotectonic Evolution of Thailand: A New Synthesis. J. Geol. Soc. (Thailand), 1, 1-20.

Clemens, J.D. and Wall, V.J. (1981) Origin and crystallization of some peraluminous (S-type) granitic magmas. Canadian Mineralogist, 19, 111-131.

Cobbing, E.J. (2011) Granitic rocks. In: Ridd, M.F., Barber, A.J. and Crow, M.J. (eds). The Geology of Thailand. J. Geol. Soc. (London), 441-457.

Cobbing, E.J., Mallick, D.I.J., M., Pitfield, P.E.J. and Teoh L.H. (1986) The granites of the Southeast Asian Tin Belt. J. Geol. Soc. (London), 143, 537-550.

Crow, M.J. and Zaw, K. (2011) Metalliferous minerals. In: RIDD, M.F., Barber, A.J. and Crow, M.J. (eds). The Geology of Thailand. J. Geol. Soc. (London), 459-492.

Davidson, J.D., Morgan, D.J. and Charlier, B.L.A. (2007) Isotopic microsampling of magmatic rocks. Elements, 3, 253-259.

Defant, M.J., Jackson, T.E., Drummond, M.S., De Boer, J.Z., Bellon, H., Feigenson, M.D., Maury, R.C. and Stewart, R.H. (1992). The geochemistry of young volcanism throughout western Panama and southeastern Costa Rica: an overview. J.Geol. Soc., London. 149, 569–579.

De Little, J.V. (2005) Geological Setting, Nature of Mineralisation, and Fluid Characteristics of the Wang Yai Prospects, Central Thailand. Unpublished BSc (Hons) Thesis, ARC Centre of Excellence in Ore Deposits (CODES), University of Tasmania, Hobert, Australia, November 2005, 109p.

Defant, M.J. and Drummond, M.S. (1990) Derivation of some modern arc magmas by melting of young subducted lithosphere. Nature, 347.

DePaolo, D.J. (1981) A neodymium and strontium isotopic study of the Mesozoic calc-alkaline granitic batholiths of the Sierra Nevada and Peninsular Ranges, California. J. Geophys. Res.: Solid Earth, 86, 10470-10488.

Department of Mineral Resources (2013) Geological Map of Thailand 1:1,000,000 (revised version). Department of Mineral Resources, Ministry of Natural Resources and Environment, Bangkok, Thailand.

Flood, R.H. and Shaw, S.E. (1975) A cordierite-bearing granite suite from the New England Batholith, N.S.W., Australia. Contrib. Mineral. Petrol., 52, 157-164.

Gatinsky, Y.G., Hutchison, C.S., Minh, N.N. and Tri, T.V. (1984) Tectonic evolution of Southeast Asia. In: Tectonics of Asia, 27th Int. Geol. Congr, Moscow, Colloq., 5, 225-241.

Henry, D.J., Guidotti, V.C. and Thomson, J.A. (2005) The Ti-saturation surface for low-to-medium pressure metapelitic biotites: Implications for geothermometry and Ti-substitution mechanisms. Am. Mineral., 90, 316-328.

Hildreth, W. and Moorbath, S. (1988) Crustal contributions to arc magmatism in the Andes of Central Chile. Contrib. Mineral. Petrol., 98, 455-489.

Hine, R., Williams, I.S., Chappell, B.W. and White, A.J.R. (1978) Contrasts between I- and S-type granitoids of the Kosciusko Batholith. J. Geol. Soc. Aust., 25, 219-234.

Hutchison, C.S. (1989) Geological Evolution of South-East Asia. Oxford Monographs on Geology and Geophysics, 13, Clarendon Press, Oxford, UK, 368p.

Hutchison, C.S. (2007) Geological Evolution of South-East Asia. Geological Society of Malaysia, Malaysia., 2nd edn., 407p.

Ikeda, K. (2017) Mineral description and ore-forming conditions of the Phu Thap Fah gold skarn deposit in northeastern Thailand. (Unpublished B.C. Thesis) Akita University, Japan, 75p.

Intasopa, S. (1993) Petrology and Geochronology of the Volcanic Rocks of the Central Thailand Volcanic Belt. (Unpubished PhD Thesis) University of New Brunswick, Fredericton, 242p.

Ishihara, S. (1977) The magnetite-series and ilmenite-series granitic rocks. Min. Geol., 27, 293-305.

Ishihara, S. (1981) The granitoid series and mineralization. Econ. Geol., 75th Ann. Vol., 458-484.

Ishihara, S. (1998) Granitoid series and mineralization in the Circum-Pacific Phanerozoic granitic belts. Resour. Geol., 48, 219-24.

Ishihara, S. and Chappell, B.W. (2010) Chemical compositions of the Miocene granitoids of the Okueyama, Hoei mine and Takakumayama plutons, Outer Zone of SW Japan. Bull. Geol. Surv. Japan, 61, 17-38.

Ishihara, S., Hashimoto, M. and Machida, M. (2000) Magnetite/ilmenite series classification and magnetic susceptibility of the Mesozoic-Cenozoic batholiths in Peru. Resour. Geol., 50, 123-129.

Ishihara, S. and Sasaki, A. (1989) Sulfur isotopic ratios of the magnetite-series and ilmenite-series granitoids of the Sierra Neveda batholith - A reconnaissance study. Geology, 17, 788-791.

Imaoka, T., Kiminami, K., Nishida, K., Takemoto, M., Ikawa, T., Itaya, T., Kagami, H. and Lizumi, S. (2011) K-Ar age and geochemistry of the SW Japan Paleogene cauldron cluster: Implications for Eocene-Oligocene thermo-tectonic reactivation. J. Asian Earth Sci., 40, 509-533.

Jacobson, H.S., Pierson, C.T., Japakasetr, T., Inthuputi, B., Siriratanamongkol, C., Prapassornkul, S. and Pholphan, N. (1969) Mineral Investigation in Northeastern Thailand. U.S.G.S, Professional Paper 618, 96p.

Kamvong, T., Charusiri, P. and Intasopa, S.B. (2006) Petrochemical Characteristics of Igneous Rocks from the Wang Pong Area, Phetchabun, North Central Thailand: Implications for Tectonic Setting. J . Geol. Soc. Thailand, 1, 9-26.

Kamvong, T., Zaw, K., Meffre, S., Maas, R., Stein, H. and Lai, C.-K. (2014) Adakites in the Truong Son and Loei fold belts, Thailand and Laos: Genesis and implications for geodynamics and metallogeny. Gondwana Res., 26, 165-184.

Kamvong, T. and Zaw, K. (2009) The origin and evolution of skarn-forming fluids from the Phu Lon deposit, northern Loei Fold Belt, Thailand: Evidence from fluid inclusion and sulfur isotope studies. J. Asian Earth Sci., 34, 624-633.

Kamvong, T. and Zaw, K. (2005) Geology and genesis of Phu Lon copper-gold skarn deposit, northeast Thailand. International conference on Geology, Geotechnology and Mineral Resources of Indochina (GEOINDO 2005), 28-30 November 2005, Kosa Hotel, Khon Kaen, Thailand, 310-318.

Kawakami, T., Nakano, N., Higashino, F., Hokada, T., Osanai, Y., Yuhara, M., Charusiri, P., Kamikubo, H., Yonemura, K. and Hirata, T. (2014) U-Pb zircon and CHIME monazite dating of granitoids and high-grade metamorphic rocks from the Eastern and Peninsular Thailand — A new report of Early Paleozoic granite. Lithos, 200, 64-79.

Khositanont, S., Panjasawatwong, Y., Ounchanum, P., Thanasuthipitak, T., Zaw, K. and Meffre, S. (2008) Petrochemistry and zircon age determination of Loei-

Phetchabun volcanic rocks. In: Chutakositkanon, V., Sutthirat, C. and Charoentitirat, T. (eds.), International Symposia on Geoscience Resources and Environments of Asian Terranes (GREAT 2008), 4th IGCP 516 and 5th APSEG, Bangkok, 272-278.

Leake, B.E. (1990) Granite magmas: their sources, initiation and consequences of emplacement. J. Geol. Soc. Lond., 147, 579-589.

Macpherson, C.G., Dreher, S.T. and Thirlwall, M.F. (2006) Adakites without slab melting: High pressure differentiation of island arc magma, Mindanao, the Philippines. Earth Planet Sci. Lett., 243, 581-593.

Mahawat, C., Atherton, M.P. and Brotherton, M.S. (1990) The Tak Batholith, Thailand: The evolution of contrasting granite types and implications for tectonic setting. J. Asian Earth Sci., 4, 11-27.

Maniar, P.D. and Piccoli, P.M. (1989) Tectonic discrimination of granitoids. Geological Society of America Bulletin, 101, 635-643.

Martin, H. (1986) Effect of steeper Archean geothermal gradient on geochemistry of subduction-zone magmas. Geology, 14, 753-756.

Maulana, A., Imai, A., Van Leeuwen, T., Watanabe, K., Yonezu, K., Nakano, T., Boyce, A., Page, L. and Schersten, A. (2016) Origin and geodynamic setting of Late Cenozoic granitoids in Sulawesi, Indonesia. J. Asian Earth Sci., 124, 102-125.

Meinert, L.D., Dipple, G.M. and Nicolescu, S. (2005) World skarn deposits. In: Hedenquist, J.W., Thompson, J.F.H., Goldfarb, R.J., Richard, J.P. (Eds.), Economic Geology 100th Anniversary Volumn. Society of Economic Geologists, Littleton, Colorado, USA, 299-336.

Metcalfe, I. (1984) Stratigraphy, palaeontology and palaeogeography of the Carboniferous of Southeast Asia. Mem. Soc. Geol. France, 147, 107–118.

Metcalfe, I. (1988) Origin and assembly of Southeast Asian continental terrances. In Gondwana and Tethys. Audley-Charles, M.G. and Hallam, A. (eds.). J. Geol. Soc. Lond. Special Publicaiton, 37, 101-118.

Metcalfe, I. (2006) Paleozoic and Mesozoic tectonic evolution and paleography of East Asian crustal fragments: The Korean Peninsula in contect. Gondwana Research, 9, 24-26.

Metcalfe, I. (2011) Tectonic framework and Phanerozoic evolution of Sundaland. Gondwana Research, 19, 3-21.

Metcalfe, I. (2017) Tectonic evolution of Sundaland. Bulletin of the Geological Society of Malaysia. 63, 27-60.

Middlemost, E.A.K. (1994) Naming materials in the magma/igneous rock system. Earth-Science Reviews, 37, 215-224.

Müller, C.J. (1999) Geochemistry, Fluid Characteristics and Evolution of the French Mine Gold Skarn System, Eastern Thailand, Unpublished BSc (Hons) Thesis, ARC Centre of Excellence in Ore Deposits (CODES), University of Tasmania, Hobert, Australia, 145p.

Müntener, O., Kelemen, P.B. and Grove, T.L. (2001) The role of H_2O during crystallization of primitive arc magmas under uppermost mantle conditions and genesis of igneous pyroxenites: An experimental study. Contrib. Mineral. Petrol., 141, 643-658.

Paipana, S. (2014) Geology and Mineralization Characteristics of Bo Thong Antimony ± Gold Deposit, Chonburi Province, Eastern Thailand. BSc (Hons) Thesis, ARC Centre of Excellence in Ore Deposits (CODES), University of Tasmania, Hobert, Australia, 100p.

Pearce, J.A., Harris, B.W. and Tindle, A.G. (1984) Trace element discrimination diagrams for the tectonic interpretation of granitic rocks. J. Petrol. , 25, 956-983.

Petrone, C.M. and Ferrari, L. (2008) Quaternary adakite-Nb-enriched basalt association in the western Trans-Mexican Volcanic Belt: Is there any slab melt evidence? Contrib. Mineral. Petrol., 156, 73-86.

Qin, Z., Wu, Y., Siebel, W., Gao, S., Wang, H., Abdallsamed, M.I.M., Zhang, W. and Yang, S. (2015) Genesis of adakitic granitoids by partial melting of thickened lower crust and its implications for early crustal growth: A case study from the Huichizi pluton, Qinling orogen, central China. Lithos., 238, 1-12.

Rapp, R.P. and Watson, E.B. (1995) Dehydration melting of metabasaltat 8–32 kbar: Implications for continental growth and crust–mantle recycling. J. Petrol., 36, 891-931.

Renne, P. R., Farley, K. A., Becker, T. A. and Sharp, W. D. (2001) Terrestrial cosmogenic argon. Earth Planet. Sci. Lett. 188, 435– 440.

Ridd, M.F. (2012) The role of strike-slip faults in the displacement of the Palaeotethys suture zone in Southeast Thailand. J. Asian Earth Sci., 51, 63-84.

Ridolfi, F., Renzulli, A. and Puerini, M. (2009) Stability and chemical equilibrium of amphibole in calc-alkaline magmas: an overview, new thermobarometric

formulations and application to subduction-related volcanoes. Contrib. Mineral. Petrol., 160, 45-66.

Robinson, B.W. and Kusakabe, M. (1975) Quantitative preparation of sulfur dioxide for $^{34}S/^{32}S$ analyses from sulfides by combustion with cuprous oxide. Anal. Chem., 47, 1179—1181.

Rodmanee, T. (2000) Genetic Model of Phu Thap Fah Gold Deposit, Ban Huai Phuk Amphoe Wang Saphung, Changwat Loei. MSc Thesis (unpublished), Chiang Mai University, Chiang Mai, Thailand, 128p.

Rodriguez, C., Selles, D., Dungan, M., Langmuir, C., and Leeman, W. (2007) Adakitic dacites formed by intracrustal crystal fractionation of waterrich parent magmas at Nevado de Longavi volcano (36.2°S; Andean Southern volcanic zone, Central Chile). J. Petrol., 48, 2033-2061.

Rollinson, H. R. (1993) Using geochemical data; evaluation, presentation, interpretation, Longman Scientific & Technical. Harlow, 352 p.

Rooney, T. O., Franceschi, P. and Hall, C. (2011) Water saturated magmas in the Panama Canal region - a precursor to adakite-like magma generation? Contrib. Mineral. Petrol., 161, 373-388.

Salam, A. (2013) A Geological, Geochemical and Metalloogenic Study of The Chatree Epithermal Deposit, Phetchabun Province, Central Thailand. Ph.D. Thesis, ARC Centre of Excellence in Ore Deposits (CODES), University of Tasmania, Hobert, Australia, 268p.

Salam, A., Zaw, K., Mefre, S., McPie, J., Cumming, G., Suphananthi, S. and James, R. (2008) Stratigraphy and geochemistry of Permian to Triassic Chatree volcanics,

Phetchabun Province, Central Thailand. International Conference on the Tectonics of Northwestern Thailand, Chiang Mai, 37-38.

Salam, A., Zaw, K., Meffre, S., McPhie, J. and Lai, C.-K. (2014) Geochemistry and geochronology of the Chatree epithermal gold–silver deposit: Implications for the tectonic setting of the Loei Fold Belt, central Thailand. Gondwana Research, 26, 198-217.

Samaniego, P. (1997) Interactions entre les magmas adakitiques et calco-alcalins: ge´ochimie des complexes volcaniques du Cayambe et du Moranda–Fuya Fuya (Equateur) Unpublished memoir, University of Clermont-Ferrand, France, 45 pp.

Sato, K. (1991) Miocene granitoid magmatism at the island-arc junction, central Japan. Mod. Geol., 15, 367-399.

Saunders, A.D., Tarney, J. and Weaver, S.D. (1980) Transverse geochemical variations across the Antarctic Peninsula: Implications for the genesis of calc-alkaline magmas. Earth Planet. Sci. Lett., 46, 344-360.

Seal, I.R. (2006) Sulfur Isotope Geochemistry of Sulfide Minerals. Reviews in Mineralogy & Geochemistry, 61, 633-677.

Searle, M.P., Whitehouse, M.J., Robb, L.J., Ghani, A.A., Hutchison, C.S., Sone, M., Ng SW-P., Roselee, M.H., Chung S-L. and Oliver, G.J.H. (2012) Tectonic evolution of the Sibumasu-Indochina terrane collision zone in Thailand and Malyasia: constraints from new U-Pb zircon chronology of SE Asian tin granitoids. J. Geol. Soc. Lond., 169, 489-500.

Seward, T. M., and Barnes, H. L. (1997) Metal transport by Hydrothermal Ore Fluids, *in* Barnes, H. L., ed., Geochemistry of Hydrothermal Ore deposits, 435-486.

Shabbani, A.T. and Lalonde, A. (2003) Composition of Biotite from Granitic Rocks of the Canadian Appalachian: A potential tectonomagmatic indicator? Can. Mineral., 41, 35-46.

Singharajwarapan, S. and Berry, R. (2000) Tectonic implications of the Nan suture zone and its relationship to the Sukhothai fold belt, northern Thailand. J. Asian Earth Sci., 18, 663-673.

Sone, M. and Metcalfe, I. (2008) Parallel Tethyan sutures in mainland Southeast Asia: New insights for Palaeo-Tethys closure and implications for the Indosinian orogeny. C.R. Geoscience, 340, 166-179.

Spycher, N. F., and Reed, M. H. (1989) As (III) and Sb(III) sulfide complexes: An evaluation of stoichiometry and stability from existing experimental data. Geochim. Cosmochim. Acta, 9, 2185-2194.

Streckeisen, A.L. (1973) Plutonic rocks, classification and nomenclature recommended by the IUGS Subcommission on the Systematics of Igneous Rocks. Geotimes, 18, 26-30.

Streckeisen, A.L. (1976) To each plutonic rock its proper name. Earth Science Reviews, 12, 1-33.

Sun, S.-s. and McDonough, W.F. (1989) Chemical and isotopic systematics of oceanic basalts: implications for mantle composition and processes. J. Geol. Soc. Lond., Special Publicaitions, 42, 313-345.

Takahashi, M., Aramaki, S. and Ishihara, S. (1980) Magnetite-series/Ilmenite-series vs. I-type/S-type granitoids. Min. Geol. Spec. Issue, 8, 13-28.

Tangwattananukul, L. and Ishiyama, D. (2017) Characteristics of Cu-Mo mineralization in the Chatree mining area, central Thailand. Resour. Geol., 68, 83-92.

Uchida, E., Endo, S. and Makino, M. (2007) Relationship between solidification depth of granitic rocks and formation of hydrothermal ore deposits. Resour. Geol., 57, 47-56.

Wang, Q., Li, X.H., Jia, X.H., Wyman, D., Tang, G.J., Li, Z.X., Ma, L. Yang, Y.H., Jiang, Z.Q. and Gou, G.N. (2012) Late Early Cretaceous adakitic granitoids and associated magnesian and potassium-rich mafic enclaves and dikes in the Tunchang–Fengmu area, Hainan Province (South China): Partial melting of lower crust and mantle, and magma hybridization. Chemical Geology, 328, 222-243.

White, A.J.R. and Chappell, B.W. (1977) Ultrametamorphism and granitoid genesis. Tectonophysics, 43, 7-22.

Williams-Jones, A. E., and Normand, C. (1997) Controls of mineral parageneses in the system Fe-Sb-S-O. Econ. Geol., 92, 308-324.

Yang, X.M. and Lentz, D.R. (2010) Sulfur isotopic systematics of grantioids from southwestern New Brunswick, Canada: implications for magmatic-hydrothermal processes, redox conditions, and gold mineralization. Miner Deposita, 45, 795-816.

Yang, J.H., Wu, F.Y., Chung, S.L., Wilde, S.A. and Chu, M.F. (2004) Multiple sources for the origin of granites: geochemical and Nd/Sr isotopic evidence from the Gudaoling granite and its mafic enclaves, NE China. Geochim. Cosmochim. Acta, 68, 4469-4483.

Zaw, K., Khositanont, T., Salam, A. and Manaka, T. (2007a) Geochronology, metallogenesis and deposit styles of Loei Fold Belt in Thailand and Lao PDR. CODES ARC Center of Excellence in Ore Deposits, University of Tasmania, Hobart, Australia, Final Report and CD-ROM, February, 2007 (unpublished).

Zaw, K. and Meffre, S. (2007b) Metallogenic relations and deposit-scale studies, final report, Geochronology, Metallogenesis and Deposit Styles of Loei Foldbelt in Thailand and Laos PDR, ARC Linkage Project.

Zaw, K., Meffre, S., Lai, C.-K., Burrett, C., Santosh, M., Graham, I., Manaka, T., Salam, A., Kamvong, T. and Cromie, P. (2014) Tectonics and metallogeny of mainland Southeast Asia — A review and contribution. Gondwana Research, 26, 5-30.

Zaw, K., Rodmanee, T., Khositanont, S., Thanasuthipitak, T. and Ruamkid, S. (2007b) Geology and genesis of Phu Thap Fah gold skarn deposit, northeastern Thailand: Implications for reduced gold skarn formation and mineral exploration. Proceeding of the GEOTHAI' 07 International Conference on Geolology of Thailand: Towards Sustainable Development and Sufficiency Economy, 93-95.

Zaw, K., Meffre, S., Kamvong, T., Stein, H., Vasconcelos, P. and Golding, S. (2009) Geochronological and metallogenic framework of Cu-Au skarn deposits along Loei Fold Belt, Thailand and Lao PDR. Proceeding of the Tenth Biennial SGA Meeting, Townsville, 309-311.

Zaw, K., Rodm anee, T., Khositanont, S. and Ruamkid, S. (2008) Mineralogy and genesis of Phu Thap Fah gold skarn deposit, Norhteast Thailand: Implication for reduced gold skarn formation. International Geological Congress (IGC), Norway, August 2008.